

**Schlieren in the South Mountain Batholith
and Port Mouton Pluton
Meguma Zone, Nova Scotia**

Krista L. McCuish

Submitted in Partial Fulfilment of the Requirements
for the Degree of Bachelor of Science, Honours
Department of Earth Sciences
Dalhousie University, Halifax, Nova Scotia
April 23, 2001



Dalhousie University

Department of Earth Sciences

Halifax, Nova Scotia

Canada B3H 3J5

(902) 494-2358

FAX (902) 494-6889

DATE 23 April 2001

AUTHOR Krista Leah McCuish

TITLE Schlieren in the South Mountain Batholith
and Port Mouton Pluton, Meguma Zone,
Nova Scotia.

Degree BSc. Convocation May Year 2001

Permission is herewith granted to Dalhousie University to circulate and to have copied for non-commercial purposes, at its discretion, the above title upon the request of individuals or institutions.

THE AUTHOR RESERVES OTHER PUBLICATION RIGHTS, AND NEITHER THE THESIS NOR EXTENSIVE EXTRACTS FROM IT MAY BE PRINTED OR OTHERWISE REPRODUCED WITHOUT THE AUTHOR'S WRITTEN PERMISSION.

THE AUTHOR ATTESTS THAT PERMISSION HAS BEEN OBTAINED FOR THE USE OF ANY COPYRIGHTED MATERIAL APPEARING IN THIS THESIS (OTHER THAN BRIEF EXCERPTS REQUIRING ONLY PROPER ACKNOWLEDGEMENT IN SCHOLARLY WRITING) AND THAT ALL SUCH USE IS CLEARLY ACKNOWLEDGED.

*We shall not cease from exploration
and the end of all our exploring,
will be to arrive where we started,
and know the place for the first time.*

--T.S. Eliot

TABLE OF CONTENTS

Table of Contents.....	i
Table of Figures	iv
Table of Tables	vi
Acknowledgements.....	vii
Abstract.....	viii
Glossary of Terms.....	ix
CHAPTER 1: INTRODUCTION.....	1
1.1 Opening Statement.....	1
1.1.1 Streaks in Nature.....	1
(i) Non-geological.....	1
(ii) Geological.....	3
1.2 Definitions.....	3
1.3 Schlieren in Granite	5
1.4 Purpose and Objectives.....	6
1.5 Scope of Study	10
1.6 Thesis Organization	12
CHAPTER 2: FIELD RELATIONS.....	13
2.1 Regional Geological Setting	13
2.2 Geology of the South Mountain Batholith.....	13
2.3 Prospect.....	15
2.4 Peggy's Cove	20
2.5 Geology of the Port Mouton Pluton.....	25
2.6 Jackies Island	25
2.7 St. Catherines River Bay.....	35
2.8 Summary.....	34
CHAPTER 3: METHODOLOGY	36
3.1 Introduction.....	36
3.2 Field Methods	36
3.2.1 Field mapping	36
3.2.2 Sampling	37
3.2.3 Photography	37
3.3 Petrography.....	37
3.3.1 Petrographic description	37
3.3.2 Sample preparation	38
3.4 Electron Microprobe Analysis	38
3.4.1 Operation of the electron microprobe	38

3.4.2 Sample preparation	40
3.4.3 Mineral analyses	40
3.5 Image Analysis.....	41
3.5.1 Sample preparation	41
3.5.2 Image analysis.....	41
3.6 Summary	41
CHAPTER 4: LABORATORY RESULTS	43
4.1 Introduction.....	43
4.2 Petrographic Description	43
4.2.1 Prospect.....	43
4.2.2 Peggy's Cove	46
4.2.3 Jackies Island	50
4.2.4 St. Catherines River Bay.....	53
4.3 Foliation Image Analysis Study.....	57
4.4 Biotite Composition Study.....	58
4.5 Summary	58
CHAPTER 5: DISCUSSION	62
5.1 Introduction.....	62
5.1.2 Homogenization vs. heterogenization.....	62
5.1.3 Dynamics of a crystallizing magma.....	62
5.2 Prospect	62
5.2.1 Major observations.....	65
5.2.2 Schlieren characteristics and working hypotheses.....	65
5.2.3 Inferred process.....	69
5.2.4 Implications of the model	71
5.3 Peggy's Cove	72
5.3.1 Major observations.....	72
5.3.2 Schlieren characteristics and working hypotheses.....	72
5.3.3 Inferred process.....	76
5.3.4 Implications of the model	78
5.4 Jackies Island	78
5.4.1 Major observations.....	78
5.4.2 Schlieren characteristics and working hypotheses.....	79
5.4.3 Inferred process.....	81
5.4.4 Implications for the model	83
5.5 St. Catherines River Bay.....	83
5.5.1 Major observations.....	83
5.5.2 Schlieren characteristics and working hypotheses.....	84
5.5.3 Inferred process.....	89
5.6 Summary	92

CHAPTER 6: CONCLUSIONS	93
6.1 Conclusions.....	93
6.2 Recommendations for future work	93
6.2.1 Prospect.....	93
6.2.2 Peggy’s Cove	96
6.2.3 Jackies Island	96
6.2.4 St. Catherines River Bay.....	96
REFERENCES	97

TABLE OF FIGURES

CHAPTER 1

1.1 Non-geological streaks in natural fluid systems	2
1.2 Geological streaks in granitoid rocks.....	4
1.3 Liquid-solid diagram for crystallizing magma	7
1.4 Location map for the four study areas	10

CHAPTER 2

2.1 Regional geology and locations of the four study areas	14
2.2 Location map of the Prospect study area	15
2.3 Detailed map of the Prospect study area.....	16
2.4 Photographs of Prospect schlieren	18
2.5 Location map of the Peggy's Cove study area.....	22
2.6 Detailed map of the Peggy's Cove study area	23
2.7 Photographs of mafic and felsic layering at Peggy's Cove	24
2.8 Location map of the Jackies Island and St. Catherines River Bay study areas	26
2.9 Location map of the Jackies Island study area.....	28
2.10 Photographs of mafic and felsic banding at Jackies Island.....	29
2.11 Detailed ink sketch of banding at Jackies Island	30
2.12 Location map of the St. Catherines River Bay study area	31
2.13 Photographs of streaked schlieren at St. Catherines River Bay.....	32
2.14 Detailed sketch of biotite schlieren trailing off metasedimentary xenoliths St. Catherines River Bay.....	33

CHAPTER 3

3.1 Diagram depicting the method of cutting thin sections for Jackies Island	39
--	----

CHAPTER 4

4.1 Photomicrographs of Prospect samples	45
--	----

4.2 Photomicrographs of Peggy's Cove samples.....	49
---	----

4.3 Photomicrographs of Jackies Island samples.....	52
---	----

4.4 Photomicrographs of St. Catherines River Bay samples	56
--	----

CHAPTER 5

5.1 Diagram of size sorting and shear flow in the wake of a rising vapour bubble or falling xenolith block.....	70
--	----

5.2 Diagram of repeated magma injection and crystal settling.....	77
---	----

5.3 Diagram of syn-magmatic shearing in the PMP disrupted by a fault-shear zone.....	82
--	----

5.4 Mineral plot of TiO_2 vs. $FeO/(FeO + MgO)$ for St. Catherines River Bay biotite composition study	88
---	----

5.5 Diagram of progressive partial melting and assimilation of metasedimentary xenoliths.....	90
--	----

5.6 Liquid-solid diagram showing the range of solids fraction at each of the four schlieren localities	91
---	----

TABLE OF TABLES

1.1 Summary table of previous work on schlieren	8
2.1 Comparison table of schlieren characteristic for all study areas.....	34
4.1(a) Detailed petrographic observations of Prospect samples	44
4.1(b) Detailed petrographic observations of Peggy's Cove samples	48
4.1(c) Detailed petrographic observations of Jackies Island samples.....	51
4.1(d) Detailed petrographic observations of St. Catherines River Bay samples.....	54
4.2 Foliation image analysis data for Peggy's Cove and Jackies Island.....	59
4.3 Mean biotite analyses of St. Catherines River Bay samples.....	60
6.1 Summary table of field relations, petrography, analytical methods, and working hypotheses.....	94
6.2 Summary table of physical processes at the four schlieren localities.....	95

Acknowledgements

I am very grateful to many people for their encouragement and support in the time it has taken me to complete this degree. In particular, I am indebted to my supervisor, Professor Barrie Clarke. His generosity with his time and resources, and his patient guidance, made this work possible. I wish to thank Professors Marcos Zentilli, Martin Gibling, Becky Jamieson, and Djordje Grujic for their helpful recommendations. I extend a warm thanks to John Adams and Brigitte Petersmann for their kind offerings of accommodation while I was doing fieldwork in Port Mouton. I am very grateful to Howard and Charlotte Callahan for navigating the “Charlotte ‘n Aye” through fog and rain, when I was stranded on Jackies Island. Thanks to Bob MacKay for his assistance with the electron microprobe and Gordon Brown for his expertise in thin section preparation. I gratefully acknowledge Richard Brunt of Parks Canada for permission to sample in the Kejimkujik Seaside Adjunct, and Dan Kontak for suggesting the Peggy’s Cove location. Thanks go to my sister, Fern, for her endless sense of humour and perceptive nature. Finally, special thanks go to my Dad for instilling a love for the outdoors and photography, and especially for encouraging me to pursue multiple careers.

Abstract

Dynamic interactions between crystals and melt can form schlieren as primary features during the various stages of the crystallization of magmas. The restricted conditions necessary for the formation and preservation of schlieren account for their relatively rare occurrence, and thus the schlieren can yield information about the chemical and physical processes in the magma prior to its solidification. This thesis presents a comparison of schlieren from four areas in the granites of southern Nova Scotia. At Prospect, schlieren features include: perturbation of the regional flow foliation, development of size-sorted biotite laminae, randomly oriented clusters of K-feldspar megacrysts, and deformation of quartz. At Peggy's Cove, schlieren features include: occurrence of subhorizontal, reversely-graded bands with cusped biotite margins and pockets of coarse-grained felsics, zoned adcumulate crystals, and myrmekitic textures. At Jackies Island, the major schlieren features are: symmetrical straight schlieren banding, zones of strong biotite and feldspar foliation with and without segregation banding, and the presence of feldspar and mica deformation microstructures. At St. Catherines River Bay, schlieren features include: spatially associated schlieren bands and metasedimentary xenolith slab swarm in host tonalite, hornfelsic texture in xenolith cores, foliated biotite aggregates on xenolith rims, and limited variation in biotite FeO-MgO-TiO₂ compositions. Schlieren at all four study localities show distinctive mineralogical, textural, and structural features indicating different physical-chemical processes of formation at each location. The inferred processes for schlieren formation are: Prospect – size sorting and shear flow in the wake of a rising vapour bubble or falling xenolith block; Peggy's Cove – repeated magma injection with gravity settling; Jackies Island – synmagmatic shearing in a shear zone with development of strong foliation and segregation banding; and St. Catherines River Bay – partial melting and assimilation of metasedimentary xenoliths. These examples demonstrate that a wide range of physical and chemical processes are responsible for the formation of schlieren in felsic magmatic systems.

Key Words: schlieren, banding, layering, foliation, segregation, microstructures, shear flow, magma injection, gravity settling, shear zone, partial melting, assimilation

Glossary of Terms

anatexis- melting of a pre-existing rock

banding- a two-dimensional feature developed in igneous rocks as layers, stripes, flat lenses, or streaks with obvious differences in mineral composition and/or texture (AGI 1987)

- *segregation banding-* compositional banding (not of primary origin) that results from a segregation of material from an originally statistically homogeneous composite material

cumulate- fractionated crystals concentrated by processes of crystallization differentiation producing a framework of touching mineral crystals and commonly showing features suggestive of gravity settling (Irvine 1987)

- *cumulate crystals-* subhedral to euhedral fractionated crystals
- *postcumulus crystals* - a later textural generation of material that cements the cumulate crystals
- *intercumulus liquid-* the liquid that originally filled the interstitial spaces between cumulate crystals becoming postcumulus material
- *adcumulate-* crystal growth represented by a continued growth of cumulus crystals by fractional crystallization of trapped intercumulus liquid (Irvine 1987)

dilatancy- an increase in the bulk volume during deformation, caused by a change from close-packed structure to open-packed structure, accompanied by an increase in the pore volume, rotation of grains, microfracturing, and grain boundary slippage (AGI 1987)

LPO- lattice-preferred orientation

- *(c)-slip(in quartz)-* slip motion parallel to c-axes at high temperature conditions ($T > 500^{\circ}\text{C}$)
- *(a)-slip(in quartz)-* dislocation glide and creep along glide planes at low temperature conditions ($T = 300\text{-}400^{\circ}\text{C}$)
- both (a) and (c)-slip produce blocky subgrain development and undulose extinction (Passchier and Trouw 1996)

foliation- a general term used to describe any planar arrangement of textural and structural features in any type of rock

- *S-foliation-* planar fabric elements
- *L-foliation-* linear fabric elements
- *S > L foliation-* planar fabric element is stronger than linear fabric element

layering- the tabular succession of different components (mineralogic, textural, structural) one upon the other in a particular rock (implies three-dimensional planar structure) (AGI 1987)

- *schlieren layering* (used synonymously with *wispy or streaky layering*)- thin wavy streaks of dark minerals which can be truncated or crossbedded and may be finely banded (McBirney and Noyes 1979)
- *symmetrical layering*- parallel, mafic bands that grade into granitic host or are sharply defined on both sides
- *asymmetrical layering*- bands with sharp lower edges that become graduated in an upwards direction
- *rhythmic layering*- layers have obvious banding that is repeated as a result of changes in the relative proportions of minerals (Hess 1960)
- *graded layering*- layers that are stratigraphically graded according to texture and composition
 - a) *normal grading*-upward gradation of minerals from coarse to fine grain size
 - b) *reverse grading*-upward gradation of mineral from fine to coarse grain size

lamina- a thin, sharply defined layer with a usual thickness of 1 cm ranging to a maximum thickness of approximately 3 cm which typically form branches, fans, bundles or truncations (laminae) and are described as wispy, streaky or schlieren layering (Wager and Brown 1967)

myrmekite- a vermicular intergrowth of quartz and plagioclase often occurring as “blebs” that replace the margins of K-feldspar. “Subsolidus deformation appears to be a prerequisite for its formation” (Vernon 2000).

CHAPTER 1: INTRODUCTION

1.1 Opening Statement

1.1.1 Streaks in Natural Systems

Streaks are “long thin usually irregular lines or bands, especially of a different colour or substance from their surroundings” (Oxford Dictionary 1994) that, in part, can occur in layered patterns in natural flowing systems. Streaks occurring in natural systems can occur in both non-geological and geological systems.

Non-geological streaks

Non-geological streaks occur in layered atmospheric cloud formations, in swirled oil patterns on a water surface, and in chaotic bands of foam or pollen particles on a water surface (Fig.1.1). Clouds consist of water droplets or ice crystals in a state of freefall, influenced by the force of drag opposing the force of gravity. If the particles are small enough, the forces balance and the particles appear suspended; if their masses increase, the force of gravity outweighs the force of drag and the particles fall. As a result, clouds can develop unique tail-like shapes with unidirectional curves called fallstreaks. These fallstreaks consist of larger crystals with increasing mass that stretch out when the magnitude of the horizontal wind speed changes with height, a feature known as vertical wind shear. Layered cloud formations (cloud streets) are also prevalent and occur as stratified bands, forming parallel to the wind direction in unstable atmospheric fluid layers. Cloud streets result from processes of thermal convection in the presence of vertical wind shear (< <http://www.personal.psu.edu/users/s/p/spz104M41W>>) (Fig. 1.1a,b).

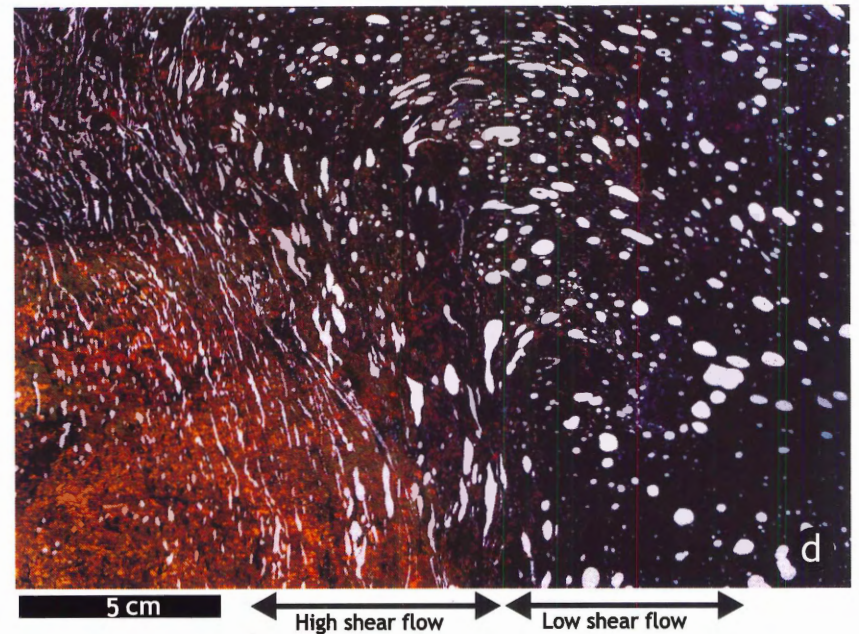
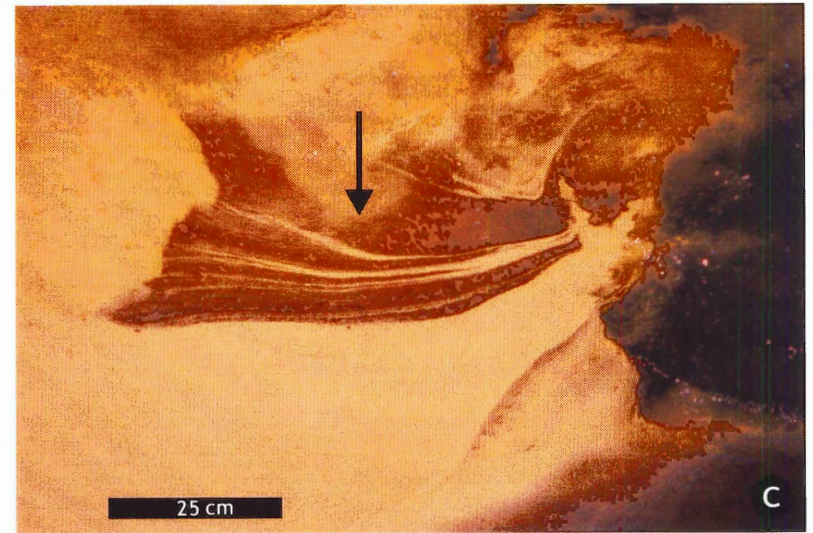
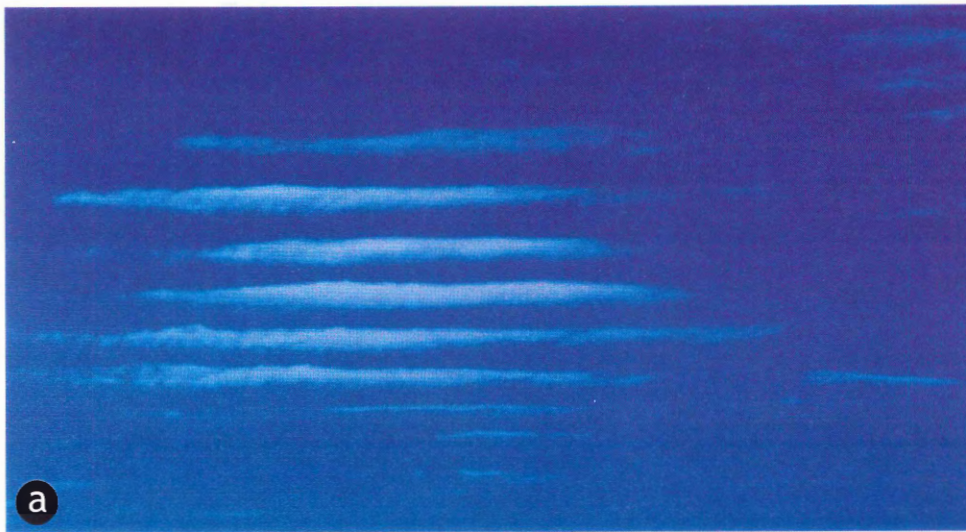


Figure 1.1: Non-geological streaks in natural fluid systems. (A) cloud streets (b) fall streaks (c) pollen particles accumulating near the shore of a lake through a complex formation of regular bands. The bands are moving in the direction of the arrow (d) foam particles

Streak patterns of accumulated foam or pollen particles on a stream surface are common banded features in regions of high velocity gradients. Fluid flow in the underlying liquid is responsible for their formation, although the factors that control the transfer of fluid motion from within the volume of fluid to the surface are poorly understood. These chaotic banded patterns are two-dimensional displays of complex structures produced on the surface of three-dimensional flowing systems (Flinders and Clemens 1996) (Fig. 1.1c,d).

Geological streaks

Geological streaks commonly occur in a variety of geological environments such as banding in obsidian lava flows, layering in mafic intrusions, and schlieren in granitoid rocks (Fig 1.2 a,b). Streaks in granitoid plutons may be the result of either homogenization or heterogenization processes (Clarke et al. 2000). In general, homogeneous materials can produce modal and textural variations (heterogeneities) as a result of physical processes (e.g., size sorting in shear flow). Heterogeneous materials may be mixed and assimilated (e.g. partial melting) to produce homogeneous materials. Streaks in granitoid plutons suggest dynamic environments during the final stages of crystallization. These structures appear as bands, layers, or thin laminae, otherwise referred to as schlieren.

1.2 Definitions

“Schlieren” (singular “schliere”) is a German word used in the early 1800’s by craftsmen to describe inhomogeneity in various substances, such as defects in glass



Figure 1.2: Geological streaks in granitoid rocks. (a) Alternating layers of felsic and mafic minerals showing reverse-graded bedding at Peggy's Cove. (b) Streaked out biotite-rich bands at St. Catherines River Bay.

disrupting its optical properties, and streaks of varying colors in cement as a product of incomplete mixing (Didier 1973). The term schlieren was first applied as a geological term by an Austrian geologist, (Reyer 1879, as cited by Didier 1973), to describe tabular bodies from 10 centimetres to several metres long, occurring in plutonic rocks. His studies on the orientation and distribution of these structures influenced the use of the term as it is described today. Schlieren have “the same general mineralogy as the plutonic rocks, but because of differences in mineral ratios they are darker or lighter; the boundaries with the rock tend to be transitional. Some schlieren are modified inclusions, others may be segregations of minerals” (American Geological Institute 1987). Irvine (1987) defined schlieren layering as “discontinuous layering characterized by thin, vaguely defined layers that inconspicuously appear and fade out.”

In this thesis, the term “schlieren” encompasses:

- (i) biotite bands occurring as tails on metasedimentary xenoliths;
- (ii) alternating bands of felsic and mafic material; and
- (iii) concentrations of biotite-rich laminae associated with clusters of megacrysts.

1.3 Schlieren in Granites

Mineral layering occurring as well-defined exposures are relatively rare features in granitic rocks. The formation of schlieren has intrigued many petrologists because the preservation of these structures can reveal information about the chemical and physical processes of formation, and can also provide information about the final stages of magma flow and solidification (Pitcher 1993).

When a crystallizing magma cools, it ultimately changes from 0% crystals ($\phi = 0$) to 100% crystals ($\phi = 100$) (Fig. 1.3). Magma is able to flow and behave as a liquid at $\phi < 55$; once the magma exceeds this degree of crystallinity, it reaches the rigidity percolation threshold (RPT) marking the liquid to solid transition (Vigneresse and Burg 2000). At $55 < \phi < 75$ %, the magma consists of a loose mush of crystals and interstitial liquid. Any structures that form may be preserved. At $\phi \geq 75$ %, the particle locking threshold (PLT), the magma consists of interlocking crystals and is no longer able to flow readily.

Some streaks of schlieren are flattened and pinched with tails of biotite that are spatially associated with metasedimentary xenoliths, whereas others consist of parallel layers that display differing mineralogies \pm mineral proportions \pm textures in which their lengths are greater than widths on the outcrop scale (Clarke et al. 2000). Table 1.1 summarizes previous work on schlieren and presents types of layering, a brief description and inferred processes.

1.4 Purpose and Objectives

Dynamic interaction between crystals and melt can form schlieren as primary features during the last stages of a crystallizing magma. The preservation of schlieren usually occurs in a narrow "window" during which flow structures are able to form when a crystallizing magma is a mush of crystals and liquid ($55 < \phi < 75$). The conditions necessary for their formation and preservation account for their relatively rare occurrence in granitic rocks.

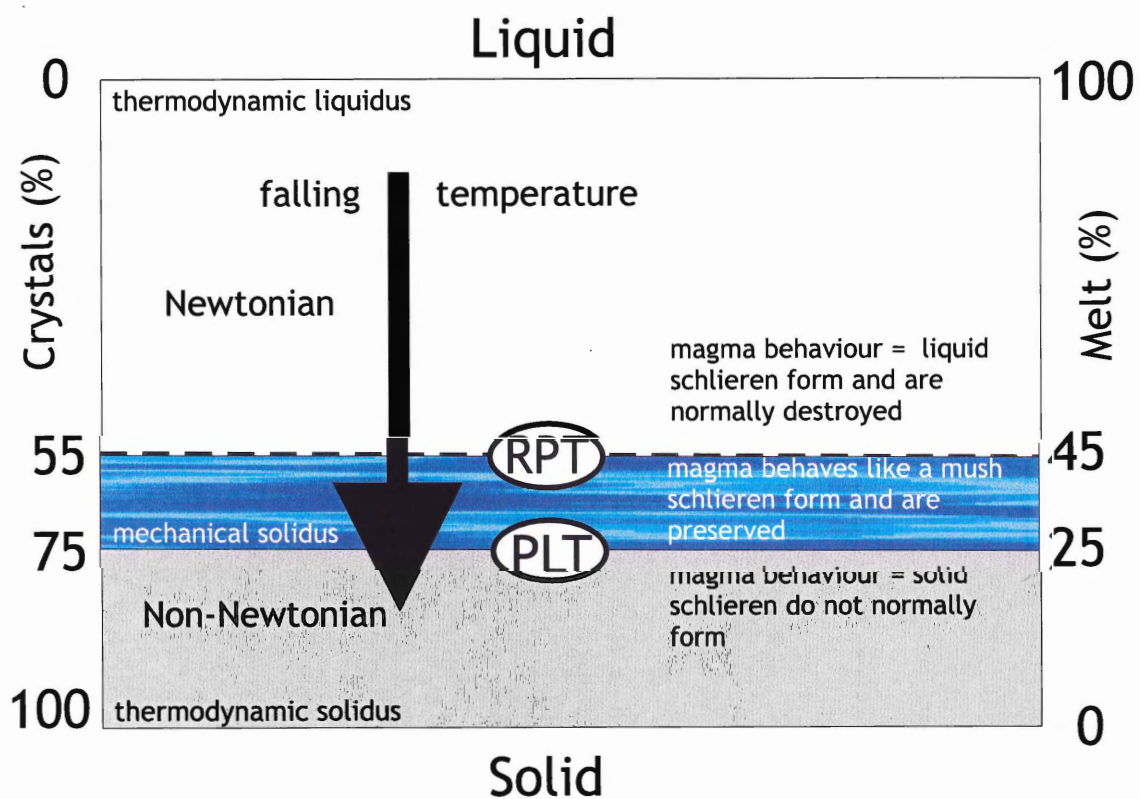


Figure 1.3 Liquid-solid diagram depicting the “window” that enables schlieren to form in a crystallizing magma (after Vigneresse and Burg 2000).

Table 1.1 Previous work on schlieren

TYPES OF LAYERS	REFERENCES	EXAMPLES	DEGREE OF CRYSTALLINITY % (Φ)	INFERRED PROCESS
melting and stretching of country rock xenoliths	Knopf 1918 Pabst 1928 Balk 1937 Dürr 1960 Gansser and Gyr 1964 Wells and Wooldridge 1931 Pitcher and Berger 1972 Link 1970 Flinders and Clemens 1996	Sierra Nevada, California Montagny, France Bergell Batholith Jersey, UK Main Donegal Granite Half Dome, Yosemite National Park, US Glen Fyne Intrusion, Scotland	$\Phi < 55 \%$	partial assimilation of xenoliths
graded layering (cumulates) reversely-graded layers; sheet-like bodies; normally-graded layers	Harry and Emeleus 1960 Hess 1960 Wahrhaftig 1979 Irvine 1987 Parsons and Becker 1987 Berry and Flint 1988 Clarke and Clarke 1998	S.W. Greenland Stillwater Complex, Montana Topaz Lake, US Muskox Intrusion, NWT Klokken, S. Greenland S. Australia Chebucto Head, South Mountain Batholith, NS	$55 \% < \Phi < 75 \%$	repeated magma injection and gravity/crystal settling

Table 1.1 continued. Previous work on schlieren

TYPES OF LAYERS	REFERENCES	EXAMPLES	DEGREE OF CRYSTALLINITY % (Φ)	INFERRED PROCESS
thin biotite laminae with associated K-fsp megacrysts	Bagnold 1954 Wilshire 1969 Barrière 1981 Abbott 1989 Pitcher 1993 Weinberg et al. 2000	(experimental work) Twin Lakes, Colorado, US Ploumanac'h massif, France South Mountain Batholith, NS Donegal, NW Ireland Travares Pluton, NE Brazil	55 % < Φ < 75 %	size sorting in shear flow
symmetric, fairly straight bands of felsic and mafic minerals	Maksaev 1986 Clarke et al. 2000 Pitcher and Berger 1972	Port Mouton Pluton, NS Port Mouton Pluton, NS Main Donegal Granite, NW Ireland	$\Phi > 75$ %	late magmatic deformation and segregation

The general purpose of this thesis is to investigate four areas of contrasting schlieren development in granitoid rocks of southern Nova Scotia, and to interpret the physical evidence in terms of their processes of formation. In detail, the research objectives of this thesis include:

- (i) description of field relations and physical characteristics of schlieren through field mapping taking into account the local and regional foliation;
- (ii) description of thin sections to determine any evidence of deformation;
- (iii) analysis of foliation images from Peggy's Cove and Jackies Island samples to determine preferred orientations of feldspar megacrysts;
- (iv) analysis of mineral chemistry to determine origin of biotite tails on streaked-out enclaves at St. Catherines River Bay;
- (v) comparison of schlieren in granites with analogues in natural flowing systems, e.g. atmosphere (clouds) and water surfaces (pollen and foam particles); and
- (vi) interpretation of physical and chemical processes, as well as analogues to determine the origin of schlieren in granitoids of southern Nova Scotia.

1.5 Scope of Study

Two areas in the South Mountain Batholith, Prospect and Peggy's Cove, show well-preserved schlieren bands and graded layering. Two areas in the Port Mouton Pluton, Jackies Island, and St. Catherines River Bay, have symmetric banding and irregular schlieren bands, respectively. The focus of this study is to incorporate all four areas into a study aimed at inferring the physical processes responsible for schlieren formation at each location (Fig. 1.4). Field mapping and petrographic observation of

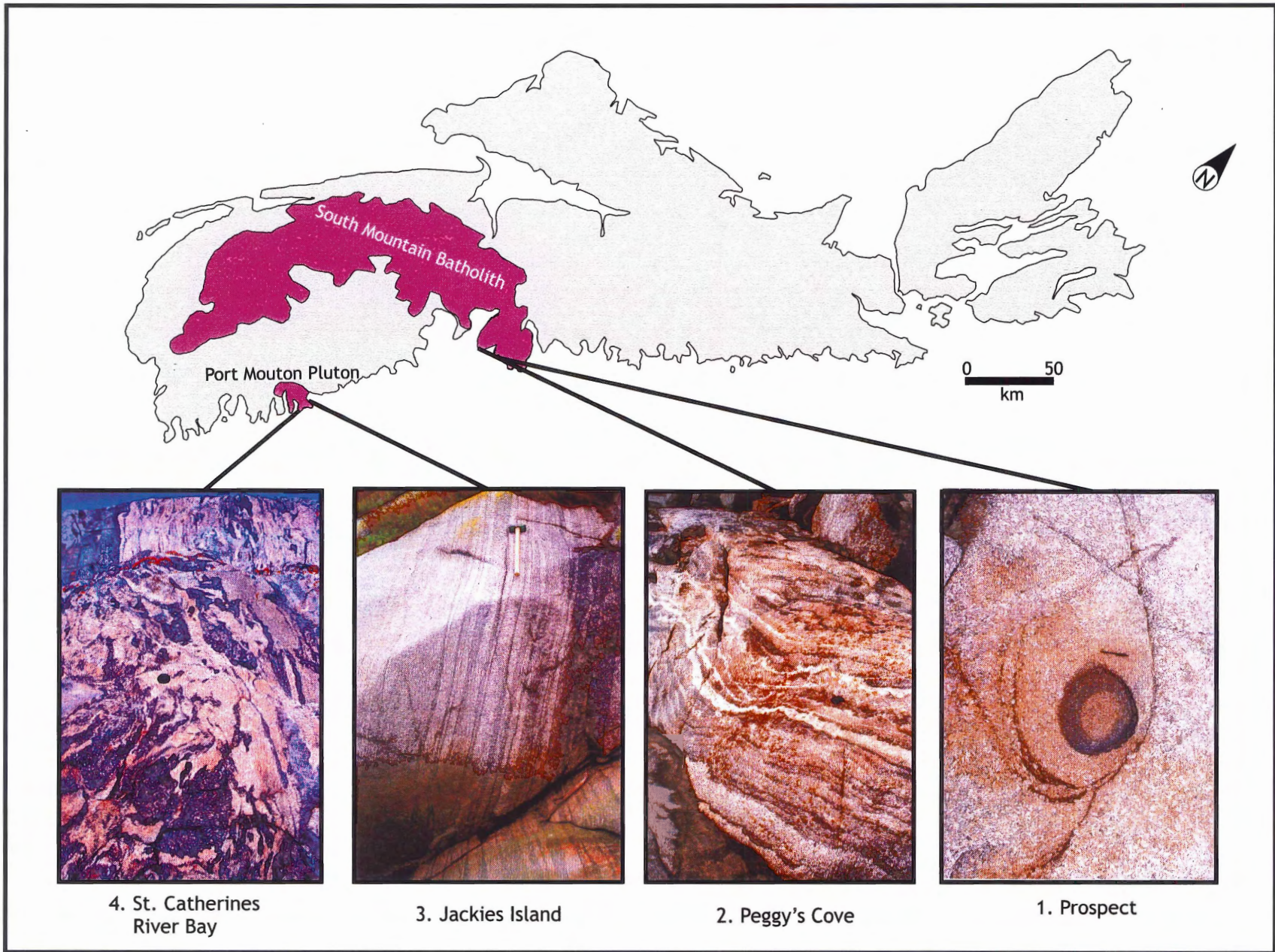


Figure 1.4 Schlieren study localities in the South Mountain Batholith and Port Mouton Pluton of southwestern Nova Scotia.

samples were completed for all study areas. Analytical methods involved foliation image analyses for samples taken from Peggy's Cove and Jackies Island; and chemical analyses of major element oxides using the electron microprobe for samples from St. Catherines River Bay. Extensive literature research, and comparison with previous works helped to analyze the Prospect study area. Neither experimental work nor mathematical modelling form part of this thesis.

1.6 Thesis Organization

Chapter 2 contains regional geology, and the geological setting of the South Mountain Batholith and Port Mouton Pluton. A detailed description of the field localities includes detailed maps, photos, sketches, and a summary comparison table. Chapter 3 discusses the methodology, including field and analytical methods. Chapter 4 includes detailed petrographic descriptions of the study areas, foliation image analysis for Peggy's Cove and Jackies Island, and a biotite composition study for St. Catherines River Bay. Chapter 5 includes a discussion of physical processes in crystallizing plutons, key field and lab evidence, working hypotheses, and inferred physical processes for each locality. Chapter 6 presents the conclusions of this study.

CHAPTER 2: FIELD RELATIONS

2.1 Regional Geological Setting

The Meguma Zone of southern Nova Scotia is the easternmost lithotectonic terrane of the Canadian Appalachians, characterized by Cambro-Ordovician flyschoid metasedimentary rocks of the Meguma Group. The Meguma Group is divided into two formations: (1) the lower, metapsammitic Goldenville Formation; and (2) the upper, metapelitic Halifax Formation (Schenk, 1995; Fig. 2.1 and inset). The Avalon Zone in the north is separated from the Meguma Zone by the Cobequid-Chedabucto fault. The Meguma Group was metamorphosed during the Acadian Orogeny between 410 and 390 Ma when it was accreted to the Avalon Zone. During the final stages of the Acadian orogeny, more than 25 peraluminous granitoid plutons intruded the Meguma crust in the Late Devonian, at ca. 372 Ma. (Clarke et al. 1997). Clarke et al. (1997) subdivided the granitoid plutons into the Central and Peripheral plutons based on spatial and compositional characteristics that required different petrogenetic interpretations.

2.2 Geology of the South Mountain Batholith

The South Mountain Batholith (SMB) outcrops over an area of 7500 km² in southern Nova Scotia and is the most voluminous central granitic pluton in the Appalachian orogen. McKenzie et al. (1974) estimated the batholith to underly one-third of western Nova Scotia with dimensions of 180 km in length and 50 km in width. The batholith has a three-dimensional “mushroom” shape defined by negative gravity anomalies with an average thickness of 5 km along the margins reaching local thicknesses of 20-25 km (New Ross-Vaughan Complex). The SMB has an estimated age

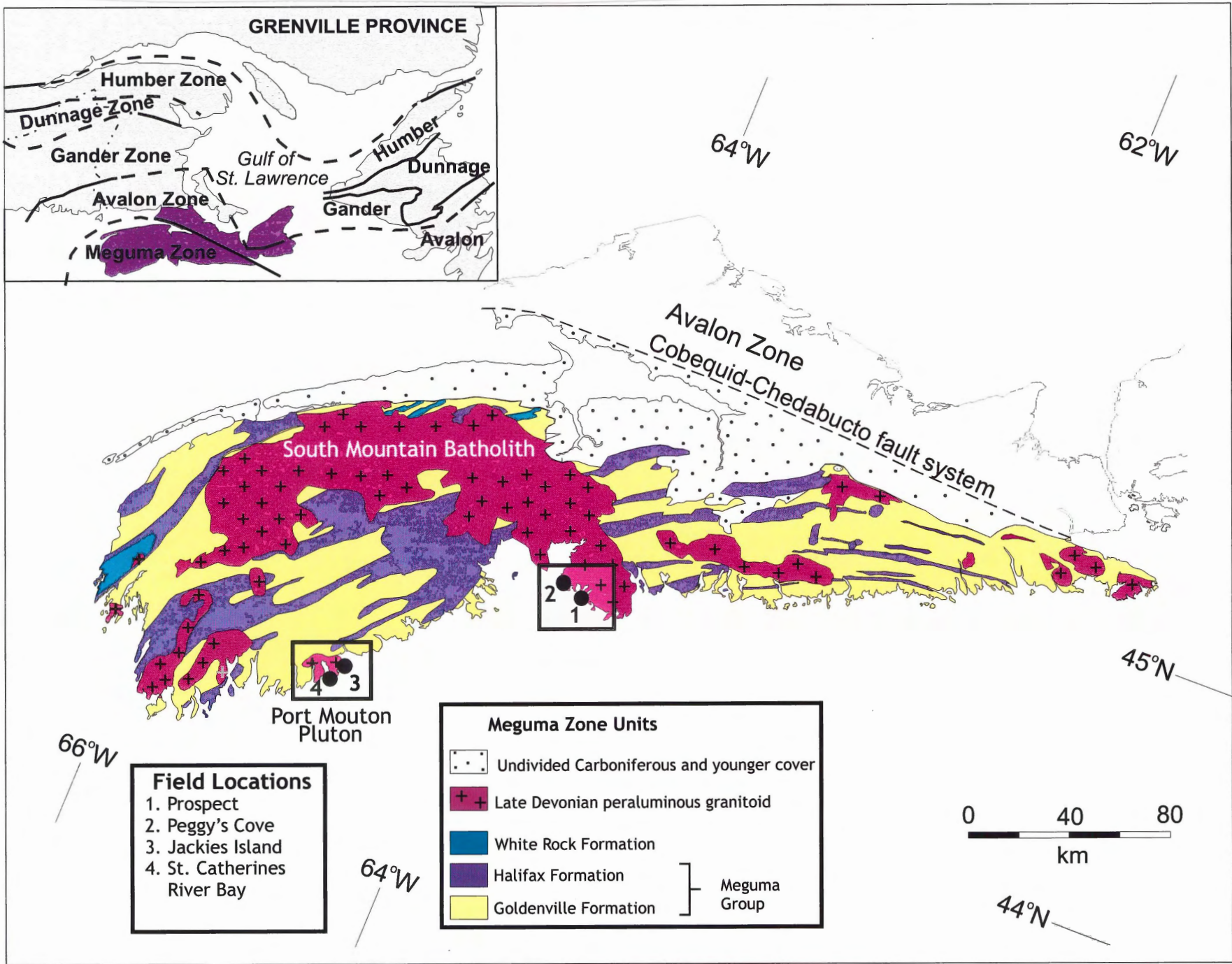


Figure 2.1. Location map for study areas in the South Mountain Batholith and the Port Mouton Pluton.

of 372 ± 3 Ma (Clarke et al 1997) and represents a massive, peraluminous batholith dominated by granodiorite and monzogranite (Clarke and Muecke 1985). McDonald et al. (1992) recognized two stages of intrusion: Stage I an earlier stage dominated by granodiorite, and Stage II, a later stage dominated by monzogranites.

Two locations in the SMB, Prospect and Peggy's Cove, show well-preserved localized development of biotite schlieren and alternating mafic and felsic layering, respectively.

2.3 Prospect

Prospect is located approximately 25 km southwest of Halifax in the southeastern part of the SMB. The host rock is a flow foliated, porphyritic, biotite monzogranite with megacrysts of K-feldspar (less than 10 cm) and numerous ellipsoidal autoliths with diameters generally less than 20 cm. The Atlantic Ocean obscures the contact with the Meguma Group, but magnetic data suggest the contact is approximately 5 km offshore (Fader and Miller 2001). The large abundance of xenoliths in the area provides further evidence for the proximity of the contact. The host rock has a weak regional flow foliation defined by a subvertical alignment of K-feldspar megacrysts that generally strike $290-345^\circ$ (Fig. 2.2).

The study area consists of a localized assemblage of long biotite wispy schlieren and isolated layered features spanning an area 40 m x 15 m along the coast above the high tide line. Figures 2.3 a-f on the location map correspond to Figures 2.4 a-f, respectively. The schlieren layers consist of high concentrations of biotite appearing as foliated biotite bands in the host granite. The biotite grains are euhedral and range in size

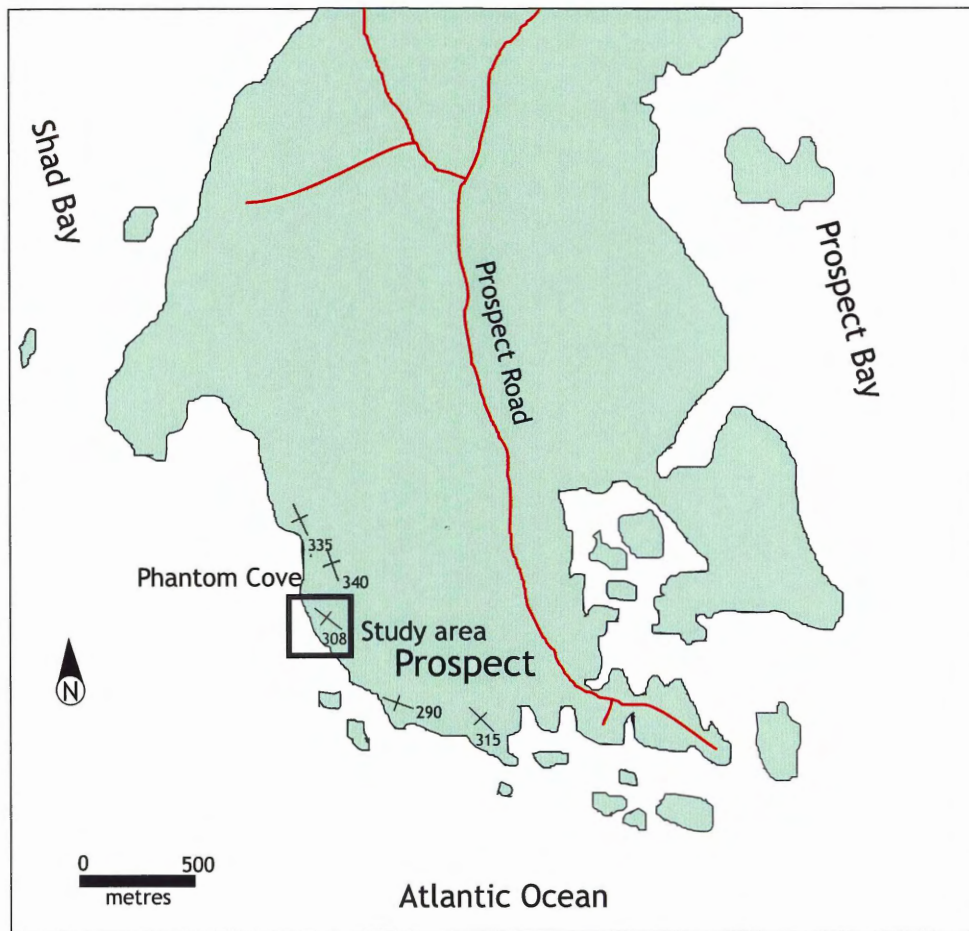


Figure 2.2. Location map of the Prospect area showing attitude of regional flow foliation.

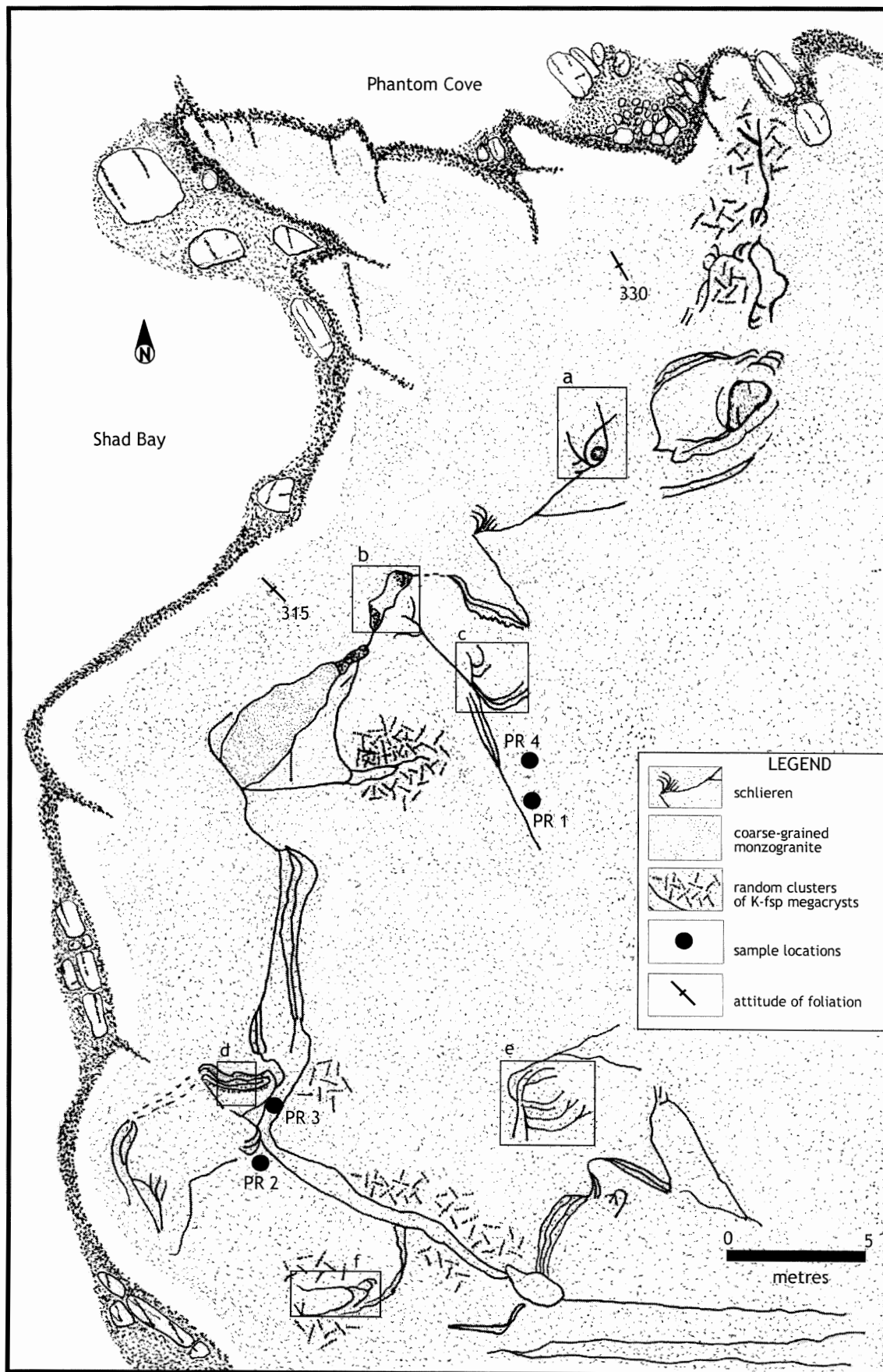


Figure 2.3. An enlarged map of the Prospect study area. The boxes marked (a) to (f) correspond to the photographs in Figure 2.4 (a) to (f).

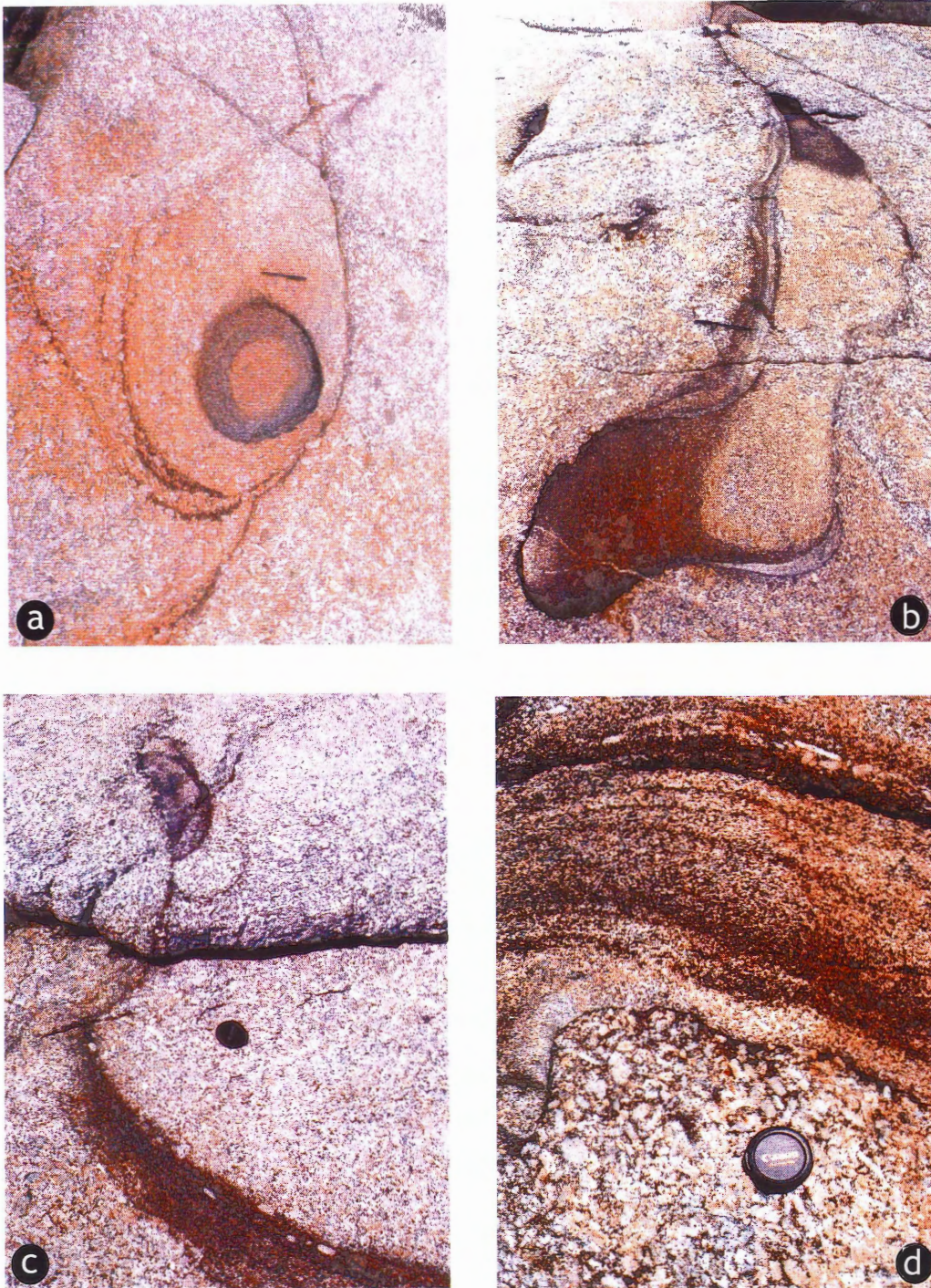


Figure 2.4. (a,b) Biotite-rimmed margins coarsening inwards surrounded by random clusters K-feldspar phenocrysts. (c) Aligned K-feldspar phenocrysts with (010) planes parallel to biotite layering. (d) Biotite layers bordered by a cluster of K-feldspar megacrysts.

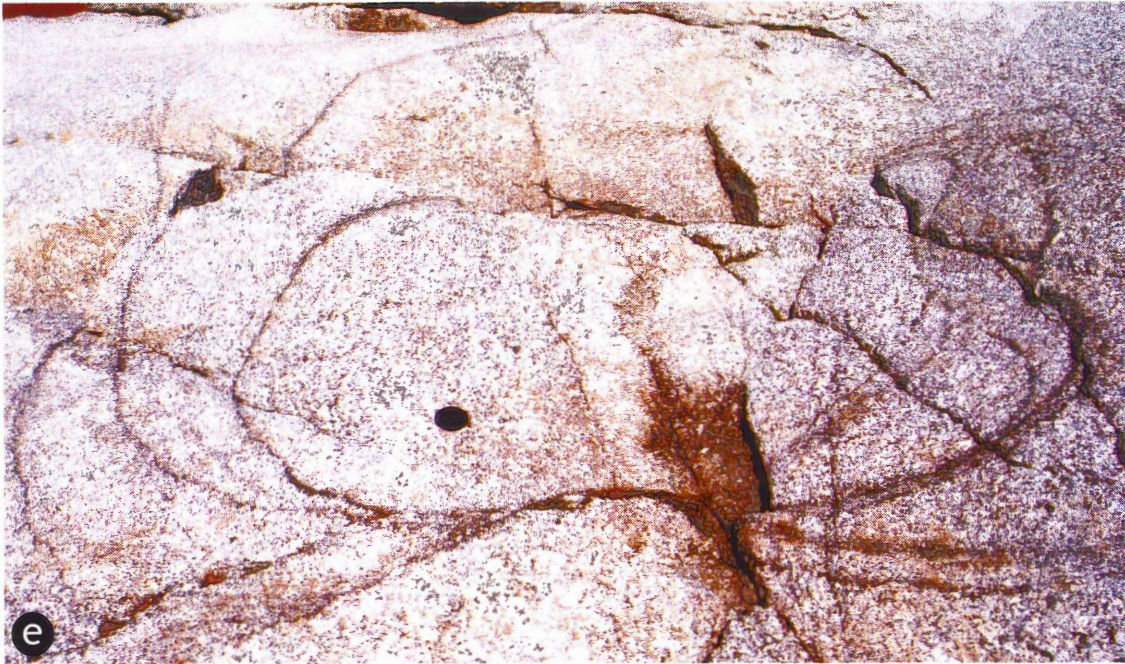


Figure 2.4(e) Eccentric rings of biotite branching and truncating other layers.
(f) Semi-circular structure with wispy biotite margins.

from 2-5 mm; the euhedral K-feldspar phenocrysts range in size from 1-10 cm. The bands are asymmetrical with varying widths ranging from 1-5 cm. The bands tend to be curved, wispy, branched, and parallel with varying sharp and gradational boundaries. Some branching schlieren layers truncate previously formed layers or pinch out, and disappear. Figure 2.3 shows that the strikes of the schlieren are widely variable, and three-dimensional exposures show that the schlieren generally dip subvertically.

Some structures in the study area demonstrate fine-grained biotite layered margins with crystals coarsening inwards, surrounded by random clusters of coarser-grained K-feldspar megacrysts (Fig. 2.4a). Figure 2.4b shows an elongated, curved structure measuring 1.5 m long and 30 cm wide. High concentrations of biotite occur on the rims at each end, and the structure pinches in the middle. The areas highly concentrated in biotite are fine-grained at the rim and coarsen inwards. Random clusters of K-feldspar megacrysts also surround this structure. Another common feature is the presence of aligned K-feldspar phenocrysts with their (010) faces parallel to biotite layering (Fig. 2.4c) and large accumulations of random clustered K-feldspar megacrysts bordering the biotite parallel layers (Fig. 2.4d). Biotite-rich layers also occur as eccentric rings in which some layers branch out or truncate others (Figs.2.4e,f).

2.4 Peggy's Cove

The Peggy's Cove study area is located in the eastern part of the SMB approximately 45 km southwest of Halifax and 1 km northwest of the Peggy's Cove lighthouse. The host rock consists of a porphyritic, biotite monzogranite with large megacrysts of K-feldspar; abundant clusters of autoliths, and xenoliths with preserved

bedding; miarolitic cavities with large quartz, feldspar, and tourmaline crystals; and many crosscutting aplite dykes (Fig. 2.5). The Atlantic Ocean obscures the contact with the Meguma Group, but magnetic data suggest the contact lies 1 km offshore (Fader and Miller 2001).

The study area consists of a localized section of well-preserved subhorizontal, asymmetrical, mafic and felsic layering dipping 20 degrees to the north restricted to an area measuring 30 m x 10 m along the coastline (Figs. 2.5, 2.6). The layered section consists of ~25 parallel, reversely-graded layers showing finer biotite-rich bases grading into coarser feldspar-rich tops. The biotite layers measure 0.5 cm- 6.0 cm in thickness where they form sharp boundaries with underlying feldspar-rich layers, but where they are gradational in an upwards direction, exact widths are difficult to determine. Feldspar-rich layers range in widths from 1-6 cm. Several distinctive feldspar layers show cusped margins against overlying biotite-rich layers. Feldspar layers range in width from 3–7 cm (Figs. 2.7a,b). In one area, six layers appear to have deformed together into concentric folds measuring 35 cm in width (Fig. 2.7c).

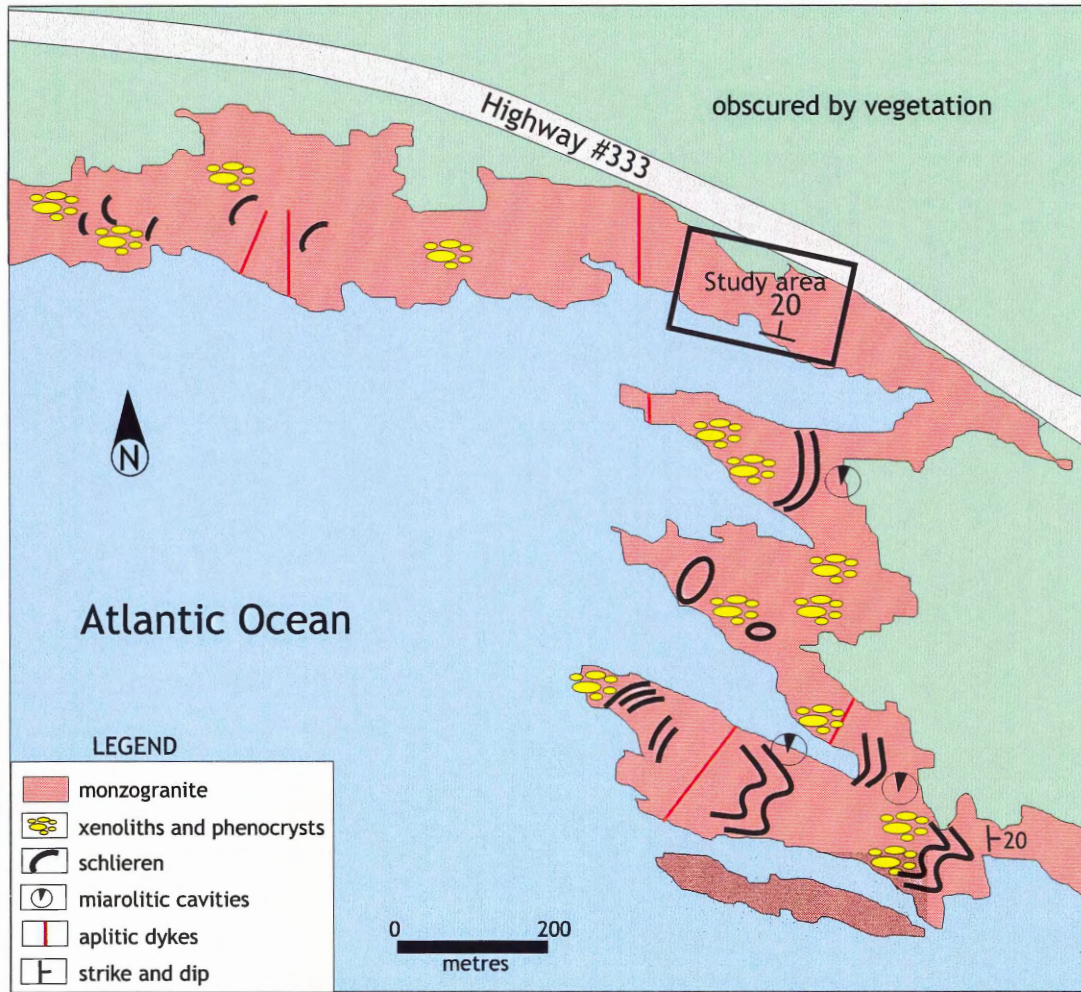


Figure 2.5 Location map for Peggy's Cove study area.

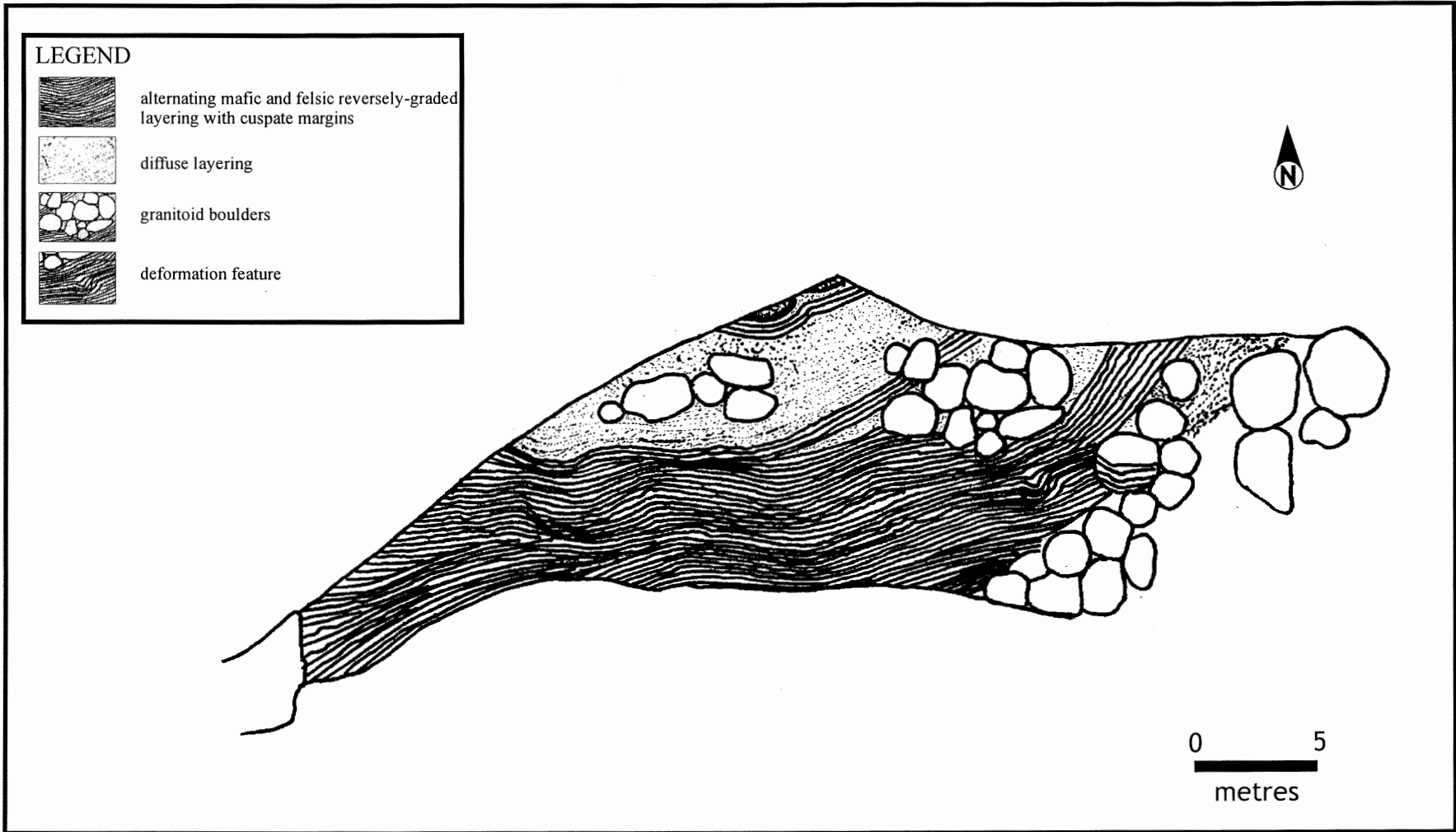


Figure 2.6 Plan view of the enlarged study area at Peggy's Cove.

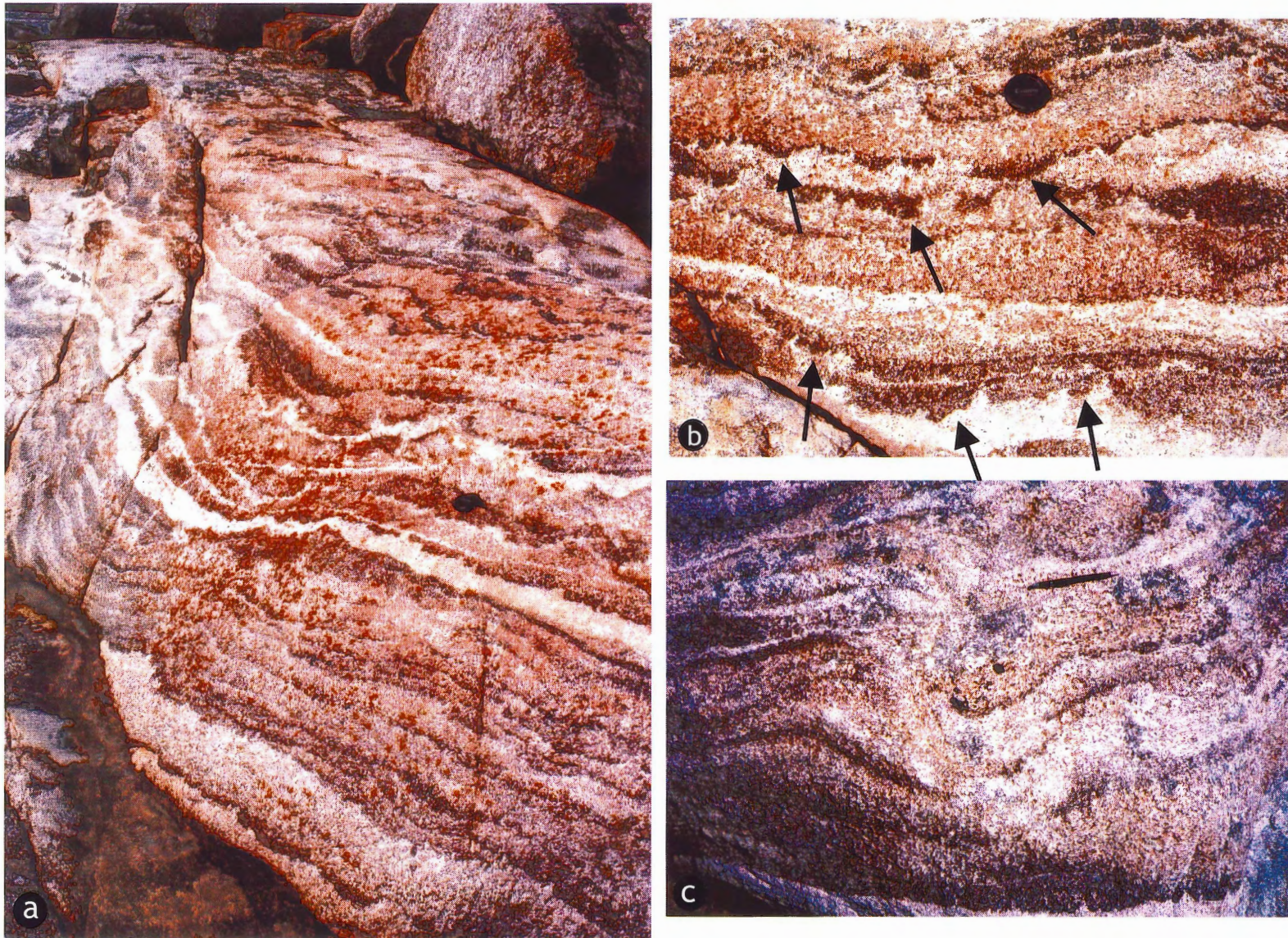


Figure 2.7 (a) Study area at Peggy's Cove shows alternating reversely-graded layers with mafic bases and felsic tops with cusped margins. (b) An enlarged view of the reversely-graded layering with cusped margins marked by arrows. (c). An area that appears to have been deformed into folds.

2.5 Geology of the Port Mouton Pluton

The Port Mouton Pluton (PMP), a smaller peripheral pluton (16 x 10 km) in southwestern Nova Scotia, represents a late or post-regional-tectonic peraluminous granitoid pluton. The PMP age estimate of 373 ± 1 Ma is similar to other granitoid plutons in the Meguma Zone. Clarke et al. (2000) noted that it has several characteristics that are distinctive compared to other plutons in the Meguma Zone: (i) it is in close contact with migmatized metasedimentary rocks of the Meguma Group; (ii) it shows a wide range of lithological and chemical variations; (iii) it shows evidence for magma mingling with Late Devonian mafic magmas; (iv) it shows the most heterogeneous and complex internal intrusive relationships (Woodend-Douma 1988); and (v) it contains the highest proportion of pegmatites. It also has physical features that are anomalous, such as symmetrical banding at Jackies Island and discontinuous biotite schlieren at St. Catherines River Bay (Fig. 2.8).

2.6 Jackies Island

Jackies Island is a part of the Port Mouton Pluton, located approximately 1 km offshore from the small village of Southwest Port Mouton (Fig. 2.8). The outcrop is exposed around the island circumference above the high tide line with the interior of the island covered by vegetation. The host rock at this location is a well-foliated medium-grained, equigranular, biotite monzogranite. The foliation in the host rock is clearly defined, on the outcrop scale, by parallel bands of concentrated biotite (0.5-2 cm wide). An adjacent island, Thrum Cap, exhibits similar lithology and shows a weak to strong foliation from the south to north end, respectively. The foliated host rock has an average

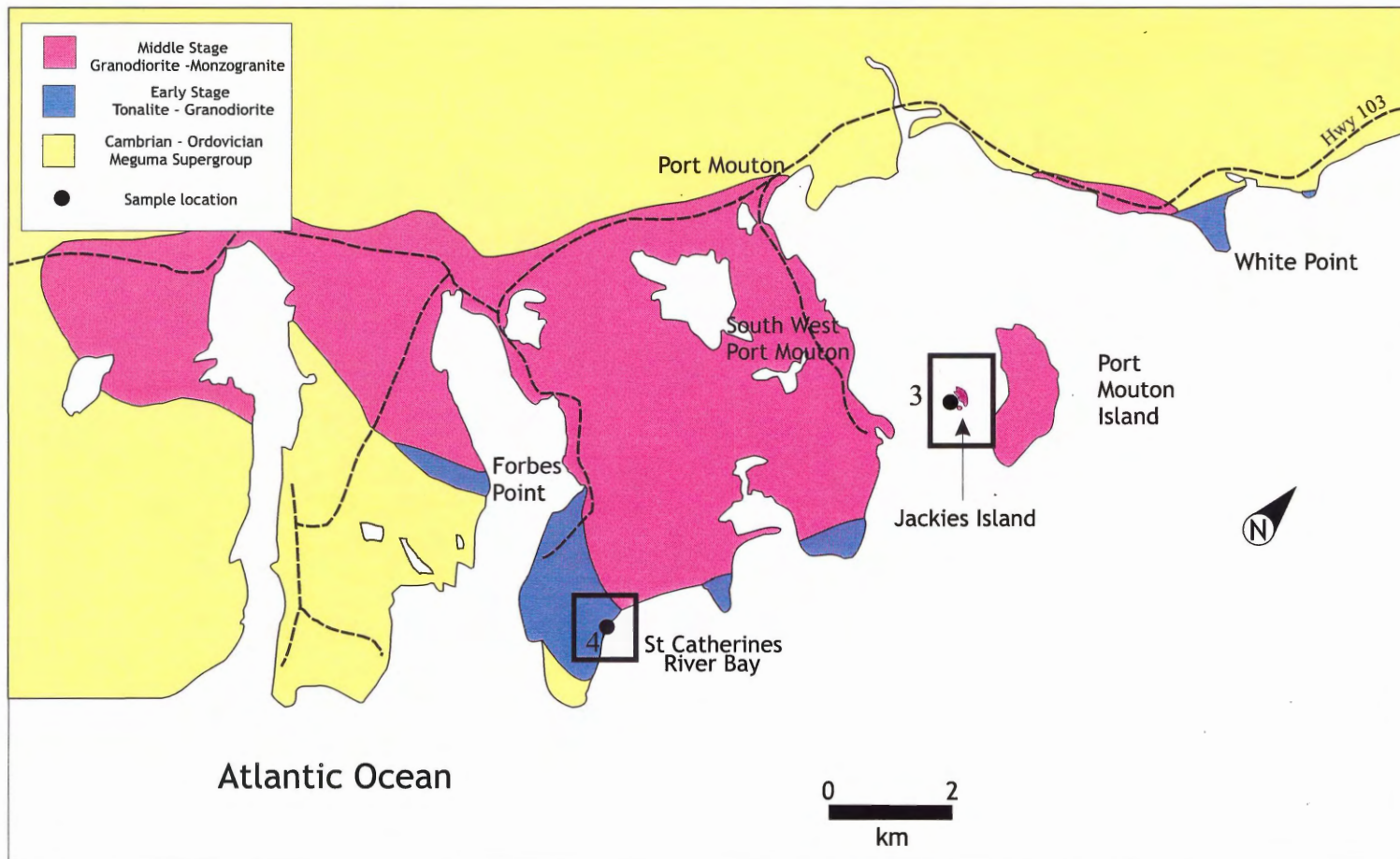


Figure 2.8 Simplified map of the Port Mouton Pluton showing the two study areas: (3) Jackies Island and (4) St Catherin es River Bay.

strike of 025 degrees northeast (Fig. 2.9). There are no observed contacts with the Meguma Group and xenoliths are absent.

The study location defines an area of strong banding and strong foliation that is parallel, symmetrical, and straight, with alternating mafic and felsic bands restricted to a zone about 10 metres wide. The bands are subvertical, and in places, the bands branch or join adjacent layers (Figs. 2.10 c,d and 2.11). Individual mafic layers tend to randomly pinch and swell along strike. Both the felsic and mafic layers range in widths from 0.5-15 cm. The areas adjacent to the strong banding and strong foliation grade into zones of weak banding, then into zones of no banding delimited by a strong foliation of aligned of lenticular aggregates of biotite (Fig. 2.10 a,b).

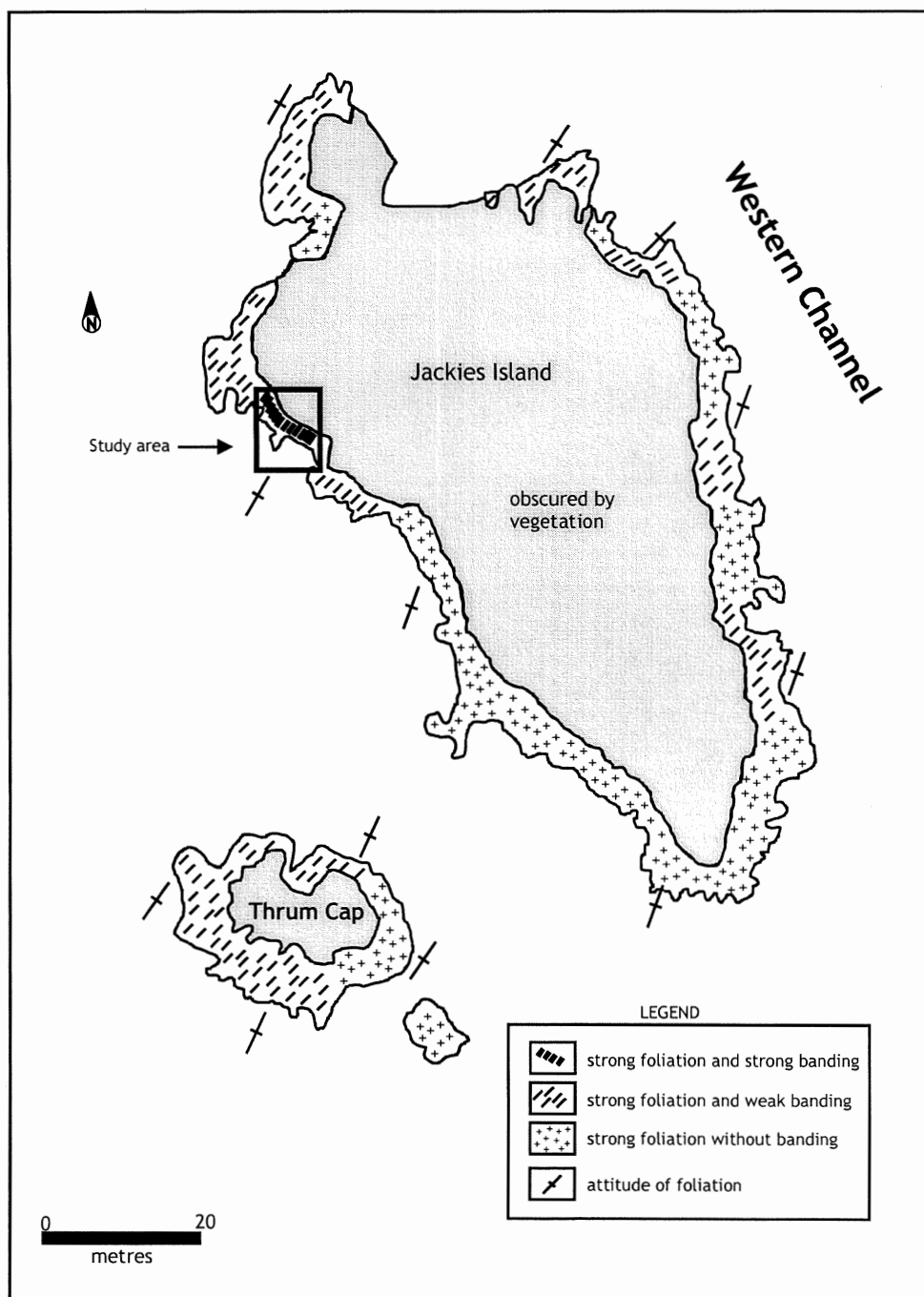


Figure 2.9 Location map of the study area on Jackies Island showing distribution of foliation and banding as well as attitude of the foliation.

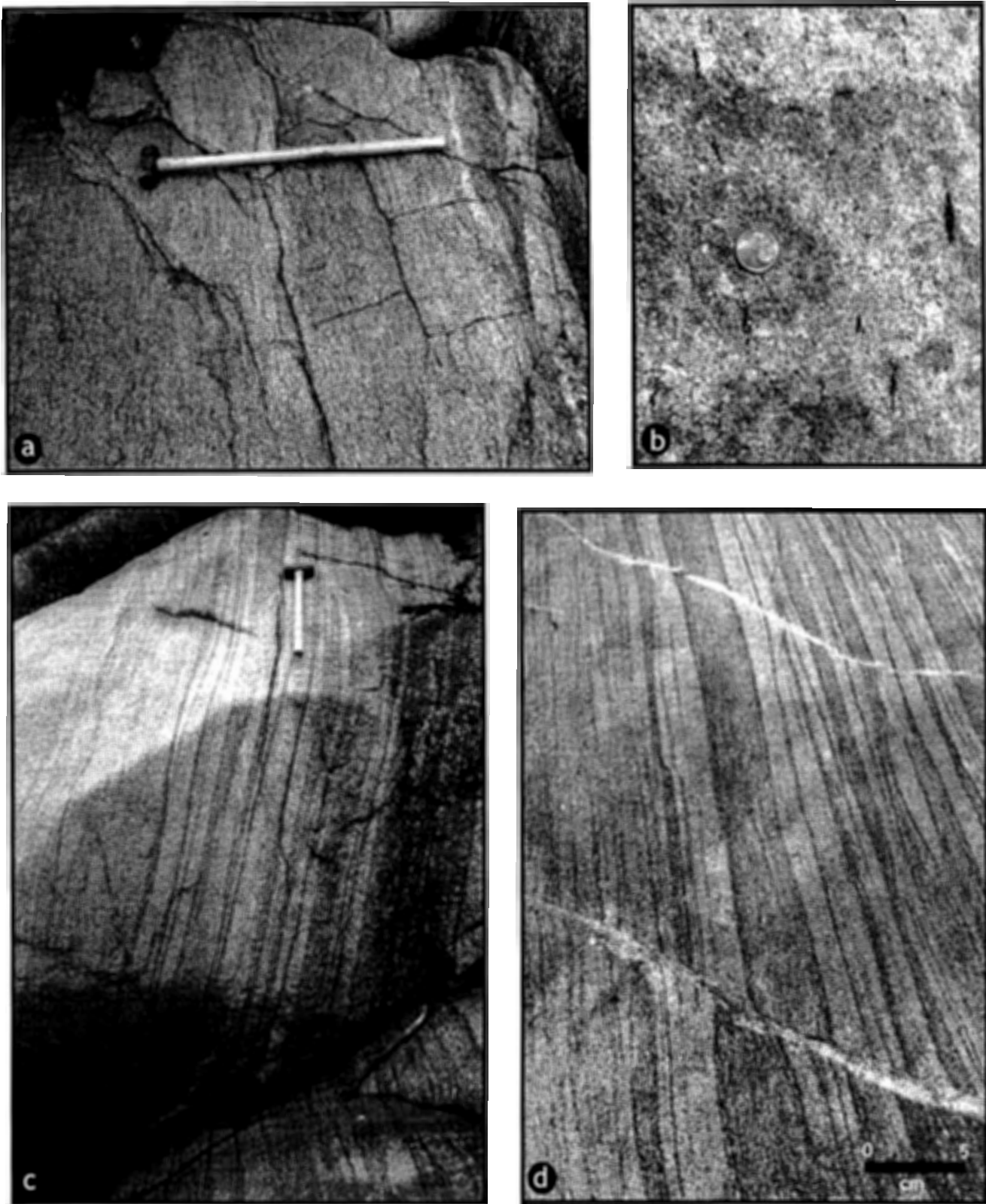


Figure 2.10. (a) Foliation located 20 metres from the study area defined by strong foliation and weak banding. (b) Enlarged photo of strong foliation defined by lenticular aggregates of biotite. (c) Subvertical schlieren banding on Jackies Island showing strong foliation and strong banding. (d) Enlarged photo of the banding showing granitoid veinlets offsetting several bands. The length of the hammer handle in photos (a) and (c) is 75 cm.



Figure 2.11. Sketch of schlieren at Jackies Island. The left side of the sketch shows symmetrical schlieren. The right side of the sketch shows a = pinch-outs and b = bifurcation.

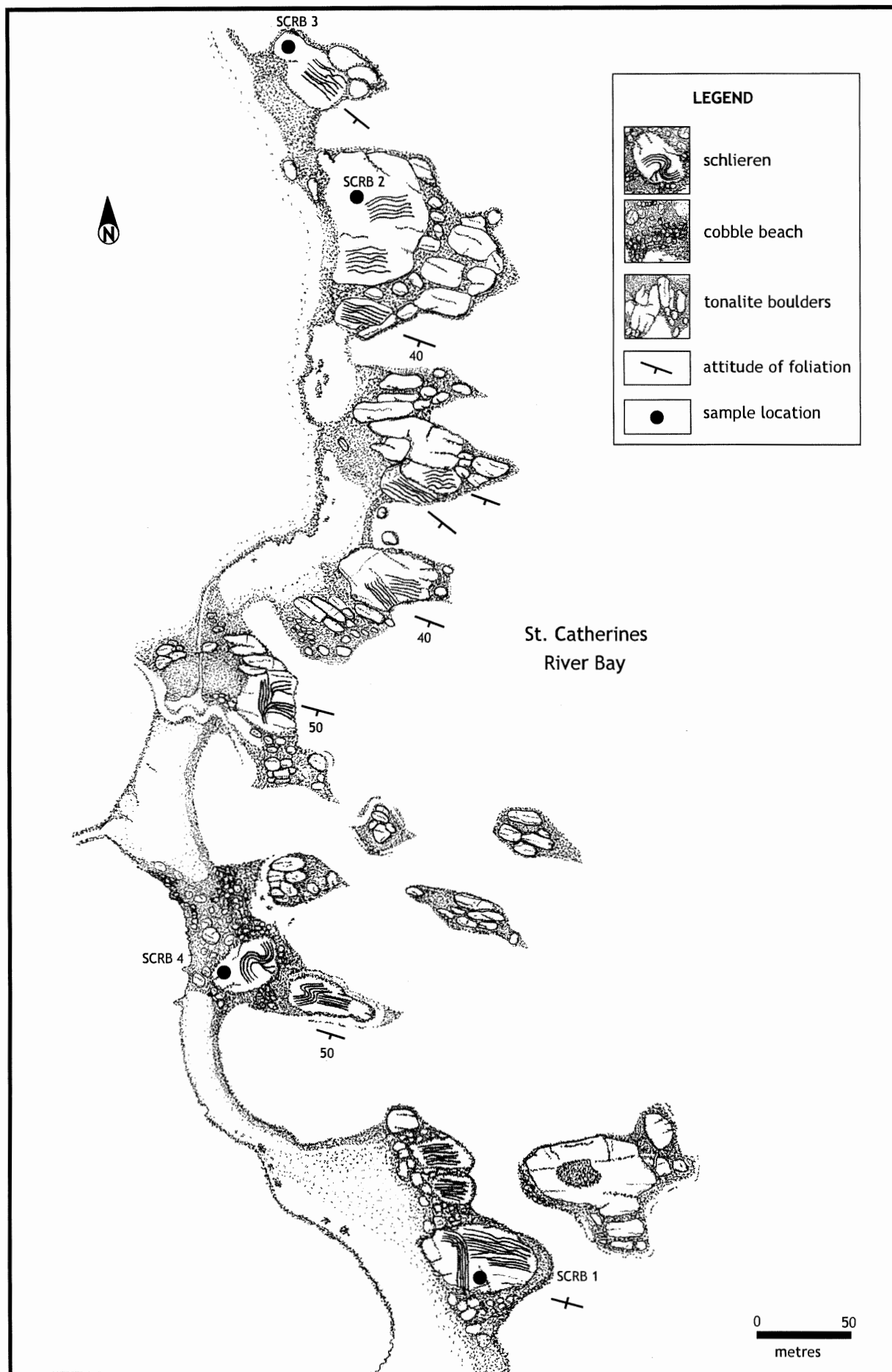


Figure 2.12. Schematic location map for St. Catherines River Bay.



Figure 2.13. Photos of schlieren at St Catherines River Bay. (a) Concentrated accumulation of metasedimentary xenoliths with schlieren bands. (b) Enlarged photo of schlieren trailing off metasedimentary xenoliths.

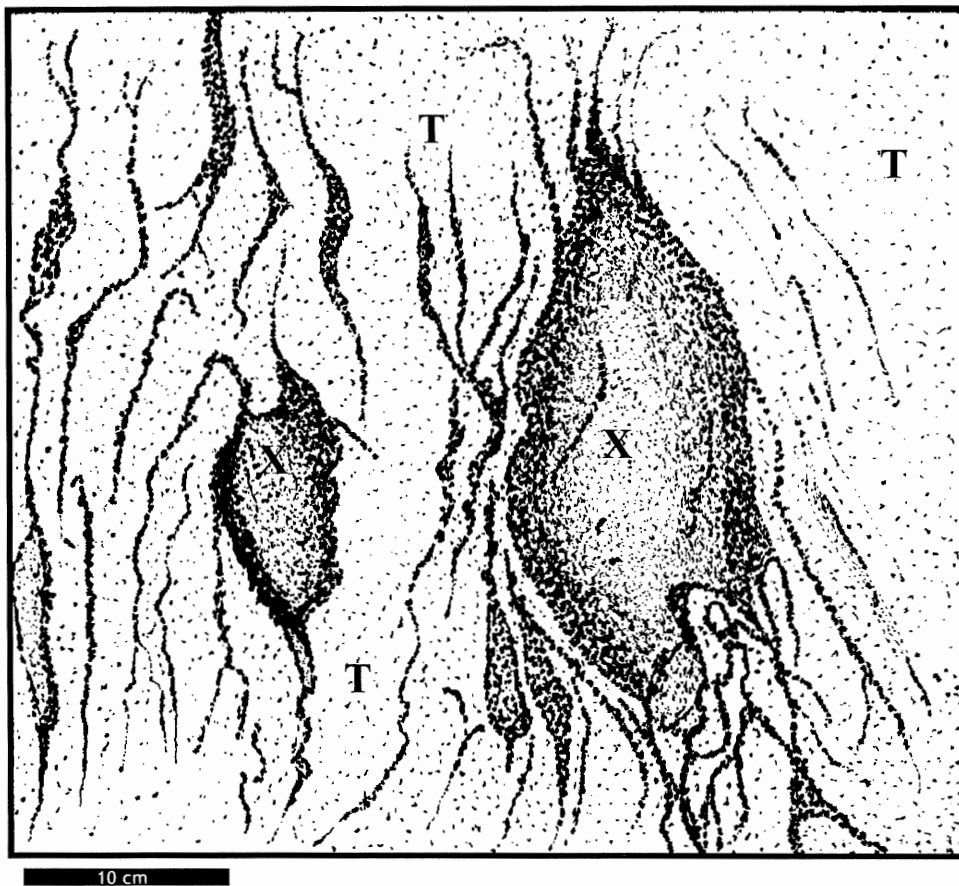


Figure 2.14 Sketch showing detail of biotite schlieren trailing off xenoliths (X) of metasedimentary country rock into the host tonalite (T).

Table 2.1 A summary table of schlieren characteristics of all the study areas.

Feature	Prospect	Peggy's Cove	Jackies Island	St. Catherines River Bay
Distance to Meguma contact	5 km	1 km	unknown	unknown
Host rocks	monzogranite	monzogranite	biotite monzogranite	biotite tonalite
Areal extent of schlieren	40 m x 15 m	30 m x 10 m	10 m x 3 km	600 m x 100 m
Schlieren composition	biotite streaks in monzogranite host	alternating mafic and felsic layers	alternating mafic and felsic layers	biotite streaks in tonalitic host
Grain size / grain shape	euhedral biotite 2-5 mm euhedral K-fsp 1-10 cm	euhedral biotite 0.5-2 mm euhedral K-fsp 0.5-5 mm	subhedral biotite 0.5-1.5 mm fsp, qz, muscovite equigranular with biotite	subhedral biotite 1-3 mm plag, qz, 0.5-5 mm, muscovite 0.5-3 mm
Band widths	1-5 cm	0.5-6 cm	0.5-30 cm	0.5-40 cm
Schlieren symmetry	asymmetrical	asymmetrical	symmetrical	asymmetrical
Regularity	irregular and wavy bands	regular curved layers	regular straight bands	irregular and wavy bands
Schlieren attitude	random strikes and dips	strike 110 dip 20 degrees N	strike 020 dip subvertical	strike 110-130
Parallel/anastomosing	anastomosing	parallel	parallel/anastomosing	anastomosing
Foliation / lineation	anomalous with local foliation	anomalous	well foliated	well foliated
Presence of xenoliths	abundant	abundant	none	abundant
Other	associated feldspar clusters	associated feldspar clusters	zones of adjacent banding and foliation	spatially associated with xenolith slab swarm to SE

2.7 St. Catherines River Bay

St. Catherines River Bay forms a part of the Port Mouton Pluton located at the southern end of the Kejimikujik Seaside Adjunct. The host rock is a moderately well-foliated, biotite-rich tonalite with an abundance of Meguma Group metasedimentary xenoliths. The area consists of highly concentrated biotite schlieren that span an approximate distance of 600 m x 100 m (Fig. 2.12) and appear to be spatially related to a swarm of rectangular xenolith blocks 300 metres to the southeast. The biotite schlieren strike 110-130° in a similar orientation to the rectangular xenolith blocks, an orientation that is perpendicular to the regional strike of the Meguma Group. Metasedimentary xenoliths in the study area tend to have ellipsoidal shapes with biotite-rich rims that appear drawn out into biotite schlieren. The schlieren are characterized by thin wisps of biotite laminae that range in widths from 0.5-10 cm with average lengths of 10- 50 cm (Figs. 2.13a,b and 2.14).

2.8 Summary

Table 2.1 presents a summary of schlieren characteristics for all the study locations. Field observations focused on the spatial relationship to the Meguma Group, regional and local foliation trends and, specifically, physical features of schlieren on the mesoscopic scale.

CHAPTER 3: METHODOLOGY

3.1 Introduction

A variety of field and laboratory methods was used to study the characteristics of schlieren in granites from four areas in southern Nova Scotia. Study locations at Prospect and Peggy's Cove involved detailed mapping using a grid method, selective sampling, photography, thin section preparation, and petrographic description. Jackies Island and St. Catherines River Bay involved the use of topographic maps (1:50 000) and enlarged air photos to construct maps of the study areas, selective sampling, detailed sketches and photography, thin section preparation, and petrographic description. Samples from St. Catherines River Bay were cut and prepared as polished thin sections and analyzed using the electron microprobe. Image analysis was used to quantify preferred orientations of minerals in thin sections from Peggy's Cove and Jackies Island study locations.

3.2 Field Methods

3.2.1 *Field Mapping*

Detailed field mapping at Prospect and Peggy's Cove required a grid system (measuring off a baseline) to construct a map for each study location. At Prospect, we marked out a 5-metre grid (interpolating between the gridlines) to measure and sketch schlieren features. Detailed maps of the Prospect and Peggy's Cove study areas were sketched from maps constructed in the field. Location maps for both areas were adapted from topographic maps (1:50 000) and airphotos also using CorelDRAW 9. Airphotos of the prospect area were used to map the regional flow foliation defined by alignments of K-feldspar megacrysts. Airphotos at Peggy's Cove were used to mark features located outside the detailed study area such as isolated schlieren structures, aplite dykes, and xenolith clusters. Maps for Jackies Island and St.

Catherines River Bay were constructed in CorelDRAW 9 using 1:50 000 scale topographic maps.

3.2.2 Sampling

A total of fifteen samples were taken at the study localities, including samples of the host granite, as well as the mafic and felsic banding where they were best observed in three-dimensional exposures. At St. Catherines River Bay, the sampling was more selective, concentrating on xenoliths of metasedimentary country rocks. Samples incorporated parts of xenolith cores, margins, and biotite tails of two xenoliths as well as samples from the host tonalite.

3.2.3 Photography

Photographs of schlieren at the four locations were taken using a Canon EOS Elan AF camera with a 28-80 mm lens. Photographs requiring greater detail were taken using a Canon AE-1P camera with a 50 mm, 1:1 macro lens. Fuji Provia professional 100 ASA slide film and Fuji Reala 100 ASA print film were the fine-grained films used to produce sharp images of schlieren. Photomicrographs of thin sections were taken with a Nikon Coolpix 990 digital camera affixed to a Wild Makroskop M420.

3.3 Petrography

3.3.1 Petrographic description

Petrographic observation of thin sections using a polarizing microscope provided an opportunity to study the differences in mineralogy of the light and dark bands, including mineral proportions, grain sizes, grain shapes, and preferred orientations of minerals. Particular attention was paid to any mineralogical or textural evidence of high temperature magmatic and/or solid state deformation in the four study areas.

3.3.2 *Sample Preparation*

A total of eight samples were collected from Prospect and Peggy's Cove, including samples of the host granite and subhorizontal mineral layering. These were made into large thin sections cut perpendicular to the plane of banding. Each of four samples from Jackies Island were cut into three sections marked a,b, and c and made into thin sections (Figure 3.1). Samples marked (a) were cut in the plane of banding, those marked (b) were cut perpendicular to the plane of banding (vertical), and those marked (c) were cut perpendicular to the plane of banding (horizontal or outcrop view). Four samples were collected from St. Catherines River Bay including three xenolith cores, three rims, two tails, and four host tonalite samples.

3.4 **Electron microprobe analysis**

3.4.1 *Operation of the electron microprobe*

The electron microprobe (EMP) laboratory at Dalhousie University has a fully automated JEOL 733 electron microprobe X-ray microanalyzer with four wavelength spectrometers and an Oxford Link eXL 137eV energy dispersive detector. The EMP provides a full quantitative chemical analysis of solid materials less than 5 microns in diameter on an elemental weight percent basis. The advantages of this system over other chemical analyses is that it provides a rapid, non-destructive method to analyze material without the need of separating minerals from their matrix (R. MacKay, written comm).

The EMP directs a very finely focused, high voltage, beam of electrons, about 1 μ m diameter, onto a target sample. The high energy electrons excite the atoms of the target sample and, when these atoms return to their normal state, they give off X-rays which have wavelengths

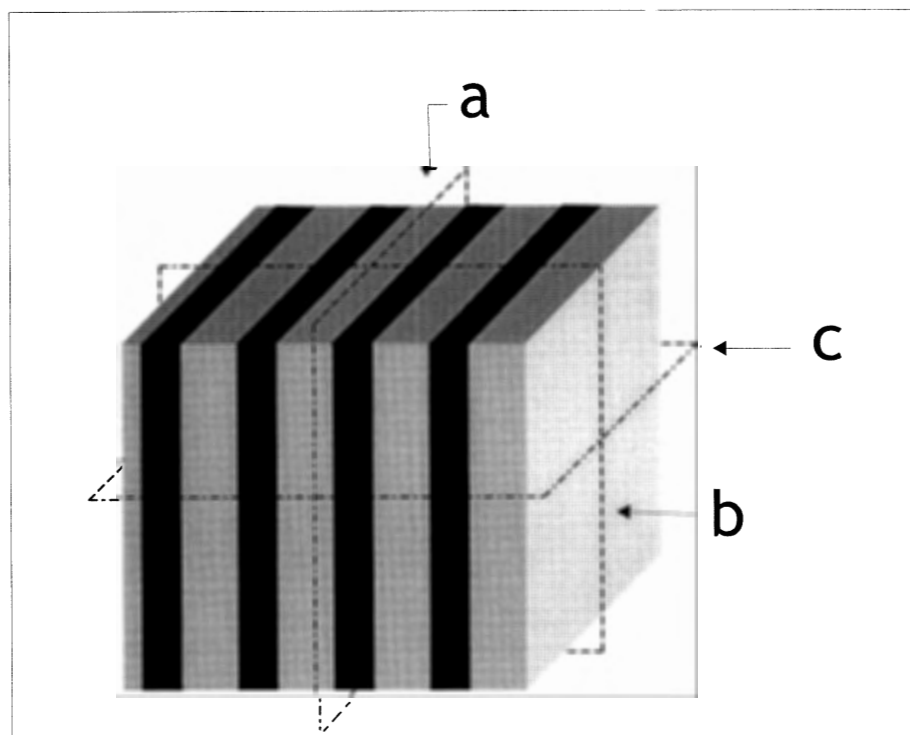


Figure 3.1 Method of cutting thin section of samples from Jackies Island. Thin sections were made in three orientations: (a) cut in the plane of banding, (b) cut perpendicular to the plane of banding (vertical), and (c) cut perpendicular to the plane of banding (horizontal).

and energies characteristic of each chemical element. The microprobe collects and counts the X-rays for each element in the sample, using a wavelength and/or energy dispersive detector. The X-ray counts of each element are compared to the X-rays counts of a standard and then a complex calculation is made to convert these X-ray counts into element concentrations to produce a complete chemical analysis according to the following formula:

$$\frac{\text{counts on sample}}{[\text{sample}] (\mathbf{X})} \sqrt{} = \frac{\text{counts on standard}}{[\text{standard}] \sqrt{}}$$

[] concentration

$\sqrt{}$ = known

X = **unknown concentration of sample** (solve for)

The accuracy for major elements is +/- 1.5 to 2.0 % relative. Detection limits for most elements using the energy dispersive system range from approximately 0.1 to 0.3 %.

3.4.2 Sample Preparation

Nine samples from St. Catherines River Bay were mounted on glass thin sections, ground, and polished to ensure flat surfaces. A thin film of conductive carbon coated the samples to provide a ground path for the electron beam.

3.4.3 Mineral analyses

Biotite mica was analyzed with the EMP using the energy dispersive system. The following standards were used for the analysis of biotite: sanidine for Si, Al, and K; jadeite for Na; kaersutite for Mg, Ca, and Ti; garnet for Fe; and MnO₂ for Mn. The resolution of the energy dispersive system was 137eV at 5.9 KeV. Each spectrum was acquired for several seconds with an accelerating voltage of 15 KV and a beam current of 15nA. The probe spot size was 10 microns. Fifty-nine individual probe points were analyzed and the raw data were corrected using the Link ZAF matrix correction program.

3.5 Image Analysis

3.5.1 Sample Preparation

The Wild Makroskop M420 with a Leica Wild MPS52 camera were used to take twenty-three black-and-white photos of thin sections from the Peggy's Cove and Jackies Island study locations. The photos were enlarged to 5 x 7" images and the orientations and lengths of feldspar twins were marked on transparencies. The resultant markings were analyzed by image analysis software associated with the electron microprobe.

3.5.2 Image Analysis

The Featurescan image analysis software is capable of morphological measurements of minerals including primary morphology (based on feret projections), e.g. feature length, convex area, and orientation. The determination of the feret or projected diameter forms the basis of morphological measurements. "The feret represents the distance between two parallel tangents which are opposite sides of a particle. The measurement of orientation expresses the angle between the maximum diameter (feature length) and the horizontal" (Link Analytical Featurescan operator's manual, 1991). The marked orientations of feldspar mineral grains were captured as a video image and analyzed by Featurescan software to determine if there were a preferred orientation of these minerals representative of the sample areas. This technique provided an objective and quantitative measurement of preferred orientations to supplement the subjective and qualitative petrographic descriptions.

3.6 Summary

A variety of methods were employed to study schlieren both in the field and in the laboratory. Observation and mapping in the field, petrographic observation, analysis of preferred

orientations, and chemical compositions of biotites were useful to infer possible physical processes responsible for schlieren development at each of the four study areas.

CHAPTER 4: LABORATORY RESULTS

4.1 Introduction

Several laboratory techniques were used to supplement observations made in the field at four study locations. Petrographic observation of thin sections from these study areas provided qualitative description of mineralogical and textural relationships. Foliation image analysis studies of Peggy's Cove and Jackies Island samples provided quantitative evidence for preferred orientations of feldspars. A biotite composition study of St. Catherines River Bay xenolith and host tonalite samples was used to assess the origin of the schlieren. The laboratory results were summarized and used to determine the physical processes responsible for schlieren banding at each study location (Chapter 5).

4.2 Petrographic description

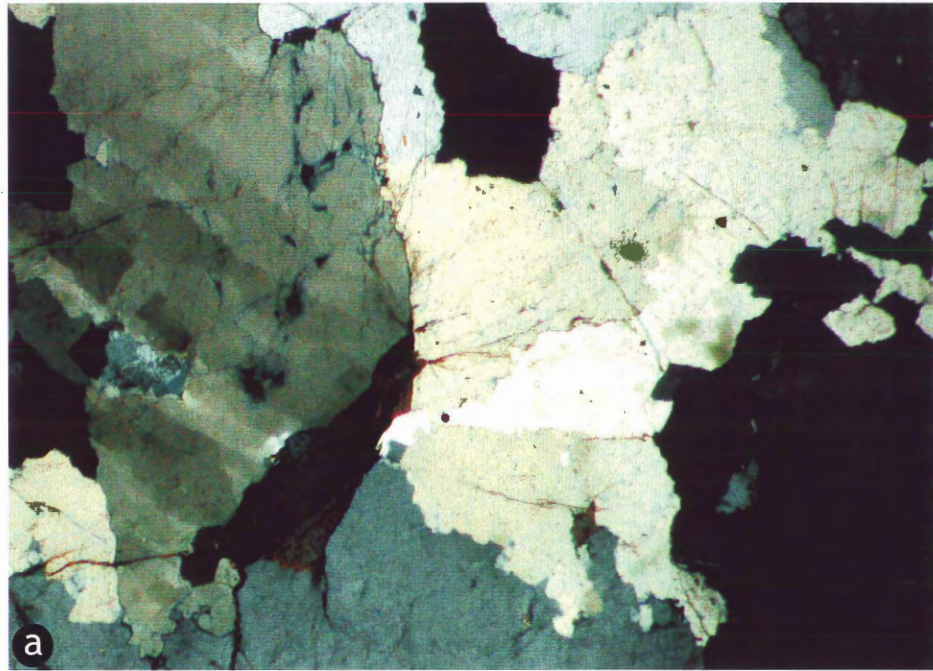
The predominant mineral phases within schlieren samples are quartz, plagioclase, K-feldspar, biotite, and muscovite. Petrographic observation focused on mineralogical and textural variations and evidence for late stage magmatic deformation and/or high temperature solid-state deformation. The following scale was used for grain size: (i) fine < 1mm, (ii) medium 1-5 mm, (iii) coarse 5-10 mm, and (iv) very coarse >10 mm. Table 4.1 lists detailed observations for all samples.

4.2.1 Prospect

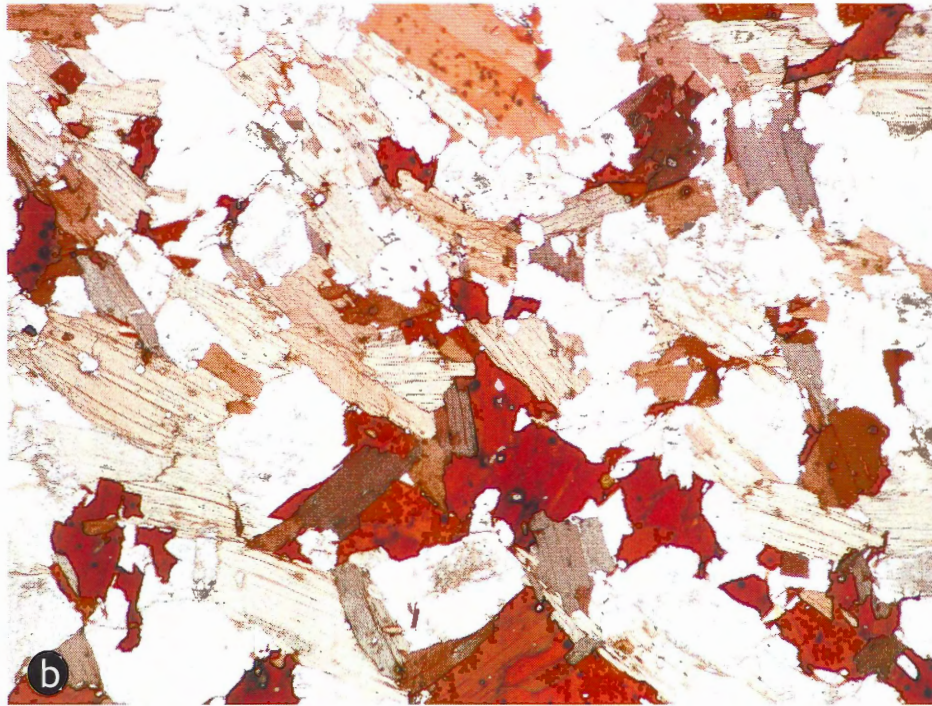
Quartz. In these samples, quartz forms aggregates of large, equidimensional, anhedral grains with a larger percentage of grains concentrating in the felsic bands. Quartz grains have irregular boundaries and show (c)- and (a)-slip, producing minor subgrain development with undulose extinction (Fig. 4.1a).

Table 4.1a Petrographic features of Prospect samples.

Sample	Quartz	Feldspar		Micas		Comments
		Plagioclase	K-Feldspar	Biotite	Muscovite	
Prospect (PR-1 HOST) host monzogranite Fig. 2.3	coarse-grains 1-7 mm, equidimensional, anhedral aggregates	very coarse grains 0.5 cm to 1 cm, albite twinning, oscillatory zoning, sericitic alteration	very coarse grains 2-5 cm, Carlsbad twinning, perthitic exsolution	euhedral, pleochroic haloes of zircon inclusions	subhedral <10%	feldspar-rich aggregate with a NW/SE trending foliation attitude of feldspar megacrysts
Prospect (PR-2) mafic and felsic banding (subvertical) Fig. 2.3	large grains, equidimensional, mosaic extinction with (c) and (a) slip and development of subgrains, irregular boundaries, greater abundance in felsic bands	oscillatory zoning, sericitic alteration, bent grains	large grains with Carlsbad twins, perthitic texture, larger grains toward middle of felsic layers	euhedral grains with pleochroic haloes of zircon inclusion, strong preferred orientation of biotite grains	n/a	section cut perpendicular to banding, foliation of biotites, size sorting with feldspar megacrysts to center of felsic bands and biotite to the margins
Prospect (PR-3) mafic and felsic banding (subvertical) Fig. 2.3	irregular boundaries, equidimensional, mosaic extinction with beginning of subgrains, recrystallized small grains at boundary edges greater abundance in felsic bands	oscillatory zoning, sericitic alteration, bent grains, preferred orientation in felsic bands plag > ksp	euhedral, coarse-grained with Carlsbad twins and fine microperthite, poikilitic, preferred orientation in felsic bands	strong preferred orientation in dark bands, weak kink banding	small intersitial grains <10%	section cut perpendicular to banding, foliation of biotites, size sorting with feldspar megacrysts to center of felsic bands and biotite to the margins (Fig. 4.1)



1 mm



1 mm

Figure 4.1 (a) Quartz grains showing irregular boundaries, and both (c) and (a) slip with minor blocky subgrain development (XN). (b) Biotite grains show a preferred orientation from upper left to lower right corner of photo (PPL).

Plagioclase. Plagioclase occurs as large phenocrysts ranging in size from 0.5-1cm with a large percentage showing a preferred orientation in felsic bands. The grains have oscillatory zoning with sericitized cores, inclusions of quartz, and appear slightly bent.

K-feldspar. K-feldspar occur as large phenocrysts ranging in size from 2-5 cm with a large fraction of grains concentrating in the middle of felsic bands with their (010) faces showing a preferred orientation. Grains are generally euhedral and platy with Carlsbad twins and perthitic texture.

Biotite. Biotite grains are euhedral and make up the main fraction of the dark bands with their [001] planes demonstrating a preferred alignment. Many grains have weak kink banding and pleochroic haloes around zircon inclusions (Fig. 4.1b).

Muscovite. Muscovite appears as small, euhedral grains in interstitial spaces of all the samples and represents less than 10% of the mineral phases present. These grains do not show any signs of deformation textures.

4.2.2 Peggy's Cove

Quartz. Quartz occurs as aggregates of large anhedral, interconnected grains with a large percentage of grains concentrating in the felsic bands. These grains have irregular, "amoeboid-type" boundaries with undulose extinction. In a few felsic bands there are small, recrystallized, anhedral aggregates of quartz on the margins of K-feldspar grains. The tops of felsic bands have pockets of larger quartz aggregates with irregular grain

boundaries. On a mesoscopic scale, these pockets represent cusped layers seen in Figure 2.7 (b).

Plagioclase. Plagioclase occurs as medium-grained phenocrysts ranging in size from 1-5 mm with no obvious preferred orientations. Many grains have adcumulate textures with unzoned, sericitized cores and oscillatory zoned rims (Fig.4.2a).

K-feldspar. K-feldspar occurs as large phenocrysts ranging in size from 0.2-2 cm with no obvious preferred orientation. The grains are generally subhedral and platy with Carlsbad twins and perthitic texture. Many grains in contact with plagioclase have growths of myrmekitic “blebs” at their grain boundaries. There are small microcline grains with weakly developed “crosshatch” twinning in areas of recrystallized quartz (Fig 4.2b).

Biotite. Biotite grains are euhedral and make up the main fraction of the dark bands with their [001] planes demonstrating a preferred alignment. The grains do not show any signs of obvious deformation, although the rims are commonly altered to chlorite.

Muscovite. Muscovite appears as small, euhedral grains in interstitial spaces of all the samples and represents less than 10% of the mineral phases present. These grains do not show signs of deformation textures.

Table 4.1b Petrographic features of Peggy's Cove samples.

Sample	Quartz	Feldspar		Mica		Comments
		Plagioclase	K-Feldspar	Biotite	Muscovite	
Peggy's Cove (PC-1 HOST)	coarse-grained, equidimensional with irregular boundaries	subhedral, coarse-grained, 1-5 mm oscillatory zoning, many grains have adcumulate texture, sericitic alteration	coarse-grained 0.2-2 cm, Carlsbad twinning, perthitic texture, lobate myrmekitic "blebs" on grain margins common	large euhedral plates with pleochroic haloes of zircon inclusions, preferred orientation to the margins of mafic layers	minor interstitial grains <10%	hypidiomorphic, adcumulate texture: plagioclase has unzoned core, and zoned rims mafic layers have cusped margins (Fig 4.2a)
Peggy's Cove (PC-2) reverse-graded layers (subhorizontal) with mafic bottoms, felsic tops, cusped layers	irregular boundaries with small grains of recrystallized quartz	coarse-grained, 1-5 mm, various orientations in felsic layers, oscillatory zoning	coarse-grained 0.2-2 cm, various orientations in felsic layers, myrmekite "blebs" on grain margins, perthitic texture common, presence of microcline with weak "crosshatch" twinning	strong preferred orientation in mafic layer, mostly large euhedral grains +/- chloritized rims	minor interstitial grains <10%	pockets of coarse-grained felsics disrupt cusped margins
Peggy's Cove (PC-3) reverse-graded layers (subhorizontal) with mafic bottoms, felsic tops	irregular boundaries, large grains with recrystallized quartz boundaries	coarse-grained, 1-5 mm, plagioclase intergrowths, many grains have adcumulate texture, sericitic alteration	large, coarse-grained 0.2-2 cm, small microcline grains, myrmekite "blebs" on grain margins	strong preferred orientation of biotite composing the dark bands, chloritized grain boundaries	minor interstitial grains <10%	stress indicators include: granulation along boundaries, presence of microcline, and cracked microcline grains (Fig 4.2b)

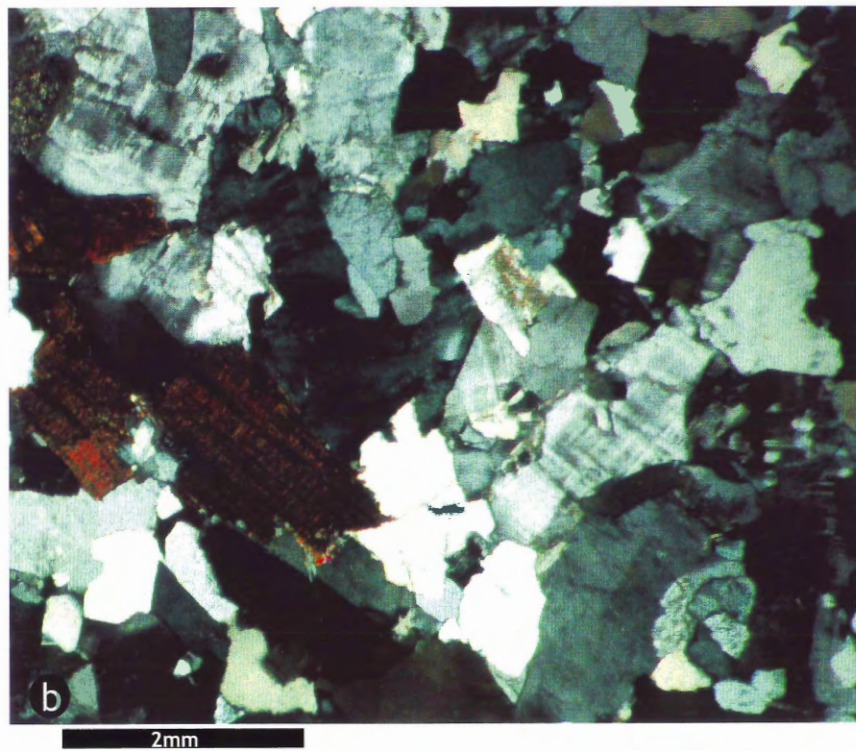
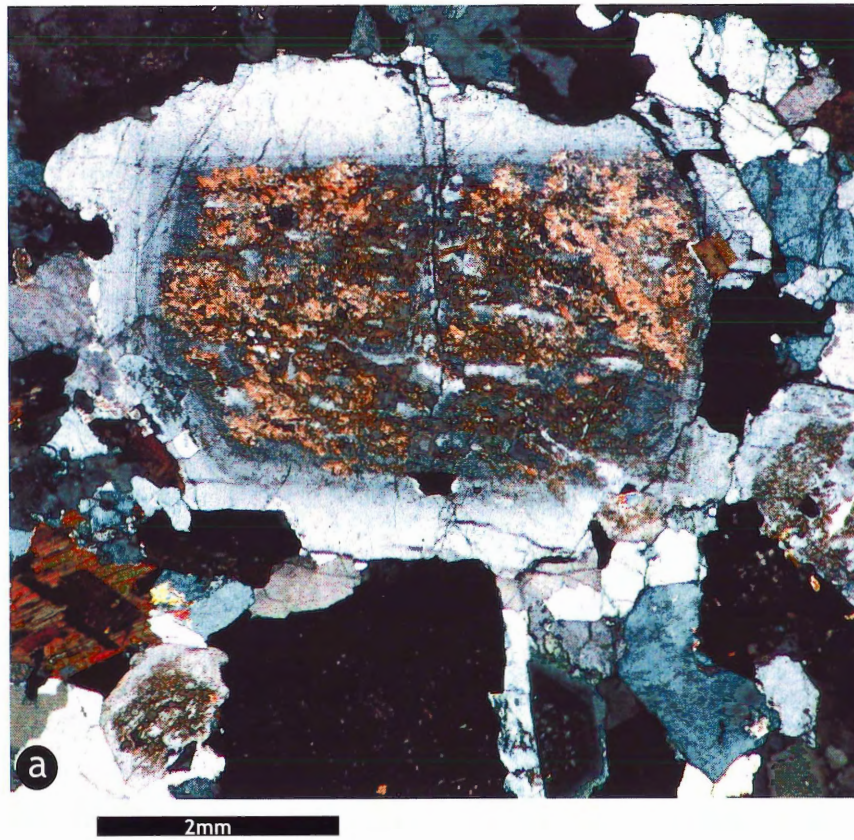


Figure 4.2 (a) Plagioclase grain shows an adcumulate textural feature (unzoned core and oscillatory zoned rim) (XN). (b) Microcline grains show weak “crosshatch” twinning and small quartz grains with irregular boundaries (XN).

4.2.3 Jackies Island

Quartz. In these samples, quartz forms aggregates of medium, equidimensional, anhedral grains. Quartz grains have irregular boundaries and demonstrate (c) and (a) slip, producing minor blocky subgrain development with undulose extinction (Fig. 4.3b).

Plagioclase. Plagioclase consists of fine grains ranging in size from 0.5-1mm in varying orientations. Many grains are weakly kinked with tapering deformation twins, offset albite twinning, deformation bands and undulose extinction (Fig. 4.3 d).

K-feldspar. K-feldspar occurs as small grains ranging in size from 0.5-0.8 mm. The grains are generally subhedral with flame perthitic texture. At least 30% of K-feldspar occurs as microcline with well-developed “crosshatch” twinning and deformation bands. Microcline grains appear bent with undulose extinction, and many are cracked with infillings of small muscovite grains (Fig. 4.3 c,e).

Biotite. Biotite grains are euhedral and make up the main fraction of the dark bands with their [001] planes demonstrating a preferred alignment in (b) and (c) sections cut perpendicular to banding. The (a) sections, cut in the plane of the banding, expose a large percentage of (001) basal grains. Many biotite grains are bent, and have moderate kink banding and undulose extinction.

Table 4.1c . Petrographic features of Jackies Island samples.

Sample	Quartz	Feldspar		Mica		Comments
		Plagioclase	K-Feldspar	Biotite	Muscovite	
Jackies Island 1a, 2a, 3a, 4a symmetrical, anastomosing/ parallel, subvertical banding	medium-sized grains with development of blocky subgrains, undulose extinction, LPO with (c) slip no elongated grains	small grains 0.5-1 mm, tapering deformation twins, sericitic alteration	larger than plagioclase grains at 0.5-0.8 mm, microcline with crosshatch twinning, deformation banding	biotite in basal sections (001) most common, grains weakly bent, undulose extinction	moderate kinked grains with undulose extinction	all (a) sections cut in the plane of banding, large concentration of basal biotite sections
Jackies Island 1b,2b,3b,4b symmetrical, anastomosing/ parallel, subvertical banding	medium-sized grains with development of blocky subgrains, undulose extinction, LPO with (c) and (a) slip, no elongated grains	small grains 0.5-1 mm, tapering deformation twins, bent tapering twins with offset bands, deformation banding, undulose extinction	larger than plagioclase at 0.5- 0.8 mm, flame perthite, deformation banding, microcline grains bent and cracked with in-filling of muscovite	subhedral grains bent with weak kink banding, undulose extinction, preferred orientation of biotite	subhedral with strong kink banding and undulose extinction	all (b) sections cut perpendicular to the plane of banding(vertical), orientation of biotites obvious in this plane (Fig. 4.3a-e)
Jackies Island 1c,2c,3c	medium-sized grains with development of blocky subgrains, undulose extinction, some embayed grains, LPO with (c) and (a) slip, no elongated grains	small grains 0.5-1 mm, tapering deformation twins, bent tapering twins with offset bands, deformation banding at high angles to polysynthetic twins, undulose extinction	larger than plagioclase at 0.5- 0.8 mm, flame perthite, deformation banding, microcline grains bent and cracked with in-filling of muscovite	subhedral grains bent with moderate kink banding, undulose extinction, preferred orientation of biotite	subhedral with strong kink banding and undulose extinction	all (c) sections cut perpendicular to the plane of banding (horizontal), orientation of biotites obvious in this plane

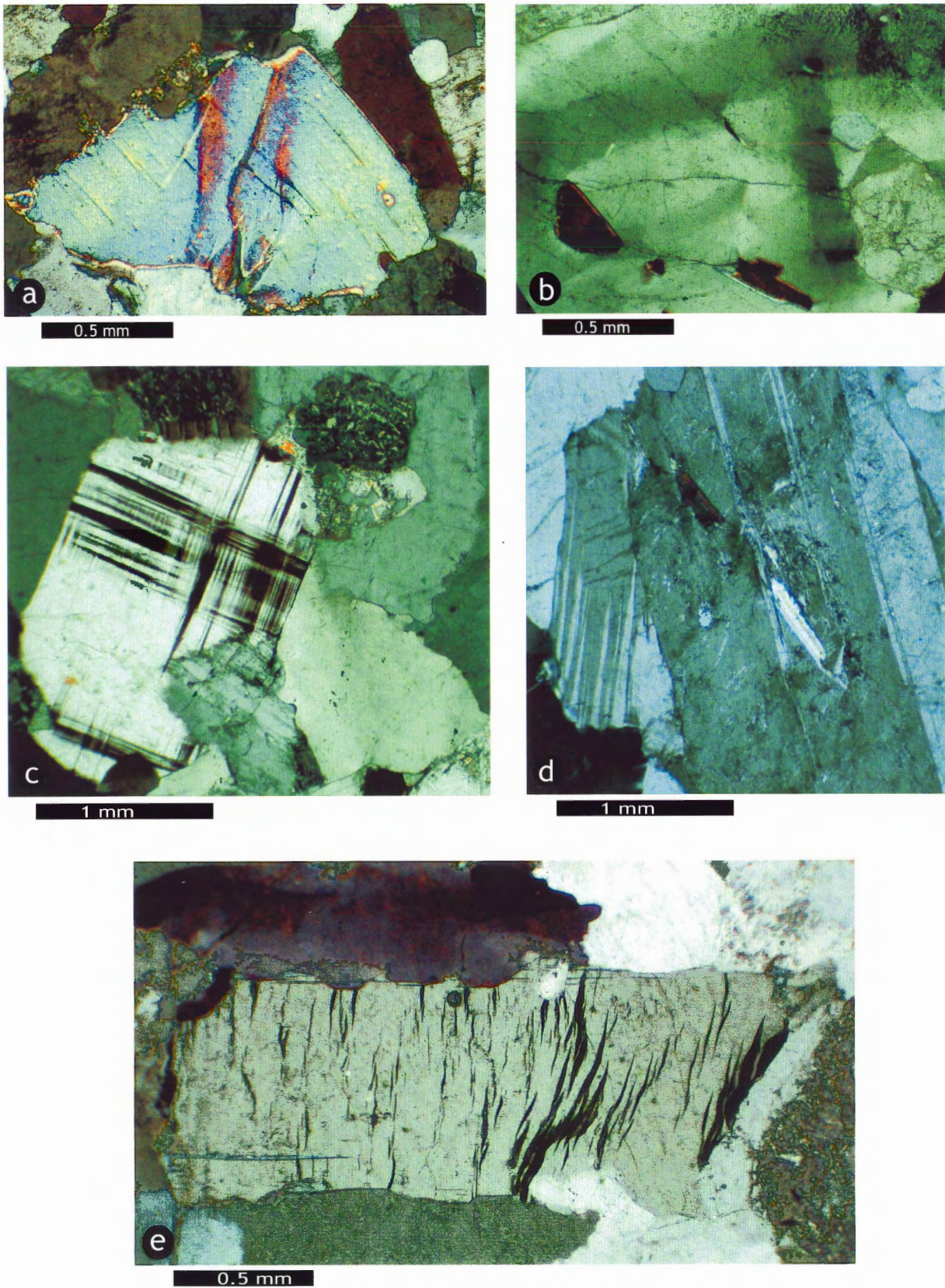


Figure 4.3 Photomicrographs from Jackie Island samples (XN): (a) Kinked muscovite. (b) Shows (c)- and (a)-slip in quartz with blocky subgrain development. (c) Microcline grain with well-defined “crosshatch” twinning. (d) Tapering deformation twins in plagioclase. (e) Flame perthite in K-feldspar.

Muscovite. Muscovite grains are subhedral and medium grained with larger sizes than biotite, ranging from .2-1.0 mm. The grains show strong kink banding with undulose extinction (Fig. 4.3 a).

4.2.4 St. Catherines River Bay

Quartz

(i) *Xenolith.* Quartz grains are small, sub-rounded, recrystallized grains ranging in size from 0.2-0.4 mm with an average abundance of 30% in the xenolith core to less than 1% at the rim (Fig 4.4a).

(ii) *Host Tonalite.* Quartz grains are anhedral, with larger sizes ranging from 0.3-2 mm. The grains have irregular boundaries with development of blocky subgrains and undulose extinction (Fig. 4.4b).

Plagioclase

(i) *Xenolith.* Plagioclase occurs as very small, subhedral, highly sericitized grains in the xenolith core and is absent in the rim.

(ii) *Host Tonalite.* Plagioclase is much more abundant than K-feldspar with well-developed oscillatory zoning, tapering deformation twins, and sericitized cores.

K-feldspar

(i) *Xenolith.* K-feldspar occurs as very small, subhedral, highly altered grains in the xenolith core and is absent in the rim (Fig. 4.4a).

Table 4.1 d Petrographic features of St. Catherines River Bay samples.

Sample	Quartz	Feldspar		Mica		Comments
		Plagioclase	K-Feldspar	Biotite	Muscovite	
St Catherines River Bay SCRB-1a (xenolith core and rim)	small to medium sized grains, irregular boundaries 30% abundance in core and decreasing to <1% at the rim	small subhedral grains in the core no obvious deformation, absent on the rim	ksp>plag small subhedral grains, no obvious deformation	bent grains with chloritized rims in the core, strongly developed kink bands with undulose extinction, well- aligned aggregates increasing to 80% abundance at the rim	highly fragmented and bent grains in the core, strongly developed kink bands with undulose extinction, parallel alignment to biotite grains at the rim	core: hornfelsic texture = granoblastic quartz and feldspar (Fig. 4.4a)
St Catherines River Bay SCRB-1b (xenolith tail)						sample lost during thin section preparation
St Catherines River Bay SCRB-1c (host tonalite)	large grains with development of blocky subgrains and undulose extinction	highly developed oscillatory zoning and plag> ksp in abundance, no obvious deformation	ksp small grains, no obvious deformation	strongly developed kink bands with undulose extinction, strong alignment of grains	strongly developed kink bands with undulose extinction	strong preferred orientation of biotites in thin section and hand sample (Fig. 4.4b)
St Catherines River Bay SCRB-2a (xenolith core)	small grains undulose extinction	n/a	small grains no deformation	small bent and kinked grains with a strong preferred orientation	large grains strongly kinked, bent, undulose extinction	fine grained quartz, ksp, biotite, larger grains of muscovite, strong foliation marked by biotite

Table 4.1d continued. Petrographic features of St. Catherines River Bay samples.

Sample	Quartz	Feldspar		Mica		Comments
		Plagioclase	K-Feldspar	Biotite	Muscovite	
St Catherines River Bay SCRB-2b (xenolith rim)	very small grains highly altered	? plag	very small grains highly altered	strongly developed kink bands with undulose extinction, stretched, tight aligned aggregates 80% abundance	strongly developed kink bands with undulose extinction, parallel alignment to biotite grains	xenolith rim surrounds the xenolith core, tightly packed aggregate of aligned, aligned biotite plates
St Catherines River Bay SCRB-2c (xenolith tail)	? quartz	? plagioclase	? ksp	tightly packed aggregate of aligned biotite flakes, strongly kinked and with undulose extinction	subhedral grains strongly kinked, aligned with biotite, undulose extinction	xenolith tail consisting almost entirely of aligned biotite plates strongly foliated
St Catherines River Bay SCRB-2d (host tonalite)	large grains with development of blocky subgrains and undulose extinction	highly developed oscillatory zoning and tapering deformation twins plag> ksp in abundance, no obvious deformation	small grains of microcline present with undulose extinction	strongly developed kink bands with undulose extinction, strong alignment of grains	strongly developed kink bands with undulose extinction	strong preferred orientation of biotites in thin section and hand sample
St Catherines River Bay SCRB-3 (host tonalite)	large grains with development of blocky subgrains and undulose extinction	highly developed oscillatory zoning and tapering deformation twins plag> ksp in abundance	small grains of microcline present with undulose extinction	strongly developed kink bands with undulose extinction, strong alignment of grains	strongly developed kink bands with undulose extinction	strong preferred orientation of biotites in thin section and hand sample
St Catherines River Bay SCRB-4 (xenolith core, rim, host tonalite)	very small grains with undulose extinction in the core, large grains with development of blocky subgrains and undulose extinction in the host	absent in core and rim, highly developed oscillatory zoning and tapering deformation twins plag> ksp in abundance in the host	very small grains, no obvious deformation in the core and rim, small grains of microcline present with undulose extinction in the host	strongly kinked, strong preferred orientation in tightly packed aggregates in core and rim, kinked, foliated and undulose extinction in the host	strongly kinked with preferred orientation, aligned with biotite at the rim, kinked, foliated and undulose extinction in the host	foliation largely marked by biotite in the core, tightly packed aggregate of biotite represents the rim, and also strong foliation of biotite in host

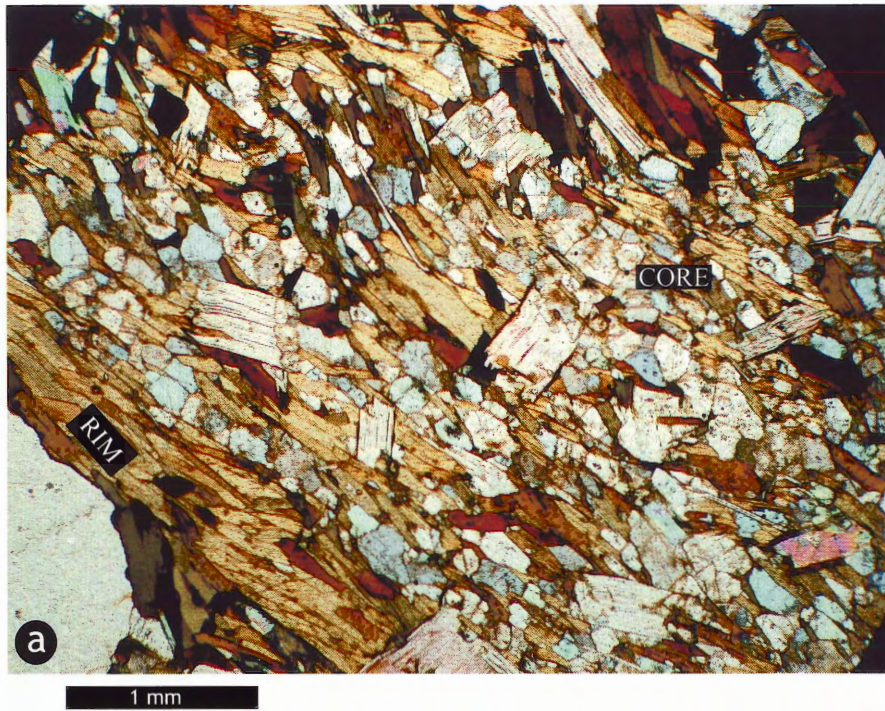


Figure 4.4 Photomicrographs from St. Catherines River Bay samples. (a) Tightly packed aggregates of aligned biotite on the rim of a metasedimentary xenolith (left side of photo)(PPL). Note small grains of quartz and feldspar in the xenolith core (right side of photo). (b) Aligned biotite grains and kinked muscovite grains in the host tonalite (partial XN).

(ii) *Host Tonalite*. K-feldspar occurs as small grains with microcline. Microcline has weakly developed “crosshatch” twinning and undulose extinction.

Biotite

(i) *Xenolith*. Biotite grains are small, aligned, subhedral plates often bent with chloritized rims in the xenolith core. At the xenolith rims they occur as tightly packed aligned aggregates with an abundance of 80%, are strongly kink banded, and have undulose extinction (Fig 4.4a).

(ii) *Host Tonalite*. Biotite grains have strongly developed kink bands, undulose extinction, and have a strong preferred orientation (Fig. 4.4b).

Muscovite

(i) *Xenolith*. Muscovite grains are larger than biotite, strongly kinked and have a strong preferred orientation parallel to biotite.

(ii) *Host Tonalite*. Muscovite grains are large, subhedral, strongly kinked grains with undulose extinction. They have a strong preferred orientation parallel to biotite grains.

4.3 Foliation Image Analysis Study

The Featurescan image analysis software quantifies the preferred orientation of minerals based on feret projections. This software measured an angle between the maximum length and a horizontal baseline to calculate the orientations of feldspars. Sample results are given as the mean direction and standard deviations (in degrees) of feldspar orientations for selected samples from Peggy’s Cove and Jackies Island. These

were compared to random standards for the same given number of samples (Table 4.2). Additional standards, one for a defined vertical orientation and one for a random orientation, are shown as comparisons at the bottom of the table.

The Peggy's Cove samples have a high standard deviation and, compared to the random standard sample, they are markedly similar. The Jackies Island samples have lower standard deviations from the mean indicating a stronger degree of foliation.

4.4 Biotite Composition Study

Biotite mica grains were analyzed in samples of xenoliths and host tonalite from St. Catherines River Bay with the electron microprobe. The mean and standard deviation of major element oxides for xenolith cores, rims, tails, and host tonalite were calculated from fifty-nine samples (Table 4.3). The $\text{FeO}/(\text{FeO} + \text{MgO})$ ratios of all biotites are statistically identical.

4.5 Summary

Petrographic observation of the four study locations demonstrate differences in terms of grain shapes, grain size distribution, orientation of minerals, and deformation textures. Foliation image analysis data used the mean direction and standard deviation of feldspar orientations to compare Peggy's Cove and Jackies Island samples with tested standards. Peggy's Cove samples demonstrated a similarity with the random orientation standard, but the data for Jackies Island samples showed much smaller standard deviations from the known directions of the banding. A biotite composition study

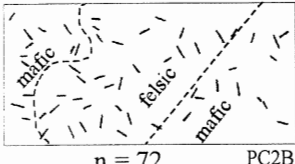
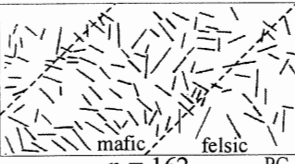
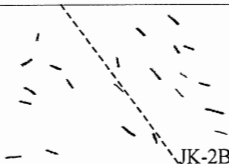
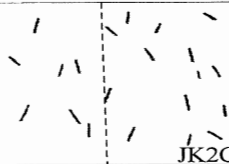
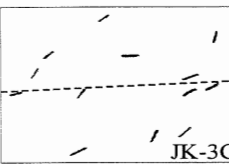
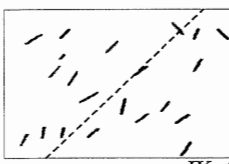
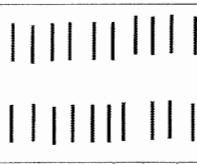

Sample	Mean Feldspar Orientation (degrees)	Standard Deviation (degrees)	Standard Deviation for random (n) (degrees)
 n = 72 PC2B	91.0	+/- 46.7	+/- 53
 n = 162 PC-3	86.4	+/- 47.0	+/- 52.4
 JK-2B n = 22	59.7	+/- 32.8	+/- 55.4
 JK2C n = 28	106.0	+/- 63.0	+/- 54.7
 JK-3C n = 13	132.5	+/- 33.2	+/- 57.9
 JK-4B n = 21	124.7	+/- 18.6	+/- 55.6
 Vertical orientation n = 20	92	+/- 2.0	+/- 0.0
 Random orientation n = 50	101.3	+/- 46	+/- 54

Table 4.2 Foliation image analysis data was calculated from the orientations of feldspar megacrysts using Featurescan software. The mean orientation and standard deviation of the megacrysts from Peggy's Cove (PC) and Jackies Island (JK) samples are shown in degrees. Dashed lines represent the foliation and/or schlieren banding in the samples as a reference direction.

<i>Oxide</i>	<i>Core</i>	<i>Core</i>	<i>Rim</i>	<i>Rim</i>	<i>Tail</i>	<i>Tail</i>	<i>Host</i>	<i>Host</i>
	\bar{X}	σ	\bar{X}	σ	\bar{X}	σ	\bar{X}	σ
n	16		16		7		20	
SiO2	34.92	0.37	34.98	0.49	34.99	0.25	34.98	0.40
TiO2	2.29	0.19	2.29	0.30	2.18	0.14	2.66	0.24
Al2O3	18.02	0.40	18.03	0.36	17.97	0.16	17.52	0.84
FeO	20.55	0.91	20.18	0.40	19.99	0.28	20.48	0.75
MnO	0.37	0.07	0.32	0.07	0.37	0.07	0.40	0.10
MgO	8.78	0.43	8.89	0.38	9.12	0.12	8.61	0.39
CaO	0.03	0.03	0.02	0.03	0.01	0.02	0.01	0.02
Na2O	0.27	0.07	0.28	0.09	0.26	0.06	0.27	0.07
K2O	9.67	0.28	9.70	0.26	9.77	0.10	9.73	0.18
Cl	0.05	0.03	0.06	0.03	0.04	0.02	0.04	0.03
P2O5	0.04	0.05	0.04	0.05	0.05	0.07	0.02	0.02
F	0.01	0.02	0.02	0.03	0.05	0.03	0.02	0.03
BaO	0.17	0.10	0.11	0.08	0.10	0.11	0.17	0.11
Total	95.16	0.97	94.92	0.90	94.91	0.46	94.92	0.84
F/(F+M)	0.70	0.02	0.69	0.01	0.69	0.01	0.70	0.01

Table 4.3 Mean biotite analyses of St. Catherines River Bay samples - Major element oxides (wt %) of xenolith core, rim, tail, and host tonalite.

involved an electron microprobe analysis of major elements in biotites from xenoliths and host tonalite at St. Catherines River Bay. The mineral chemistry (Fig 4.5) showed no systematic variation in the samples.

CHAPTER 5: DISCUSSION

5.1 Introduction

Schlieren at each of Prospect, Peggy's Cove, Jackies Island, and St. Catherines River Bay show distinctive field relations, as well as unique mineralogical and textural features, suggesting a different physical process of formation at each location. This chapter attempts to analyze, qualitatively, the physical evidence responsible for schlieren development at these four localities.

5.1.2 Heterogenization \leftrightarrow Homogenization

The formation of schlieren bands in granitoid rocks can be the result of homogenization or heterogenization processes. Heterogenization processes tend to sort statistically homogeneous materials, based on the physical properties of the individual components (size, shape, and density), to produce modal and textural variations. The development and preservation of geological streaks (schlieren banding) in this case can result from size sorting in shear flow with a suitable magma viscosity. Non-geological streaks, such as layered cloud formations, form in atmospheric fluid systems in the presence of vertical wind shear, and pollen and foam particles form streak patterns on water surfaces in shear flow. Although a direct correlation between geological processes and these non-geological fluid processes is difficult to make, the result is similar in that heterogeneous streaks develop from an originally homogeneous material.

Homogenization processes tend to make heterogeneous materials statistically uniform. Non-geological streaks such as pollen and foam particles can subsequently

become homogenized by concentration or dispersal in fluid systems. Geological streaks appear at intermediate stages between heterogeneous and homogeneous states (e.g., heterogeneities that are partially melted, stretched, and then eventually dispersed into a silicate melt).

5.1.1 Dynamics of a crystallizing magma

Magmas represent a continuum from 100 % liquid fraction to 100 % solid fraction during cooling and crystallization. Vigneresse and Burg (2000) defined two important rheological boundaries in a crystallizing magma: the rigidity percolation threshold (RPT) and the particle locking threshold (PLT), representing different degrees of crystallinity, $\phi \geq 55$ and $\phi \geq 75$, respectively. A granitic magma can deform in three ways depending on its degree of crystallinity (ϕ).

1. *magmatic flow* ($\phi < 55\%$). Paterson (1989) defined magmatic flow as deformation by displacement of melt in which crystals rotate freely without sufficient interference to produce internal deformation. When the solid fraction is low, crystals are able to rotate independently with minimal interaction with other crystals. This rotation can produce magmatic foliations with planar fabrics defined by euhedral grains. This foliation is easily destroyed unless the magma has an adequate viscosity.

2. *late stage magmatic flow* ($\phi = 55-75\%$). At a solids fraction of 55%, a rigid framework of touching crystals defines the rigidity percolation threshold (RPT). At this stage, crystals can no longer rotate freely and begin to tile and interact. Crystal interactions can result in changes in grain shapes, grain sizes, grain boundaries, and grain orientations, and can produce a foliation parallel to the flow plane (Clarke et al. 2000b).

At these higher crystal fractions, the magma is still able to deform and becomes dilatant, creating localized shear zones in which the remaining melt can segregate (Vigneresse and Tikoff 1999). Vernon (2000) suggests that minor solid-state strain can occur in the interstitial spaces between aligned euhedral crystals as a result of shearing along discrete planes, such as mica-rich folia. Schlieren layering can occur at this stage when it develops as a result of velocity gradients in shear flow. As the temperature decreases, the crystal fraction increases, thereby increasing viscosity until the close packing of crystals locks the solid framework at 75 % crystals (PLT). Foliation produced in this regime tends to be preserved.

3. solid-state overprinting at high (T) ($\phi > 75\%$) Above the particle locking threshold of $\phi = 75\%$, differentiation between late stage magmatic flow and high T solid-state flow is difficult as a result of subsolidus deformation and annealing which can overprint earlier magmatic flow. Magmatic flow structures can be modified or destroyed by crystal plasticity and recrystallization before the magma reaches its solidus (Paterson et al. 1998). Local stress conditions may be adequate to produce some plastic deformation/recrystallization in localized pockets of melt. C-slip in quartz is a common microstructure that develops at high T deformation ($T > 500^\circ\text{C}$) At lower temperatures ($T = 300\text{-}400^\circ\text{C}$), (a)-slip in quartz is common and as a result, produces blocky subgrain development. Other deformation microstructures such as deformation twinning, deformation bands, bent grains, and flame perthite are common in feldspar at these lower temperatures.

5.2 Prospect

5.2.1 Major observations

The major structural and textural features at Prospect, requiring a physical process to explain them, are:

- (i) local perturbation of the regional flow foliation;
- (ii) development of thin wispy biotite schlieren with sorting and alignment of biotite grains, and with alignment of K-feldspar megacrysts with (010) faces parallel to mafic layers;
- (iii) creation of ellipsoidal and circular structures defined by fine-grained mafic margins coarsening inwards, surrounded by randomly oriented clusters of K-feldspar megacrysts; and
- (iv) deformation of quartz.

5.2.2 Schlieren characteristics and working hypotheses

(i) local perturbation of the regional flow foliation

Pitcher (1993) suggested that porphyritic granites show flowage alignments indicative of fairly dense suspensions that can be mobile, even turbulent, and that may represent diapiric upsurges of a new magmatic pulses into the core of a pluton. Abbott (1989) mapped cylindrical structures defined by platy K-feldspar megacryst foliation and schlieren structures at Terence Bay, 5 km east of Prospect. He interpreted the foliation planes and related schlieren structures to have resulted from internal folding of the magma by forced convection during ascent or lateral injection.

Schlieren features at Prospect appear to represent complementary parts of what was originally a homogeneous flow-foliated monzogranite, similar to that at Terence Bay. The development of heterogeneities such as mafic schlieren and associated K-feldspar megacryst clusters is restricted to a small area of 40 m x 15 m. This perturbed area represents a disruption of the regional flow foliation defined by the alignment of platy K-feldspar megacrysts, generally striking 290-345°. This local disruption of the regional flow foliation, and production of schlieren structures at Prospect, might be the result of a rising vapour bubble (water-saturated magma) or a falling xenolith block (dislodged from the roof) that produced large strain and complex flow patterns in its wake.

Fan and Tsuchiya (1990) experimented with rising gas bubbles in a solid-liquid medium and described the relationship between the rising bubble and its wake. Rising bubbles produce localized areas of heterogeneity in a flow field with the development of flow instabilities downstream of bubbles, resulting in large-scale vortical motions and local solids concentration gradients. Following the ascent of a bubble, the bubble wake develops a closed laminar area represented by rotating curved surfaces (vortex rings) with narrow tails. As the bubble rises and the wake grows in size by continuously accumulating solid material from outside the wake, the symmetry of the flow will be disturbed and wake material will be shed.

Paterson and Miller (1998) examined magmatic fabric patterns around stoped blocks in tonalite in the Mount Stuart Batholith, Washington. They suggested that stoped blocks sinking in a relatively stationary or slow moving magma can move vertically downwards and disrupt any pre-existing foliation. In close proximity to the stoped block,

large strains rotate pre-existing fabrics towards the block margin and laterally around the block; therefore, large amounts of strain and fabric patterns move outwards away from the block. Zones of complex flow (vertically oriented) can occur behind sinking objects forming steeply plunging lineations or random fabrics (Paterson and Miller 1998).

Complex flow foliations around stoped blocks in the Mount Stuart Batholith are defined by inward curving arcuate patterns discordant to the block margin. Pitcher (1993) compared the falling of large blocks through magma chamber to dropstones in a glacial environment. He stated that at depth the blocks become disoriented and appear to tumble as they react to the flow or strain pattern of the host.

(ii) development of thin biotite schlieren +/- foliated K-feldspar

Crystals in a suspension tend to move away from the margins of a magma body with their rate of movement highly dependent on their physical properties (e.g., sizes and shapes). The flow of magma past static margins creates differential shear stress in the viscous liquid as a result of a velocity gradient near the contact (Wilshire 1969). Magma flows around larger crystal sizes (megacrysts) and as a result of its differential motion, it exerts pressure on the grains, forcing the grains apart and away from the contact. Bagnold (1954) experimented with this grain dispersive pressure and suggested that mixed sand sizes in a dry sand flow produced size sorting from induced shear flow. Wilshire (1969) also applied Bagnold's theory to mafic and felsic layers in granodiorite of Twin Lakes, Colorado. He inferred that K-feldspar grains migrated to areas of minimal shear stress and biotite grains concentrated in areas of high shear stress along the contact with wall

rock. The highest mafic concentrations occur on the same side of the layers with sharp contacts. Wilshire (1969) attributed these observations to size-sorting in shear flow.

Thin wispy biotite laminae at Prospect are characterized by sharply defined biotite margins, in some places pinching out, and in other places occurring in parallel repeated laminae. In some places, K-feldspar megacrysts are aligned with their (010) faces parallel to the biotite layers, and in other places, biotite laminae appear as fans and truncating branches. Sharp fine-grained mafic boundaries grading into coarse-grained K-feldspar megacryst clusters also occur at Prospect (Figs. 2.4 a-f). There are also petrographic observations that indicate further evidence for size-sorting in shear flow. Biotite grains tend to concentrate in mafic margins in areas of higher shear stress and coarse K-feldspar grains tend to concentrate in the center of felsic layers in areas of minimal shear stress. Biotite grains show a preferred orientation parallel to the mafic margins.

Barrière (1981) described similar types of biotite laminae at Ploumanac'h, France, and attributed them to shear flow occurring in small-scale convection cells. He applied his experimental work on size-sorting in flowing suspensions to his interpretations, based on the earlier work of Bagnold (1954).

(iii) creation of ellipsoidal and circular structures

If vortices formed behind a rising bubble or falling block, flow patterns may have formed arcuate, inwards curving patterns discordant to the bubble or xenolith block. Shear flow may have induced size sorting explaining the fine-grained biotite margins and clusters of coarse-grained K-feldspar megacrysts.

(iv) deformation of quartz

Quartz shows evidence of weak deformation with irregular grain boundaries and (c)- and (a)-slip with blocky subgrain development indicating evidence for flow at a high solids fraction.

5.2.3 *Inferred Process*

Any physical process responsible for the development of schlieren at Prospect must explain the anomalous distribution of schlieren features at this locality disrupting the regional foliation; size-sorting occurring in ellipsoidal and circular structures with fine-grained biotite margins that coarsen inwards; associated K-feldspar megacryst clusters; and thin, wispy biotite laminae. I propose the following model to account for most of the observed schlieren features at Prospect (Fig. 5.1):

Stage 1. Prior to schlieren development, the magma was a homogeneous flow-foliated mush. The new schlieren features must have developed at a relatively high crystal fraction of $\phi = 55-75\%$ when the granitic magma was fluid enough to segregate crystals from melt, and on the other hand, solid enough to preserve the new structures.

Stage 2. A large vapour bubble was rising, or a large xenolith block was sinking, through the magma chamber, producing large strains and complex flow patterns in its wake. These flow patterns formed curved arcuate patterns turning inward, discordant to the rising bubble or sinking block. Shear flow induced size sorting with fine-grained

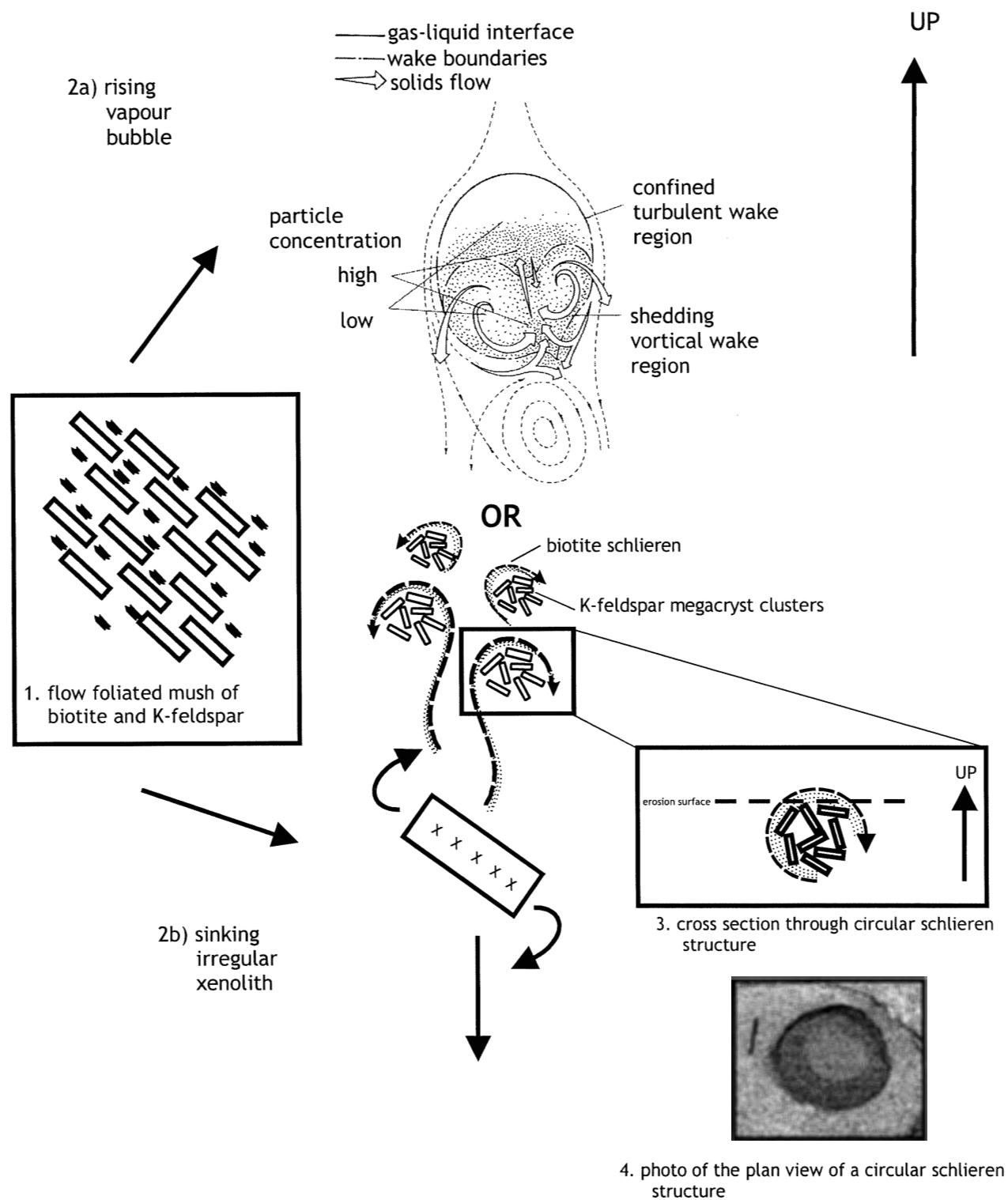


Figure 5.1 Schematic diagram illustrating the possible physical process responsible for schlieren development at Prospect. 1. Flow-foliated mush of crystals and melt. 2a) Rising vapour bubble (after Fan and Tsuchiya 1990). 2b) Sinking irregular xenolith block forming complex flow patterns in its wake. 3. Cross section through circular schlieren structure showing fine-grained margins and coarse-grained interior. 4. Photo of plan view of circular schlieren structure showing fine-grained biotite margins coarsening inwards.

biotite accumulating in areas of high shear flow, and K-feldspar megacrysts accumulating in clusters in areas of minimal shear flow.

Stage 3. After the passage of a rising vapour bubble or a falling xenolith block, the solids fraction was high enough to preserve the newly formed schlieren structures.

5.2.4 Implications of the Model

Benn (1997) used the anisotropy of magnetic susceptibility to map biotite fabrics throughout the South Mountain Batholith, deducing that the magmatic fabrics have been reworked by Acadian tectonic deformation. He suggested that an increase in magma viscosity following emplacement of the batholith with resultant locking-up of fabrics, might have concentrated tectonic strain into “corridors” of tectonic deformation. He stated that the foliation mapped by Abbott (1989) suggested a northwest-southeast “conjugate corridor” of tectonic deformation. He used regional horizontal northeast-southwest magnetic lineations to infer a syntectonic emplacement model for the SMB suggesting that the Acadian orogeny continued until 370 Ma, the cooling age of the batholith (Benn 1997). The orientations of the schlieren structures at Prospect are anomalous relative to the regional foliation and do not conform to a NW-SE compression.

At Prospect, field observations do not appear to comply with fluid dynamic parameters. For example, the ratio of the relative strength of inertial to viscous forces in a moving fluid is expressed by Reynolds numbers (Prothero and Schwab 1996). Several parameters such as: an estimated diameter of a pipe (50 m), estimated velocity (10m/s),

density of the magma (2500 kg/m^3), and viscosity (10^5 kg/m-s) were used to calculate a Reynolds number of $Re = 12.5$. This number is too low to allow a turbulent flow regime that, according to fluid dynamic laws, requires a much higher Reynolds number of $Re > 4000$. Further work is needed to correlate schlieren features with principles of fluid dynamics.

5.3 Peggy's Cove

5.3.1 Major observations

The major structural and textural features at Peggy's Cove, requiring a physical process to explain them, are:

- (i) occurrence of shallowly dipping, rhythmic schlieren, showing reversely-graded bands with fine-grained mafic bottoms and coarse-grained felsic tops;
- (ii) presence of adcumulate textures in plagioclase, formation of myrmekite, apparent random orientations of feldspars;
- (iii) development of cusped margins and pockets of coarse-grained felsic minerals; and
- (iv) development of deformation structures.

5.3.2 Schlieren characteristics and working hypotheses

- (i) shallowly dipping, rhythmic schlieren, with reversely-graded bands

Many examples of repeated accumulations of mafic and felsic minerals have a number of common elements in their explanations: the presence of solid particles dispersed in a fluid, a density contrast between the particles and the fluid, gravitational

forces, and adequate time for accumulation of layers to occur (Wadsworth 1973). An initial injection of magma into a magma chamber or into a fracture contains a mixture of felsic and mafic crystals suspended in a melt. Crystal fractionation involves the differential movement and physical separation of crystals from the melt during solidification as a result of density differences, affected by crystal settling as a result of gravitational forces. Rates of crystal settling are calculated using Stokes' Law of settling velocity taking into consideration, non-spherical crystal shape, drag forces, and the possible Bingham behaviour of magma. Clarke and Clarke (1998) modelled the evolution of rhythmic layering at Chebucto Head, Nova Scotia, and their physical model predicted settling times of approximately 10 years for fine-grained biotite-rich bottom layers.

The rhythmic schlieren features at Peggy's Cove are restricted to an area 30 m x 10 m characterized by asymmetrical bands dipping 20° to the north. The rhythmic sequences consist of ~25 distinct, reversely-graded, layers characterized by fine-grained, biotite bases, grading into coarse-grained felsic tops. The rhythmic, shallow dipping, asymmetrical banding and zoned adcumulus growth on plagioclase, suggest the development of layering that formed sequentially toward the roof of the magma chamber. Rhythmic, shallow dipping, asymmetrical layering suggest the sequence is in an upright orientation.

Wahrhaftig (1979) suggested that such types of asymmetric schlieren, consisting of alternating mafic and felsic layers with gradational and sharp boundaries, represented turbiditic sedimentation. He suggested that this type of sedimentation results from episodes of "turbidite-like" deposition from a fluid magma onto a solid crystal mush

indicating solidification in an upwards direction. This process is unlikely at Peggy's Cove given the limited thickness of the sequence (~10 m).

(ii) adcumulate textures in plagioclase, formation of myrmekite, and random orientations of feldspars

In general, gravity settling produces cumulates typically characterized by euhedral to subhedral crystals. Cumulates become cemented together by a later generation of postcumulus materials crystallizing from the intercumulus liquid (Irvine 1987). At Peggy's Cove, the nearly random orientation of feldspars in felsic layers is more likely the result of gravity settling of randomly oriented grains than the result of shear flow (Table 4.2).

The presence of zoned adcumulus growth textures in plagioclase in the Peggy's Cove samples suggests that the initial growth of the cumulate crystals (e.g., unzoned cores) occurred as a result of materials being able to exchange freely with the liquid of the main magma chamber prior to injection in the layered sequence. After injection, the intercumulus liquid became trapped, and the cumulate crystals grew by fractional crystallization developing zoned rims.

(iii) development of cusped margins and pockets of coarse-grained felsic mineral

Cusped margins at the mafic base of each sequence have convex-downward shapes that appear to form around individual feldspar crystals in the underlying felsic layer with many upwellings forming felsic pockets. Wiebe (1974) observed similar structures in mafic magmas overlying leucogranite layers in the Coastal Maine Plutons

and noted their similarity to sedimentary load structures. He noted that the chilled bases molded around large feldspar crystals in the underlying granite, and veinlets of granitic melt pressed out of the underlying granitic mush perforating the bases. Parsons and Becker (1987) also noted similar features in the laminated syenites of the Klokken intrusion, in southwest Greenland. They attributed load structure formation to result from discontinuous movements during compaction producing shock waves and subsequent deformation of the crystal mush.

(iv) deformation structures

The Peggy's Cove sequence has a deformation feature characterized by several concentric layers that have deformed together into a synformal-type fold (Fig. 2.7c). The deformation feature measures 35 cm in width and appears to affect six layers disrupting the cusped biotite bases and felsic components. This structure indicates that several schlieren layers were able to deform together and that the solids fraction was probably $\phi = 55-75\%$, enabling deformation and preservation of the structure.

The presence of microcline and myrmekitic textures in the felsic-rich pockets, as well as granulated boundaries on feldspar and quartz, could represent deformation mechanisms that took place near the solidus. Vernon (2000) suggests that the presence of microcline and myrmekite are typical of rocks deformed in the solid-state, but that some "solid-state" microstructures can develop when there is still some melt present near the solidus. Collins (1996) suggested that myrmekite results from granitization processes in which layering represents relict bedding. The possibility that these schlieren layers represent "ghost stratigraphy", however, is unlikely because their stratigraphic features

(layer thickness, graded layering, and load structures) do not resemble the Meguma Group.

5.3.3 Inferred Process

A physical process responsible for the schlieren features at Peggy's Cove must explain the asymmetric, reversely-graded, shallowly dipping layers, deformation features, cusped margins with felsic pockets, random orientation of feldspar, and accumulated plagioclase, myrmekite, and microcline. I propose the following model to explain the observed schlieren features at Peggy's Cove (Fig 5.2):

Stage 1. An initial injection of magma into a subhorizontal fracture in cooling and contracting roof rock, consisted of felsic and mafic crystals suspended in a melt.

Stage 2. Density contrasts between mafic and felsic components produced differential settling rates resulting in physical separation of crystals, so that small dense biotite crystals sank first, followed by larger less dense feldspar crystals (asymmetric, reversely-graded layers).

Stage 3. The tops of layers were still a crystal mush when another injection of magma took place, and the sinking of new biotite crystals produced cusped margins resembling load structures. The upwelling of intercumulus liquid was squeezed from the layers below and produced the felsic pockets.

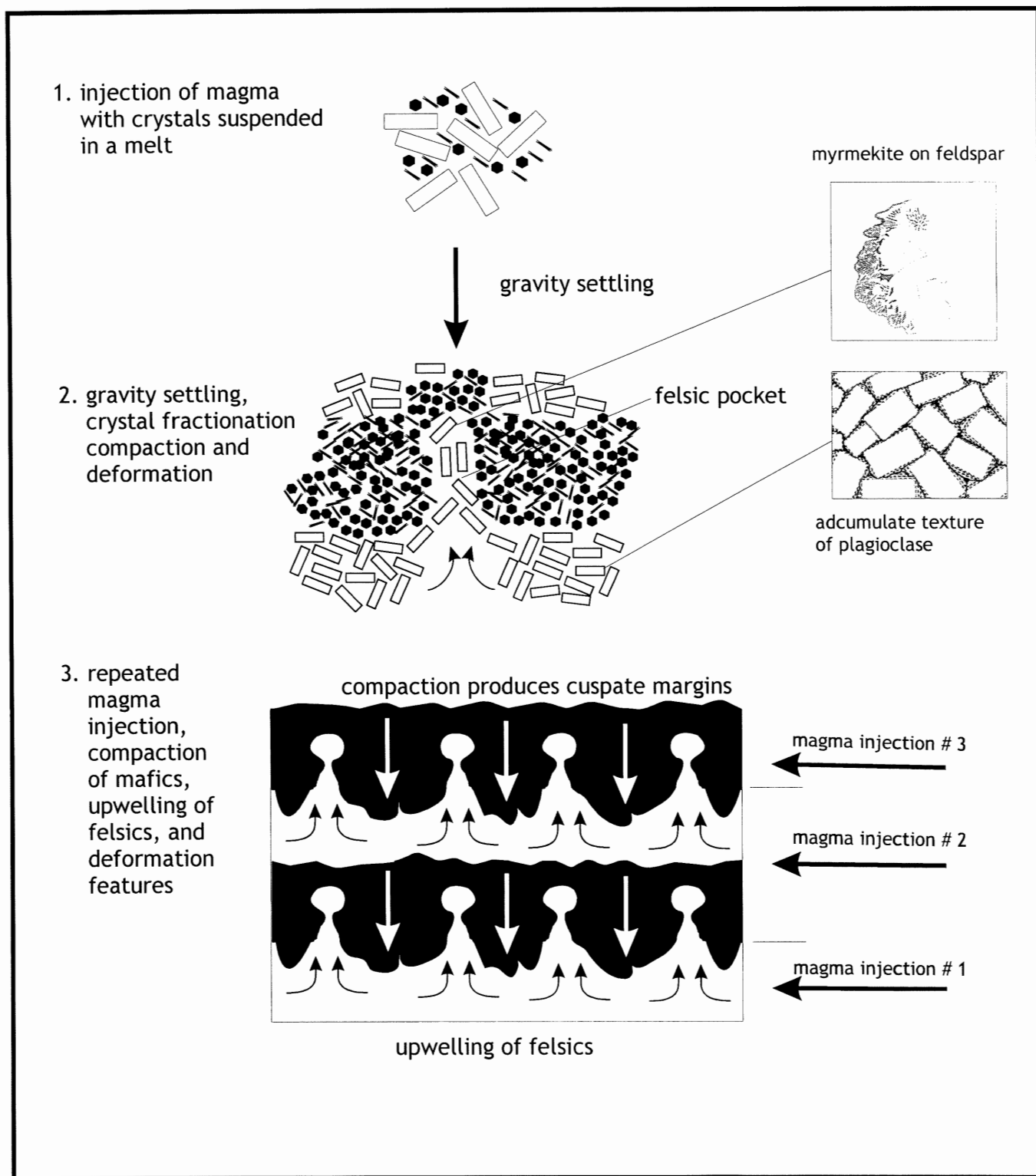


Figure 5.2 Schematic diagram illustrating the possible physical process responsible for schlieren layering at Peggy's Cove. Stage 1. Magma injection of crystals suspended in a melt. Stage 2. Gravity settling, crystal fractionation (accumulative texture in plagioclase), compaction, and deformation. Stage 3. Repetitious magma injection, continued compaction of mafics accompanied by upwelling of felsic intercumulus melt.

Stage 4. Repeated magma injections produced repeated layers, and discontinuous movements prior to complete crystallization produced deformation structures.

5.3.4 Implications of the Model

In addition to two similar layered sequences at Chebucto Head and Pennant Point, the Peggy's Cove exposure represents an additional example for the development of such structures close to the contact of the South Mountain Batholith. Clarke and Clarke (1998) suggested that the proximity of the contact, combined with rapid cooling rates, are significant factors required for creating the necessary conditions for the development of layering.

5.4 Jackies Island

5.4.1 Major observations

The major structural and textural features at Jackies Island, requiring a physical process to explain them, are:

- (i) a zone of strong foliation combined with subvertical, symmetrical, straight schlieren banding, and $S > L$ foliation, flanked by zones of strong foliation with weak (diffuse) banding, and zones of strong foliation with no banding; and
- (ii) presence of microstructures, such as kinked mica, tapering deformation twins and bent feldspar grains, flame perthite in K-feldspar, strongly defined "crosshatch" twinning in microcline, and quartz with (c)- and (a)-slip producing blocky subgrain development.

5.4.2 Schlieren characteristics and working hypotheses

(i) foliation and banding

The well-developed schlieren banding on Jackies Island covers a zone 10 m wide and extends along strike 020 - 035° for several kilometres northeast to Port Mouton Island and southwest to Bull Point. The areas adjacent to the strong foliation and banding zone are characterized by a decrease in the intensity of banding until it disappears and only a foliation marked by lenticular biotite aggregates remains. The individual schlieren bands have sharply defined margins, in some places branching and pinching out, and in other places occurring as symmetrical, parallel, alternating mafic and felsic bands.

The regularity, straightness, and repeated nature of the bands suggest that they did not form at a solids fraction of $\phi = < 55\%$ as a result of partial melting and stretched-out heterogeneities (for further discussion on the relationships between xenoliths and schlieren, see following section on St. Catherines River Bay), but rather formed at a higher solids fraction of $\phi = 55-75\%$ and involved a segregation of melt and solids.

Vigneressee and Burg (1999) indicated that, at this stage of crystallization, grains can no longer rotate freely and begin to tile and interact, developing a foliation aligned parallel to the flow plane. At these crystal fractions, the magma can deform and become dilatant forming localized shear zones in which residual melt can segregate. This residual melt can produce leucocratic bands. The shear strain is predominantly taken up by the melt phase, allowing undeformed solids to develop preferred orientations. Also, the symmetrical, straight banding at Jackies Island clearly indicates that blocky feldspars

separated from platy mica defining both the strong foliation and strong segregation banding.

The strong foliation and banded zone is bordered by zones of strong foliation and weak banding grading to zones of foliation with no banding. This variation suggests that their formation may be the result of syn-magmatic shearing in a ductile shear zone in which only the high strain zones develop segregation banding. The absence of grain size reduction, shear sense indicators (porphyroclasts), and elongated or recrystallized grains indicates that banding on Jackies Island does not represent a ductile mylonite zone.

Petrographic observations show a good foliation of biotite with (001) faces parallel to segregation banding, reasonably good foliation of K-feldspar with (010) faces parallel to the segregation banding (Table 4.2), but little or no evidence of lineation of long axes of the feldspars in the plane of foliation, therefore, $S > L$ foliation.

(ii) microstructures

Several notable microstructures provide further evidence of deformation (Fig. 4.3 a-e). *Quartz* shows (c)-slip indicating slip motion parallel to c-axis ($T > 500^{\circ}\text{C}$), as well as (a)-slip indicating low temperature conditions ($T = 300\text{-}400^{\circ}\text{C}$) that likely induced dislocation glide and creep along basal glide planes (Passchier and Trouw 1996). As a result, the quartz grains show blocky subgrain development and undulose extinction. *Plagioclase* shows tapering deformation twins, deformation bands, bent grains, and undulose extinction, suggesting low-temperature deformation ($T = 300\text{-}400^{\circ}\text{C}$). *K-feldspar* shows flame perthite, predominance of microcline with well-developed “crosshatch” twinning, bent grains, deformation bands, and undulose extinction. *Mica*

grains define the plane of foliation with evidence of ductile deformation represented by kinking, bent grains, and undulose extinction.

Vernon and Paterson (1993) suggested that the effects of weak solid-state deformation had been superimposed on magmatic foliation in the form of well-defined microcline twinning with stronger solid-state deformation evident by the presence of flame perthite in feldspar. Tribe and D'Lemos (1996) described magmatic flow features overprinted by solid-state microstructures in diorite complexes of the Channel Islands, UK, and they suggested that continuous deformation during cooling could occur when strain rates are high (e.g. where a pluton intrudes a shear zone). Vernon (2000) noted that many plutons show evidence of solid-state deformation superimposed on magmatic flow, but it is difficult to establish a continuity in time. Therefore, it is reasonable to assume that deformation can extend from magmatic temperatures to subsolidus temperatures.

5.4.3 Inferred Process

The physical process responsible for the development of schlieren banding on Jackies Island must explain the grading zones of foliation and segregation banding, and deformation microstructures. I propose the following model for the development of foliation and segregation banding on Jackies Island (Fig. 5.3):

Stage 1. Prior to the development of foliation and segregation banding, the solids fraction was $\phi = 55-75\%$ with a random orientation of feldspar and biotite in the magma mush.

Stage 2. A fault/shear zone through the partially crystalline Port Mouton Pluton at

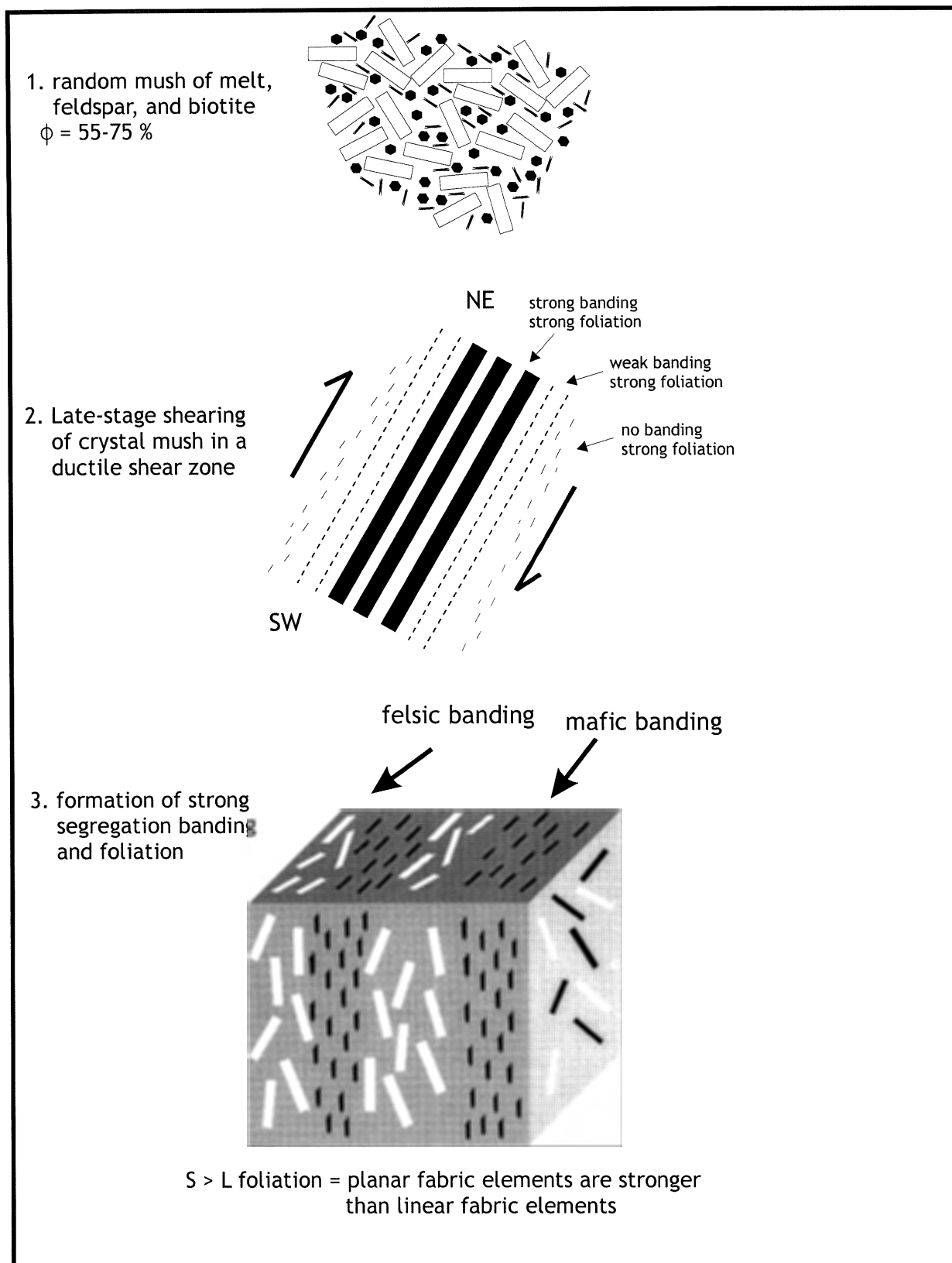


Figure 5.3 Schematic diagram representing the physical process responsible for subvertical schlieren and banding on Jackies Island. Stage 1. Random orientation of feldspar and biotite with crystal fraction of $\phi = 55-75\%$. Stage 2. Shearing of crystal mush in a ductile shear zone. Stage 3. Formation of strong segregation banding and strong foliation.

$\phi = 55-75$ % produced strong segregation banding and foliation as well as quartz microstructures such as (c)-slip parallel to their c-axes at high temperatures ($T > 500^{\circ}\text{C}$).

Stage 3. Continued movement on the shear zone produced continuous deformation during cooling down to the mechanical solidus $\phi = 100$ %. Lower temperatures produced solid-state deformation features: (a)-slip in quartz with the development of blocky subgrains, deformation twins in plagioclase, and flame perthite in K-feldspar.

5.4.4 Implications of the Model

Clarke et al. (2000) observed similar features in samples from Port Mouton Island (PMI) which further substantiates the presence of a shear zone extending along strike between the two locations. Such a major shear zone must have implications for the tectonic setting at the time of emplacement of the PMP.

5.5 St. Catherines River Bay

5.5.1 Major observations

The major structural and textural features at St. Catherines River Bay, requiring a physical process to explain them, are:

- (i) proximity, and similar orientation, to a large xenolith slab swarm almost perpendicular to regional strike of the Meguma Group;
- (ii) irregular wispy biotite schlieren trailing off abundant metasedimentary xenoliths into the host tonalite; and

- (iii) hornfelsic texture in xenolith core, and foliated biotite aggregates on the xenolith rim; and
- (iv) virtually identical biotite compositions in all lithologies.

5.5.2 Schlieren characteristics and working hypotheses

- (i) relationship to the xenolithic slab swarm and
- (ii) wispy biotites trailing off metasedimentary xenoliths

The well-developed schlieren banding at St. Catherines River Bay (SCRB) covers a zone 600 m x 100 m in a well-foliated tonalite host of the Port Mouton Pluton (PMP). The schlieren bands have sharply defined margins that on a small-scale appear irregular, but on a larger scale, tend to strike 110-130° and dip steeply. The bands are characterized by discontinuous, sinuous, wispy biotite lenses that appear concentrated around the rims of metasedimentary xenoliths trailing into the host tonalite (Figs. 2.13, 2.14).

Approximately 300 metres southeast of the schlieren banding at SCRБ, hundreds of rectangular metasedimentary xenolith blocks are exposed in a sub-parallel alignment in the host tonalite. These xenolith blocks have sharp angular contacts indicating either chilling of the magma following incorporation of the blocks so that they have spent less time in the magma, or the blocks are refractory, or both. The close spatial relationship between the schlieren and the angular xenoliths suggests a genetic connection.

Vignerresse and Burg (1999) suggest that, at low solids fractions, crystals can rotate freely with minimal interference from other crystals, and that this rotation can produce magmatic foliation. Gansser and Gyr (1964) noted the relationship between

xenoliths and the development of schlieren and suggested that magmatic movements were able to draw out xenoliths into parallel schlieren, a process indicating the fluidity of magma at the time. Link (1970) noted that differential movement in the magma could disrupt xenoliths and disperse their components. Flinders and Clemens (1996) discussed the stretching and dispersal of enclaves (xenoliths) in which shear forces in the silicate melt caused stretching and disintegration of the enclaves.

At St. Catherines River Bay, the lenticular nature of the schlieren bands and high concentration of biotite on the xenolith rims suggest that they represent refractory residue from the partial melting and mechanical disintegration of metasedimentary source rocks that become streaked-out by shear.

The common occurrence of country rock at the margins of granitoid intrusions has led to the interpretation of stoping as a classic mechanism for the emplacement of granitoid magmas. Clarke et al. (1998) showed that stoped blocks must undergo continuous thermal stress fracturing and spalling as they sink into the hotter regions of a magma. In such cases, the break-up of country rocks provides a dramatic increase in surface area that further enhances the mechanical and chemical interactions (Pitcher 1993).

Assimilation of country rock into granitic hosts by partial melting is restricted to the available thermal energy in the magma. The country rocks must first be heated by the magma to their melting point, and then partially melted, for assimilation to take place (Winter 1999). During assimilation, the magma cools quickly, and the outer margin of the intrusion may undergo rapid cooling. Such rapid cooling may explain the preservation of

angular xenolith blocks and schlieren bands in their observed orientations and partially assimilated state.

Didier (1973) noted the difficulty in determining the origin of xenoliths, especially the occurrence of large blocks which could represent roof pendants, wall apophyses, or screens separating successive intrusions. Dürr (1960) noted that the least-changed enclaves in the Montagny granite were angular, leading to a progression into elongated shapes with micaceous tails, and then to a gradual disappearance with only ghost-like schlieren traces remaining. Didier (1973) stated that xenoliths could also indicate boudinage during late tectonic activity which could impose a regional scale foliation.

The source of xenoliths at St. Catherines River Bay may originate from a roof pendant that has detached from the roof, because the strike of the xenoliths is almost perpendicular to the regional strike of the Meguma Group.

(iii) hornfelsic textures and biotite aggregates

Petrographic observations show hornfelsic texture in the xenolith cores with the quartz and K-feldspar grains appearing as small, recrystallized grains with a granoblastic texture. They have a greater modal abundance in the core, and become rare to absent at the xenolith rim. Toward the outer margin of the xenoliths, the biotite grains are concentrated in tightly-packed aggregates with strong kink banding and wavy extinction, increasing to 80 % modal abundance at the xenolith rims, and 90% abundance in the xenolith tail. The high biotite concentration on the xenolith rims to the tails appears to represent the refractory residue from partial melting of the xenolith. In the host tonalite, the biotite grains have kink banding and show a strong preferred orientation. Plagioclase

is rare or absent in the xenoliths, but shows weak oscillatory zoning in both the host tonalite and rim of one xenolith, indicating growth under the same conditions (T, P, H₂O).

(iv) identical biotite compositions

Two kinds of geochemical evidence support the assimilation model for schlieren development at SCRB. At the mineralogical level, an examination of the compositions of biotite grains analyzed from the xenolith cores to the host tonalite shows minimal variability among the major and minor oxide elements. A plot of TiO₂ vs. FeO/(FeO + MgO) (Fig. 5.4) shows fields representing xenolith core, rim, tail, and host tonalite. The fields overlap to a large extent, indicating highly similar biotite compositions. The simplest possible explanation is that all biotites represent the refractory residues of the partial melting of xenoliths. At the whole-rock level, Clarke et al. (2000a) used Sr and Nd mass balance equations to deduce that the PMP tonalites could be explained by an assimilation-fractional crystallization model involving 0.701 mantle + 0.450 upper crust (Meguma) - 0.150 lower crust. The large schlieren zone at SCRB could represent an extensive area of assimilation of upper crustal Meguma rocks into the PMP. The adjacent xenolith blocks may represent the more resistant metapsammitic Goldenville Formation, of the Meguma Group, and the schlieren banding likely represents country rock with a greater pelitic component.

The localized abundance of heterogeneous metasedimentary xenoliths with “streamers” of biotite schlieren likely represent a low solids fraction of $\phi < 55\%$ and a high liquid component, indicating a shear flow regime.

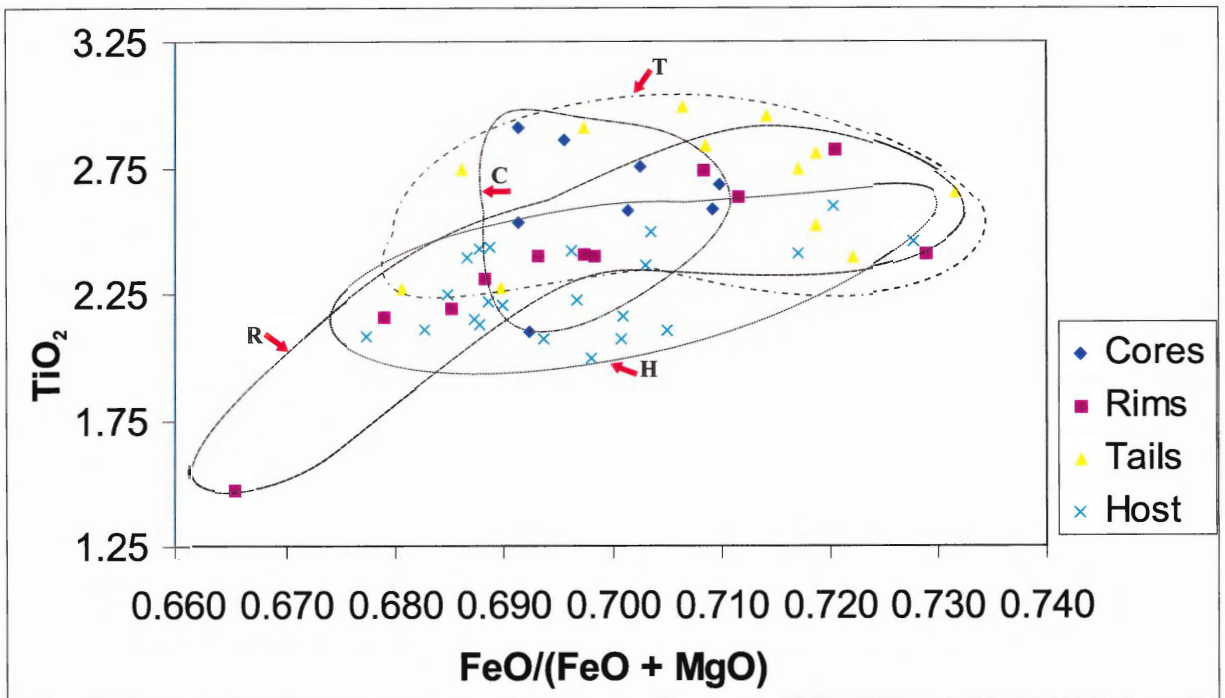


Figure 5.4 A TiO_2 vs. $\text{FeO}/(\text{FeO} + \text{MgO})$ plot of analyzed samples showing fields for xenolith core (C), rim (R), tail (T), and host tonalite (H).

5.5.3 *Inferred process*

The development of schlieren banding at St. Catherines River Bay must explain the spatial association of the biotite schlieren with metasedimentary xenoliths, their discontinuous nature, and similar biotite compositions between the xenolith core, rims, biotite schlieren tails, and host tonalite.

I propose the following model to explain the relationship between the xenoliths and host tonalite (Fig. 5.5):

Stage 1. The Port Mouton Pluton was emplaced by stoping. Thermal stress fracturing caused dislocation of roof blocks or detachment and disintegration of a roof pendant.

Stage 2. The localized abundance of heterogeneous metasedimentary xenoliths with “streamers” of biotite schlieren likely represent a low solids fraction of $\phi < 55\%$ and a high liquid component, indicating a shear flow regime. The increased surface area caused by the mechanical disintegration of xenoliths further enhances thermal and chemical interactions. The streaking-out of heterogeneous xenoliths represents an intermediate stage in the homogenization process in which the xenoliths are eventually assimilated and dispersed in a granitic host.

Stage 3. Biotite schlieren became dispersed in the magma which was progressively homogenized.

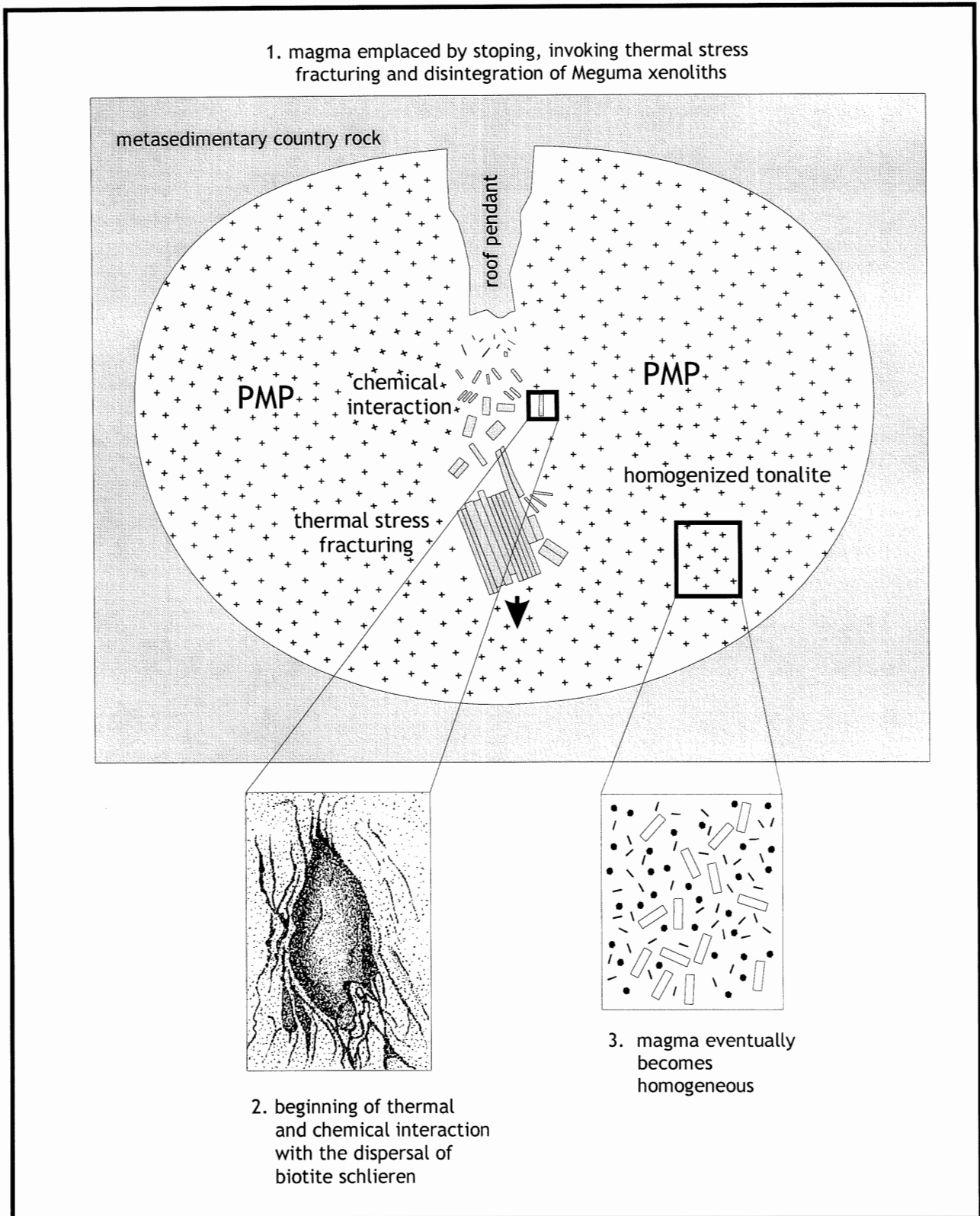


Figure 5.5. Schematic diagram of the physical process responsible for schlieren development at St. Catherines River Bay. Stage 1. The Port Mouton Pluton is emplaced by stoping and causes thermal stress fracturing and disintegration of a roof pendant. Stage 2. The increased surface area caused by the mechanical disintegration of xenoliths further enhances thermal and chemical interactions. Stage 3. Biotite schlieren become dispersed in the magma which becomes progressively homogenized.

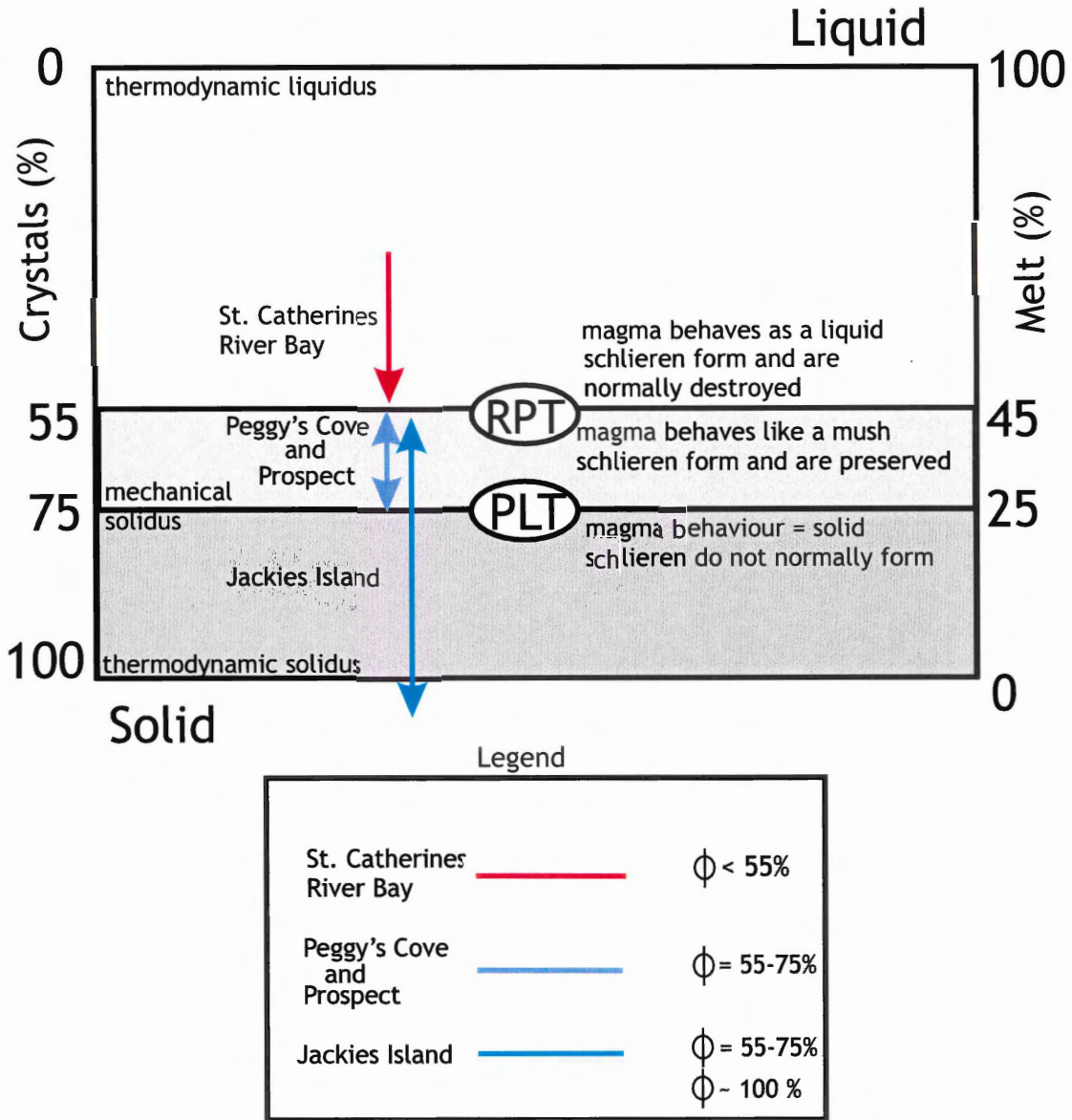


Figure 5.6. Liquid-solid diagram showing the range of solids fraction over which each of the four schlieren localities formed. Note that, at Jackies Island, the deformation continued below the thermodynamic solidus.

5.5.4 Implications of the Model

As at Prospect, the attitudes of the schlieren banding at SCRB and the nearby xenolith slab swarm are at a high angle to the regional Acadian compression, suggesting that, at least, the compressional phase of deformation had ended before the intrusion of the PMP.

5.6 Summary

Schlieren features at all four study localities show distinctive structural and textural features that require different physical process of formation at each location. Figure 5.6 represents each of the four localities on the liquid-solid diagram representing a continuum in magmas between 100 % liquid fraction to 100% solids fraction.

CHAPTER 6: CONCLUSIONS

6.1 Conclusions

Schlieren form as the result of complex interactions between melt and crystals. The features that develop are a function of many variables: temperature; degree of crystallinity; viscosity; physical properties such as size, shape, and density; shear flow; chemical reactions, such as assimilation, resulting from disequilibrium between melt and solids; and thermal stress fracturing and mechanical disintegration.

Table 6.1 reviews and compares field relations, petrographic observations, analytical methods, and multiple working hypotheses. Table 6.2 compares the inferred physical processes at the four schlieren study localities in granitoid rocks of southern Nova Scotia. The features and processes are unique at each locality and each example of schlieren must be examined on the basis of its individual mineralogical, textural, structural, and chemical characteristics.

6.2 Recommendations for Future Work

6.2.1 Prospect

Further investigation is required in the form of mathematical modelling and experimental work to understand the effects of fluid dynamic behaviour and its relationship to the development of schlieren structures and disruption of the regional flow foliation.

Table 6.1 Summary of field relations, petrography, analytical methods, and working hypotheses.





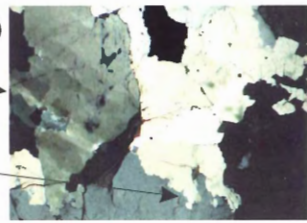
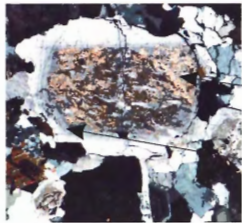
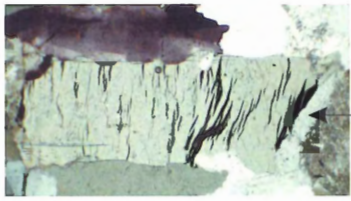
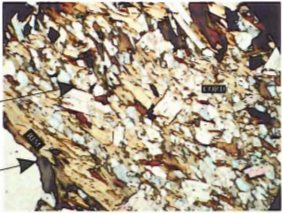
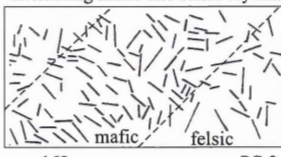
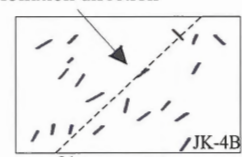
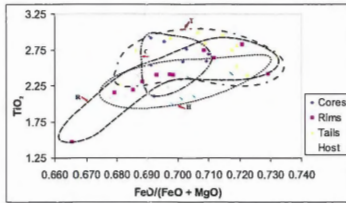
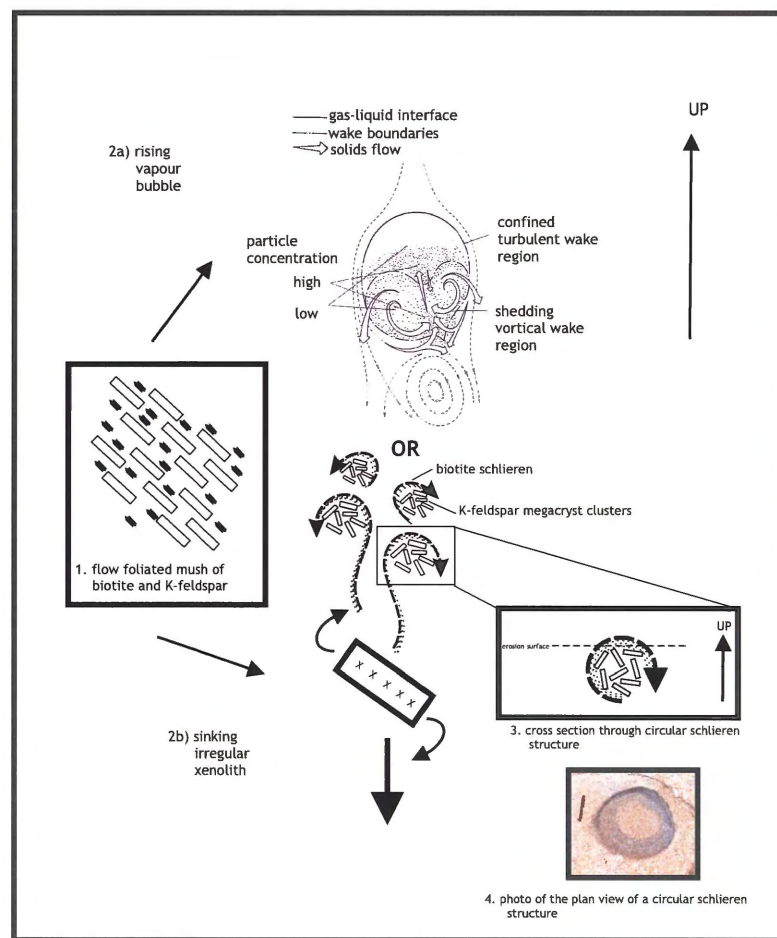
Feature	Prospect	Peggy's Cove	Jackies Island	St. Catherines River Bay
Field photograph				
Field relations: schlieren characteristics	wispy biotite laminae associated with clusters of K-feldspar megacrysts, circular and ellipsoidal structures; perturbation of the regional flow foliation	subhorizontal, asymmetrical, reversely-graded bands with cusped margins and felsic pockets, and deformation structures	subvertical, symmetrical, straight felsic and mafic bands; zones of strong segregation banding and strong foliation	metasedimentary xenoliths with biotite schlieren trailing into tonalite; spatial association with xenolith slab swarm
Petrography: photomicrographs	<p>1. (a) and (c) slip in qz</p> <p>2. irregular qz grain boundaries</p> 	 <p>1. plagioclase with unzoned core</p> <p>2. oscillatory zoned rim</p>	 <p>K-fsp with flame perthite</p>	<p>1. xenolith core with granoblastic qz + fsp</p> <p>2. aligned biotite aggregates</p> 
Petrographic observations	biotite grains are concentrated in mafic margins, K-feldspar grains are concentrated in center of felsic layers; alignment of biotite grains; quartz shows (a) and (c)-slip with blocky subgrain development and irregular grain boundaries	zoned adcumulus growth in plagioclase; presence of myrmekite texture on feldspar grain boundaries and weak crosshatch twinning in microcline in felsic pockets	(c) and (a)-slip in quartz ; plagioclase shows deformation twins, bent grains, and undulose extinction; K-feldspar shows flame perthite, bent grains, well-defined microcline crosshatch twinning; mica shows strong alignment with kinking and undulose extinction	hornfelsic texture in xenolith cores (granoblastic qz + fsp); biotite shows a strong alignment with tightly packed aggregates at the xenolith rims; plagioclase has weak oscillatory zoning in the xenoliths and host tonalite
Analytical methods	no analytical methods were used for this locality although an extensive literature review related field evidence to other previous work such as shear flow around dropstones in a glacial environment, rising vapour bubbles, and falling xenolith blocks	<p>alternating mafic and felsic layering</p>  <p>image analysis indicates a ~ random distribution of feldspar</p> <p>n = 162 x = 91.0° σ = 47° for PC-3 σ = 52.4° for random standard</p>	<p>foliation direction</p>  <p>image analysis indicates a tighter distribution = preferred orientation of feldspar</p> <p>n = 21 x = 124.7° σ = 18.6° for JK-4B σ = 55.6° for random standard</p>	 <p>biotite compositions from the xenolith core-rim-tails-host show minimal variability</p>
Working hypotheses	size sorting in shear flow develops as a result of: 1. syntectonic emplacement 2. rising vapour bubble 3. falling irregular xenolith block	asymmetrical rhythmic schlieren layering form as a result of: 1. granitization process 2. turbidite-like sedimentation 3. repeated magma injection with gravity settling	strong foliation and segregation banding form as a result of: 1. partial melting of metasedimentary xenoliths 2. solid state deformation 3. synmagmatic shearing in a fault-shear zone	biotite schlieren form as a result of: 1. partial melting and assimilation of metasedimentary xenoliths

Table 6.2 Summary of physical process at the four schlieren localities.

SOUTH MOUNTAIN BATHOLITH

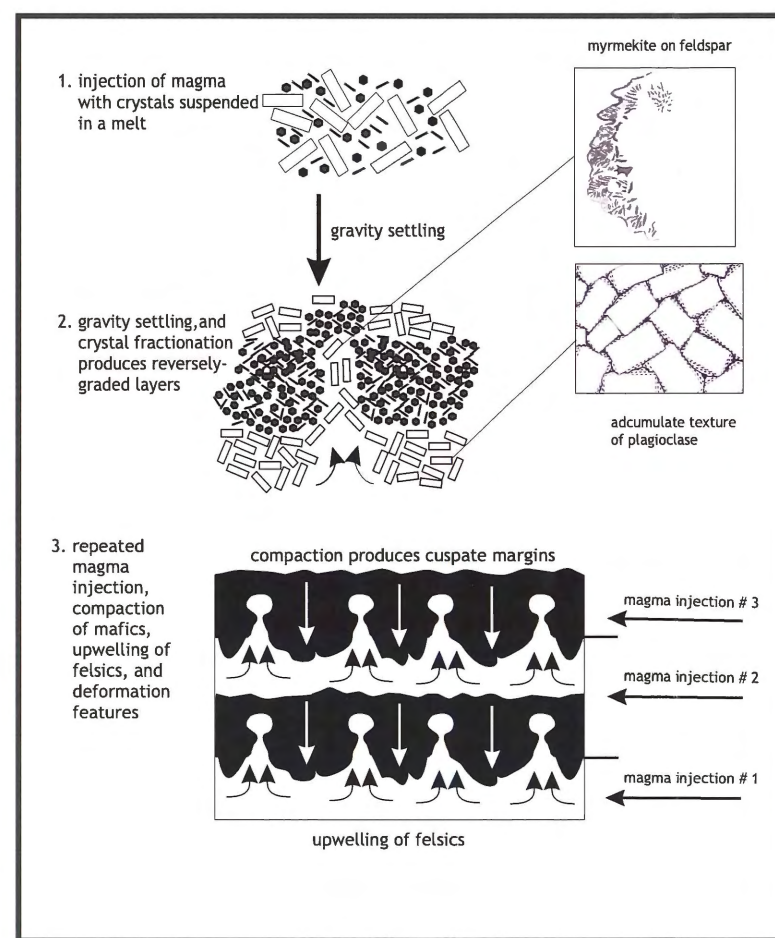
PORT MOUTON PLUTON

PROSPECT



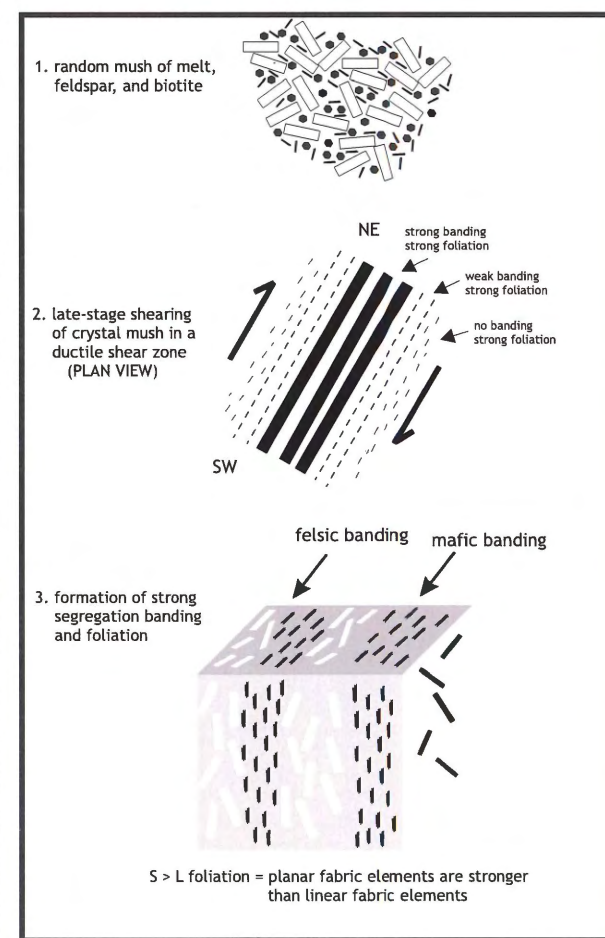
PROCESS 1.
SIZE SORTING AND SHEAR FLOW
IN THE WAKE OF A RISING VAPOUR
BUBBLE OR FALLING XENOLITH

PEGGY'S COVE



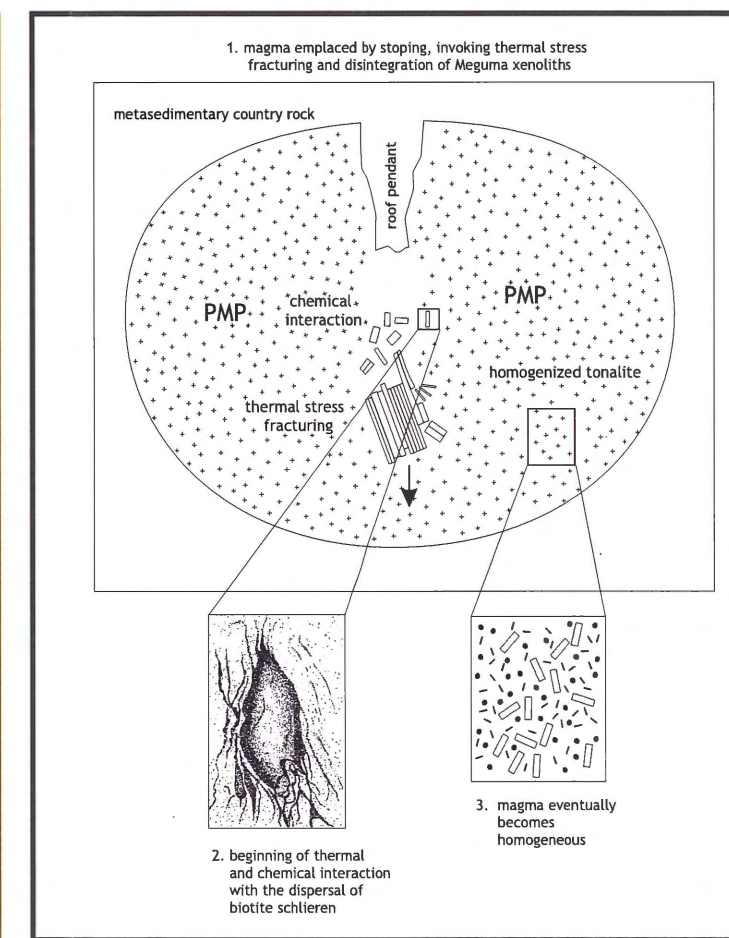
PROCESS 2.
REPEATED MAGMA INJECTION
WITH GRAVITY SETTLING

JACKIES ISLAND



PROCESS 3.
SYNMAGMATIC SHEARING
WITH DEVELOPMENT OF
SCHLIEREN BANDING

ST CATHERINES RIVER BAY



PROCESS 4.
PARTIAL MELTING AND ASSIMILATION
OF METASEDIMENTARY XENOLITHS

6.2.2 *Peggy's Cove*

Further work is needed to determine the systematic variation of layers, their compositional differences, lateral extent and continuity to establish if there is a genetic connection between Chebucto Head, Pennant Point and Peggy's Cove layering.

6.2.3 *Jackies Island*

A detailed structural investigation is needed to further understand the nature of the NE-SW trending shear zone (e.g., mesoscopic and microscopic shear sense indicators) and unexplained structural features. Electron backscattered diffraction could also be used to quantify crystallographic orientations of aligned grains. Such work may provide additional evidence for the tectonic setting and emplacement of the PMP.

6.2.4 *St. Catherines River Bay*

Additional sampling with mineralogical and textural observation, as well as detailed chemical analyses (e.g. isotopic studies, trace elements) would further substantiate the origin of schlieren and their relationship to the composition of the Port Mouton Pluton. Further structural investigation would be useful to understand the NW-SE trending strike of the schlieren and xenolith slab swarm, and might provide additional evidence for the tectonic setting and emplacement of the PMP.

REFERENCES

- Abbott, R.N. 1989. Internal structures in part of the South Mountain Batholith, Nova Scotia, Canada. *Geological Society of America Bulletin*, **101**: 1493-1506.
- Bates, R.L., and Jackson, J.A. 1987. *Glossary of geology*. 3rd ed. American Geological Institute, Alexandria, Virginia, pp. 788.
- Bagnold, R.A. 1954. Experiments on a gravity free dispersion of large solid spheres in a Newtonian fluid under shear. *Proceedings of the Royal Society of London. Series A*, **225**: 49-63.
- Balk, R. 1937. *Structural behaviour of Igneous Rocks*. Geological Society of America, Memoir 5.
- Barrière, M. 1981. On curved laminae, graded layers, convection currents and dynamic crystal sorting in the Ploumanac'h (Brittany) subalkaline granite. *Contributions to Mineralogy and Petrology*, **77**: 214-224.
- Benn, K. 1997. Syn-Acadian emplacement model for the South Mountain Batholith, Meguma Terrane, Nova Scotia: magnetic fabric and structural analyses. *Geological Society of America Bulletin*, **109**: 1279-1293.
- Berry, R.F., and Flint, R.B. 1988. Magmatic banding within Proterozoic granodiorite dykes near Streaky Bay, South Australia. *Transactions of the Royal Society of South Australia*, **112**: 63-73.
- Clarke, D.B. 1992. Field Relations. *In Granitoid Rocks, Edited by T. H. van Andel*, Chapman and Hall, London, pp. 23-59.
- Clarke, D.B., and Clarke, G.K.C. 1998. Layered granodiorites at Chebucto Head, South Mountain Batholith, Nova Scotia. *Journal of Structural Geology*, **20**: 1305-1324.
- Clarke, D.B., Fallon, R., and Heaman, L.M. 2000a. Interaction among upper crustal, lower crustal, and mantle materials in the Port Mouton pluton, Meguma Lithotectonic Zone, southwest Nova Scotia. *Canadian Journal of Earth Sciences*, **37**: 579-600.
- Clarke, D.B., Henry, A S., and White, M.A. 1998. Exploding xenoliths and the absence of "elephants' graveyards" in granite batholiths. *Journal of Structural Geology*, **20**: 1325-1343.
- Clarke, D.B., MacDonald, M.A., and Tate, M.C. 1997. Late Devonian mafic-felsic magmatism in the Meguma Zone, Nova Scotia. *Geological Society of America Memoirs*, **191**: 107-127.

- Clarke, D.B, McCuish, K.L, Vernon, R.H., Makshev, V., and Miller, B.V. 2000b. The Mouton Shear Zone: intersection of a crustal scale fracture with a crystallizing granitoid pluton. *Lithos* (submitted)
- Clarke, D.B., Muecke, G.K. 1985. Review of the petrochemistry and origin of the South Mountain Batholith and associated plutons, Nova Scotia, Canada. *In* High heat production (HHP) granites, hydrothermal circulation and ore genesis. The Institute of Mining and Metallurgy, London, pp. 41-54.
- Didier, J. 1973. Schlieren. *In* Granites and their enclaves: the bearing of enclaves on the origin of granites. Elsevier Scientific Publishing Company, Amsterdam, pp. 343-355.
- Dürr, S. 1960. Le granite de Montagny et ses enclaves (feuille de Lyon au 1/80.000). Université de Clermont-Ferand, pp. 30. (unpublished).
- Fader, G.B.J and Miller, R.O. 2001. Surficial geology of Halifax Harbour. Geological Survey of Canada Bulletin (in press).
- Fan, L.S. and Tsuchiya, K. 1990. Bubble flow in liquid-solid suspensions. *In* Bubble wake dynamics in liquids and liquid-solid suspensions. Butterworth-Heinemann, Stoneham, MA, pp. 811-855.
- Featurescan Operator's Manual. 1991. Link Analytical Limited, England.
- Flinders, J. and Clemens, J.D. 1996. Non-linear dynamics, chaos, complexity and enclaves in granitoid magmas. *Transactions of the Royal Society of Edinburgh: Earth Sciences*, **87**: 217-223.
- Gansser, A. and Gyr, T. 1964. Über Xenolithschwarze aus dem Bergeller Massiv und probleme der intrusion. *Eclogae Geol. Helvetica*, **57**: 577-598.
- Harry, W.T. and Emeleus, C.H. 1960. Mineral layering in some granitic intrusions of S.W. Greenland. International Geological Congress, Report of the twenty-first session. Norden, Copenhagen, **XIV**: 172-181.
- Hess, H.H. 1960. Stillwater Igneous Complex, Montana: a quantitative mineralogical study. Geological Society of America, Memoir 80.
- Irvine, T.N. (1987a) Appendix 1. Glossary of terms for layered intrusions. *In* Origins of Igneous Layering, *Edited by* I. Parsons. NATO Advanced Science Institute Series C., Mathematical and Physical Sciences D. Reidel, Amsterdam, pp. 641-647.
- Irvine, T.N. (1987b) Appendix II. Processes involved in the formation and development of layered igneous rocks. *In* Origins of Igneous Layering, *Edited by* I. Parsons. NATO

- Advanced Science Institute Series C., Mathematical and Physical Sciences, D. Reidel, Amsterdam, pp. 649-656.
- Knopf, A. 1918. A geological reconnaissance of the Inyo Range and the eastern slope of the Southern Sierra Nevada, California. US Geological Survey Professional Paper, **110**: 60-67.
- Link, A.J. 1970. Inclusions in the Half Dome quartz-monzogranite, Yosemite National Park, California. PhD thesis, Northwestern University, Evanston, Illinois.
- MacDonald, M.A., Horne, R.J., Corey, M.C., and Ham L.J. 1992. An overview of recent bedrock mapping and follow-up petrological studies of the South Mountain Batholith, southwestern Nova Scotia, Canada. *Atlantic Geology*, **28**: 7-28.
- Maksaev, V. 1986. The origin of banding in the Mouton Island granite, southern Nova Scotia. Dalhousie University, Geology Research Paper, pp. 48.
- McBirney, A.R., and Noyes, R.M. 1979. Crystallization and layering in the Skaergaard intrusion. *Journal of Petrology*, **20**: 487-554.
- McKenzie C.B. and Clarke, D.B. 1974. Petrology of the South Mountain Batholith, Nova Scotia. *Canadian Journal of Earth Sciences*, **12**: 1209-1218.
- Miller, R.B. and Paterson, S.R. 1994. The transition from magmatic to high-temperature solid-state deformation: implications from the Mount Stuart Batholith, Washington. *Journal of Structural Geology*, **16**: 853-865.
- Parsons, I., and Becker, S.M. 1987. Layering, compaction and post-magmatic processes in the Klokken intrusion. *In* *Origins of Igneous Layering*, Edited by I. Parsons. NATO Advanced Science Institute Series C., Mathematical and Physical Sciences, D. Reidel, Amsterdam, pp. 29-92.
- Passchier, C.W. and Trouw, R.A.J. 1996. *Microtectonics*, Springer-Verlag, Berlin, pp. 289.
- Paterson, S.R., Fowler, T.K., Schmidt, K.L., Yoshinobu, A.S., Yuan, E.S., and Miller, R.B. 1998a. Interpreting magmatic fabric patterns in plutons. *Lithos*, **44**: 53-82.
- Paterson, S.R. and Miller, R.B. 1998b. Stopped blocks in plutons: paleo-plumb bobs, viscometers, or chronometers? *Journal of Structural Geology*, **20**: 1261-1272.
- Paterson, S.R., Vernon, R.H., Tobisch, O.T. 1989. A review of criteria for the identification of magmatic and tectonic foliations in granitoids. *Journal of Structural Geology*, **11**: 349-363.

- Pitcher, W.S. 1993. The physical nature of granitic magmas. *In* The nature and origin of granite. Blackie Academic and Professional, London. pp. 48-67.
- Pitcher, W.S., and Berger, A.R. 1972. The main Donegal pluton; and The fabric of granitic rocks: comments on granite tectonics, the interpretation of textures, and on ghost stratigraphy. *In* The geology of Donegal: A study of granite emplacement and unroofing, Regional Geology Series *Edited by* L.V. De Sitter. Wiley-Interscience, New York, pp. 215-220, 328-337.
- Prothero, D.R. and Schwab, F. 1996. Clastic transport and fluid flow. *In* Sedimentary geology an introduction to sedimentary rocks and stratigraphy. W.H. Freeman and Company, New York, pp. 27-41.
- Reid, J.B., Murray, D.P., Hermes, O.D., and Steig, E.J. 1993. Fractional crystallization in granites of the Sierra Nevada, How important is it? *Geology*, **21**: 587-590.
- Schenk, P.E. 1995. Meguma Zone. *In* Geology of the Appalachian-Caledonian orogen in Canada and Greenland. *Edited by* H. Williams. Geological Survey of Canada, Geology of Canada 6, pp. 261-277.
- Stephenson, P.J., 1990. Layering in felsic granites in the main East pluton, Hinchinbrook Island, North Queensland, Australia. *Geological Journal*, **25**: 325-336.
- Trent, D.D., 1995. Schlieren in granitic rocks of the Sierra Nevada, California. *Geological Society of America Programs with Abstracts*, **13**: 111.
- Tribe, I.R. and D'Lemos, R.S. 1996. Significance of a hiatus in down-temperature fabric development within syn-tectonic quartz diorite complexes, Channel Islands, UK. *Journal of the Geological Society of London*, **153**: 127-138.
- Vigneresse, J.L. and Burg, J.P. 2000. Towards a comprehensive rheological model of partly molten felsic rocks. *Journal of Petrology* (submitted).
- Vigneresse, J.L. and Tikoff, B. 1999. Strain partitioning during partial melting and crystallizing felsic magmas. *Tectonophysics*, **312**: 117-132.
- Vernon, R.H. 2000. Review of microstructural evidence of magmatic and solid-state flow. *Electronic Geoscience* 5.
- Wadsworth, W.J. 1973. Magmatic sediments. *Minerals Science Engineering*, **5**: 25-35.
- Wager, L.R. and Brown, G.M. 1968. Layered igneous rocks. Oliver and Boyd. Edinburgh, pp. 588.

- Wahrhaftig, C. 1979. Significance of asymmetric schlieren for crystallization of granites in the Sierra Nevada batholith, California. *Geological Society of America Abstracts with Programs*, **11**: 133.
- Weinberg, R.F., Sial, A.N., Pessoa, R.R., and Ferreira, V.P. 1999. Magma flow within the Tavares pluton, NE Brazil: Diapirs, ladder dykes, and thermal plumes. In: *The origin of Granites and related rocks IVth Hutton Symposium*, Clermont-Ferrand, France.
- Wiebe, R.A. 1974. Coexisting intermediate and basic magmas, Ingonish, Cape Breton Island. *Journal of Geology*, **82**: 74-87.
- Wilshire, H.G. 1969. Mineral layering in the Twin Peaks granodiorite, Colorado. *Geological Society of America Memoir*, **115**: 235-261.
- Winter, J.D. 1999. Diversification of magmas. *In Igneous and metamorphic petrology (first draft)*. Prentice-Hall, US, pp. 1-19.
- Woodend-Douma, S.L., 1988. The mineralogy, petrology, and geochemistry of the Port Mouton Pluton, Nova Scotia, Canada. M.Sc. thesis, Dalhousie University, Halifax, Nova Scotia.
- Yuan, E.S. and Paterson, S.R. 1993. Evaluating flow from structures in plutons. *Geological Society of America Abstracts with Programs*, **25**: 305.
- Zelinka, S. Meteo 471W-Assignment 3 Fallstreaks
<<http://www.personal.psu.edu/users/s/p/spz104M471W/Assignment3/>>
(23 July, 2000)